High-speed resistance mash seam welding of tinplate-packaging steels for three-piece can manufacture

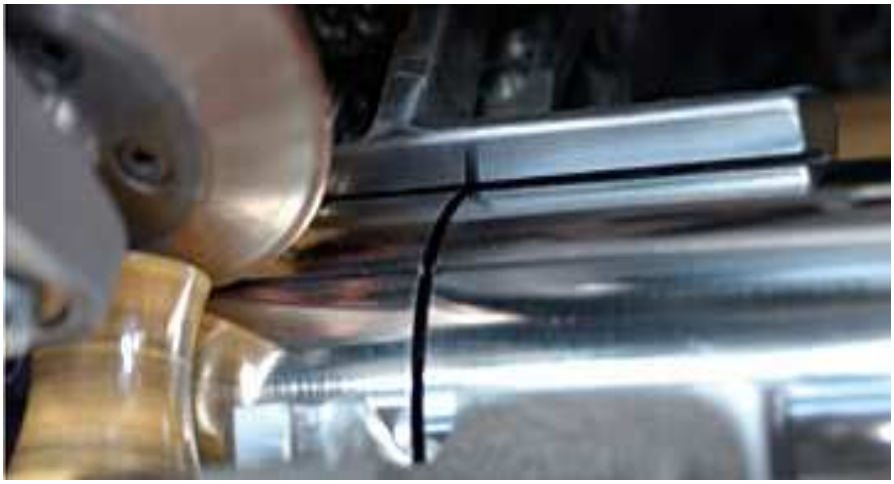

– A Literature Review –

Date: November 2006

By: Adriaan H. Blom

Supervisor: Prof. Dr. Ian M. Richardson

Delft University of Technology

Materials Science and Enigineering

Mekelweg 2

2628 CD Delft

The Netherlands

Delft University of Technology

Abbreviations

AC	Alternating Current
BA	Batch Annealed
CA	Continuous Annealed
CCT	Continuous Cooling Transformation
CHT	Continuous Heating Transformation
DC	Direct Current
DR	Double Reduced
DRD	Drawn and Redrawn
DWI	Drawn and Wall-Ironed
ECCS	Electrolytic Chrome-Coated Steel
FE	Finite Element
GTA	Gas Tungsten Arc
HAZ	Heat-Affected Zone
HSRW	High Speed Resistance (mash seam) Welding
HSS	High Strength Steels
LDR	Limiting Drawing Ratio
LSS	Low Strength Steels
LTS	Low Tin Substrates
MHD	Maximum Heat Development
PWM	Pulse Width Modulation
SR	Single Reduced
TFS	Tin Free Steel
TZM	Titanium Zirconium Molybdenum
WIMA	WIre MAsh

Abstract

Containers for food products, pressurised aerosols and general line goods are characterised by the use of high-speed resistance mash seam welding. This industrial application for fabricating the body of three-piece containers mostly uses double reduced tinplate material of around 0.2 mm thick. The can body is made from a rectangular piece of tinplate, formed into a cylinder, welded followed by insertion and double seaming of the end caps. Resistance mash seam welding is most commonly applied to the welding of the longitudinal cylinder seams, where the automated character of the process achieves speeds of 80 to 115 m/min. A good quality weld consists of intermittently repeated overlapping weld nuggets, which create a continuous gas tight welded seam along the total height of the can body.

To ensure good weldability with high quality joints, a welding parameter range is appoint, within which the materials are welded. This operating window is bounded by a lower limit, above which good mechanical behaviour is established and an upper limit, below which no material ejection (formation of splash) is encountered.

Despite the simple principles of the welding process there is an extra demand on the process potentials and product performance to utilise this to its optimum, therefore a more profound understanding of the welding procedure itself is required (i.e. a link between the process parameters, thermal-mechanical history and microstructural phenomena) and thereby a definitively based understanding of joining under different process conditions (i.e. current, force, speed, etc.) with associated material features.

To this aim, this literature review is written to first of all describe the present state of knowledge in the process of three-piece can manufacture. This is done by looking at, the development of the process, its relation to other container manufacture processes, up- and downstream processes in three-piece can manufacture, process characteristics, the effect on the materials employed, and the modelling part of the welding process.

The high-speed resistance mash seam welding process developed rapidly into a very fast and highly automated welding process, which despite other much more suitable processes is still able to maintain more than half of the steel container packaging market.

Three-piece container production consists mainly of forming operations whereby many limitations and restrictions on the tinplate influence the welding procedure. Nevertheless, welding is a major influential process step, which has a lifetime effect to what happens to the can body material and its properties in the final product.

The welding process is characterised by the (contact) resistance, which shows the effect of heat generation and temperature balances on the final joint and associated metallurgical features. The contact resistance is directly influenced by the welding parameters and tinplate properties to operate the process to its maximum speed and optimum working window, whereby the dynamic character of the welding process in combination with the welding and material parameters makes it difficult to classify the process to one type.

The welding process is settled in terms of the can manufacture specifications, yet very little is known or published on the actual mechanism of weld formation. The existing ones are based on some rather ambiguous and indistinguishable assumptions. Even though a lot of time and resources are invested in understanding the process and associated materials, especially related to protective layers with several thicknesses, it has been studied without considerably looking at the behaviour of the materials during processing. Large parameter studies or data-mining in combination with statistical analyses were employed to find material-process connections.

Given all the different parameters that should be included, only 2-D models of the HSRW process written in commercial codes appear to exist. Even though modelling the process is very difficult, it provides a great deal of useful information, otherwise unattainable form experimental studies. Both commercial and in-house codes are numerical approximations by which an exact answer is most probably not possible and requires validation by experimental studies.

To accomplish an optimisation in the process and material in the future, understanding on a more profound basis with the use of different process conditions is reached by focussing on the metallurgical and physical alterations around the weld interface line.

Contents

1 Introduction

Aerosol and food can manufacture is characterised by the use of high-speed resistance (mash seam) welding (HSRW). This industrial application for fabricating the body of three-piece cans uses Double Reduced (DR) tinplate-packaging steel material. The body of the can is made from a rectangular piece of tinplate, formed into a cylinder and welded. Even though high-speed resistance welding is an apparently well established and understood production method for packaging aerosols, food and general line cans, the actual process is rather complex, involving aspects of many different scientific phenomena, which occur simultaneously. A good quality weld consists of intermittently repeated overlapping weld nuggets, which create a continuous solid-state bond along the total height of the can body. Three-piece can manufacture implies that the containers are made from the seam welded can body, followed by insertion and double seaming of the two end caps.

In order to ensure good weldability with high quality joints a welding parameter range is defined, within which the materials are welded. The welding parameter range is bounded by a lower limit, above which good mechanical behaviour is established and an upper limit, below which no material ejection (formation of splash) is encountered.

Despite the simple principles of the HSRW process, there are a lot of limitations and unrecognisable phenomena occurring in this process. The relationships of many of these phenomena to each other or to the welding process are not yet clearly understood.

Worldwide, welded steel containers represent the most predominant form of packaging for human and pet food products; approximately 90% of the world’s food cans are three-piece containers. Occasionally, in Asia, three-piece cans are even used for beer and beverage markets due to the quality control required for drawn and wall-ironed (DWI) cans. Although high-speed resistance welding can achieve speeds of 1.2 m/s there is an extra demand on the process potentials and product performance to utilise this to its optimum, therefore a more profound understanding of the welding procedure itself is required (i.e. a link between the process parameters, thermal-mechanical history and microstructural phenomena, and thereby a definitively based understanding of joining under different process conditions (i.e. current, force, speed, etc.) with associated material features.

This literature review is written to describe the present state of knowledge in the process of three-piece can manufacture. In this way, contribution to the incomplete research on the materials tin layer and microstructural development during the joining process can be better guaranteed. The goal of the unfinished research, besides generating a definitive understanding of the welding

process, is focused on joining under different process conditions and with material conditions in order to optimise the joining process, whilst gaining knowledge on the formation of the welds, which finally forms a basis for material development in the future. An understanding of the weld formation can also open up new ways to enlarge the working window of the welding process. In particular, when appropriate adjustments can be made to chemical composition, microstructure, metallic coating type and/or thickness, it might be possible to bring down the lower limit of the welding current range. Of most interest for the steel supplier and can manufacturer would be the idea of making difficult to weld materials weldable by widening the operating window to an acceptable level, but also to make increasingly complicated commodity can shapes, after welding. Even for easily weldable materials, for which there are no direct necessities to alter the weld range in terms of process control, energy savings can be made by can manufacturers to run at lower currents, and with higher safety margins. In the end not only industry, but also the end-users or consumers will benefit.

In dealing with these issues, the following aspect will be considered:

- How did the high-speed resistance mash seam welding process develop and what is the relation to other container processes?
- What is the relation of the welding process to the up and downstream processes in three-piece can manufacture?
- What are the high-speed resistance mash seam welding process characteristics and what is their mutual relation?
- What is the effect of the welding process on the materials employed?
- What is done on the modelling side to understand the HSRW process?

These questions are addressed by means of reviewing the high-speed resistance mash seam welding history and competitive processes in can manufacture, three-piece can manufacture from start to end, and examining process details, such as weld quality/weldability, welding parameters, material factors and standards and the influence of the joining process on the materials. The review is based on different literature resources ranging from tinplate and tinplate container manufacturers to researchers and educational books as well as material data references.

The process of resistance mash seam welding at high speed is, in principle, well understood and easy to explain. First, two pieces of sheet are brought into an overlap contact after which they are fed through two electrode wheels. The main process parameters that contribute to the quality of the joint are electrode force, alternating current (AC) through the electrodes and sheets, the speed

of sheet passage between the electrode wheels and the total of the material overlap. Because of the contact resistance between the two overlapping sheets, heat is generated between the sheets, which are then mashed, and supported by enough heat generation, joined as shown in figure 1.1. Mashing involves deformation of the material to forge the sheets together.

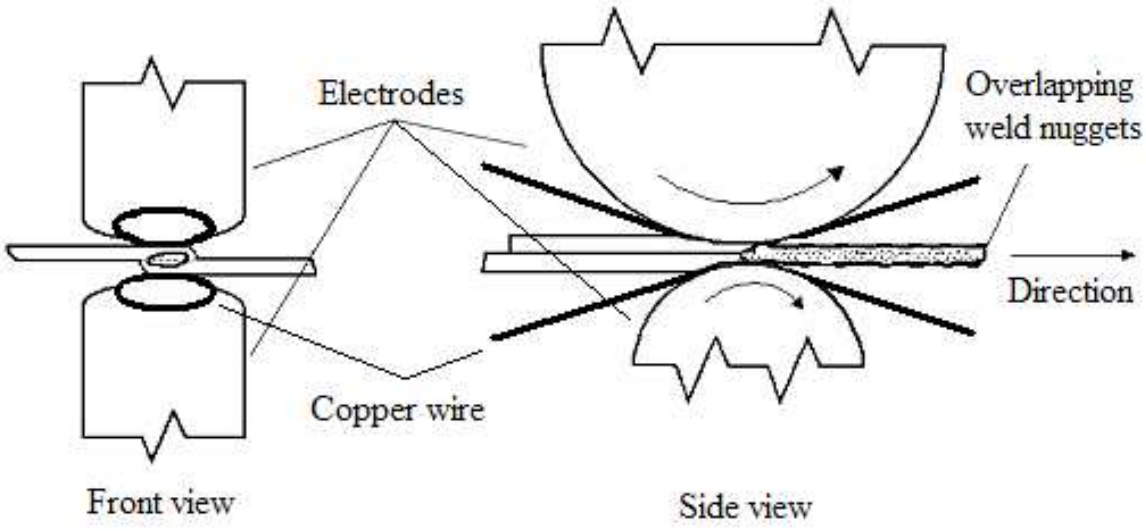

Figure 1.1: Schematic of resistance mash seam welding with on the left–hand side a front view and on the right–hand side a side view. The radii of the copper electrode wheels are different in size for the various can diameters and a copper wire moves between the electrode wheels and sheet material to prevent problems of electrode contamination and degradation.

The process involves semi-continuous sequential welds or weld nuggets to produce a solid–state, gas tight weld seam. In present day production, speeds between 80 and 115 m/min (1.3 to 1.9 m/s) are achieved (typically some 750 cans/min) without the need of any pre-treatment and with generally small material overlap distances, being in the order of 0.4 to 0.6 mm. During mash seam welding, the lap forges down to produce a total joint thickness typically 1.1 to 1.4 times the original sheet thickness. Thickness strains in the order of 30 to 50 % are applied to the joint, which is unsatisfactory for cold pressure bonding and therefore welds are primarily formed due to thermal processes in which strains on the sheet surface play an important role. The successive weld nuggets are made with current oscillation frequencies ranging from 200 to 1000 Hz. An electrode wire-feeding system is used to overcome problems of electrode degradation, the wire being placed between the electrodes and the sheet material to be welded [1 to 6].

In the process the tinplate is exposed to thermal histories in which various physical and chemical alterations take place, which determine the final properties of the joint. Generally, the demands on these properties are considerable, especially in a high quality products, such as

commodity-shaped and aerosol containers. Diffusion, recrystallisation, recovery, precipitation and dissolution are all influenced by thermal history of the joint (formation). In general, material properties can be improved by welding with higher currents, leading to greater peak temperatures, and lower welding speeds, resulting in longer times at elevated temperatures [7]. Each parameter variation indicates an alteration in the temperature gradients and heat balance across the resistively heated overlapping sheets and therefore different associated temperature cycles, final shapes (i.e. more or less deformation) and microstructures.

Heating of the sheets is also affected by the use of the differently sized copper electrode wheels (see figure 1.1). A smaller contact area of the smaller electrode wheel (i.e. at the inside of the can body cylinder) introduces a higher current density than the larger electrode wheel. Consequently, more heat generates at the side where the sheets pass the smaller electrode wheel. As an example figure 1.2 shows a final weld seam shape and associated metallurgical features taken parallel to the welding direction in the centre of the weld seam [1, 2, 8 and 34].

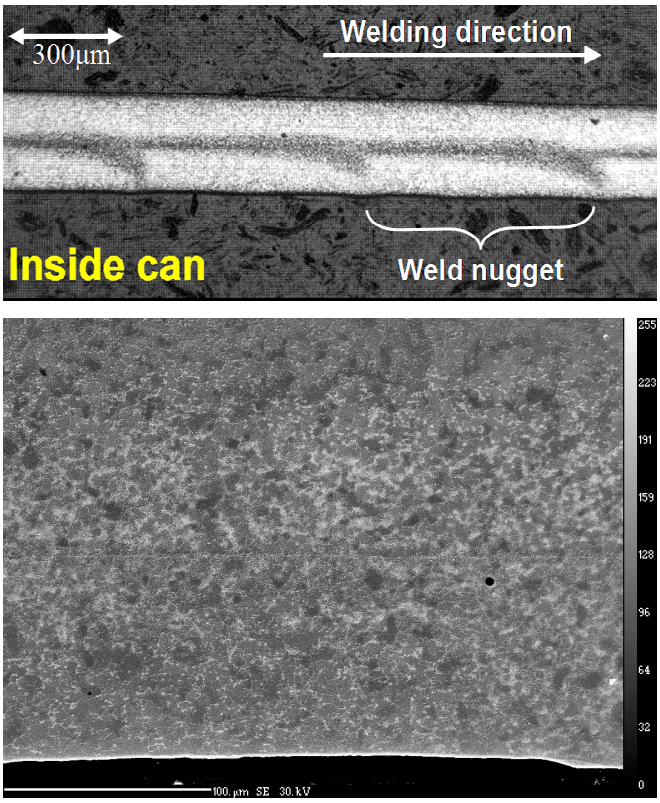

Figure 1.2: Images of two weld seam samples, intersected in the middle of the welds parallel to the welding direction. The top picture shows the shape of some weld nuggets and their associated heat pattern, whereby the darker regions indicate a higher temperature. The bottom picture shows the related microstructures. In both pictures, the side of the smaller electrode wheel was positioned at the bottom. The sample on top was etched with a picral solution to make the heat patterns visible, whilst the bottom sample was etched with a 2% nital solution for five seconds to show the microstructure. The distance scales are 300 and 100 µm for the top and bottom picture respectively [1].

A welding current establishes the welding current range used for acceptable welding (i.e. weldability). This welding operating window or weldability range comprises a lower and upper welding limit. The lower limit is determined by a mechanical tear test of the weld, by which no cold welds may form. Cold welding gives an indication that the weld has not been sufficiently warm to produce a mechanically adequate weld. The upper limit is determined by visual detection of formation of splash, which involves

metal particle ejection from the welded seam edges. The welding current range is a mapping of the current (i.e. temperature) and mostly one other main governing welding factor or parameter (e.g. welding speed, weld nugget length, electrode force, etc). Figure 1.3 gives an illustration of a weld range, associated with images of a cold and hot weld. A good weld quality is reflected by means of the weld properties or metallographic features such as grain type, size, etc.

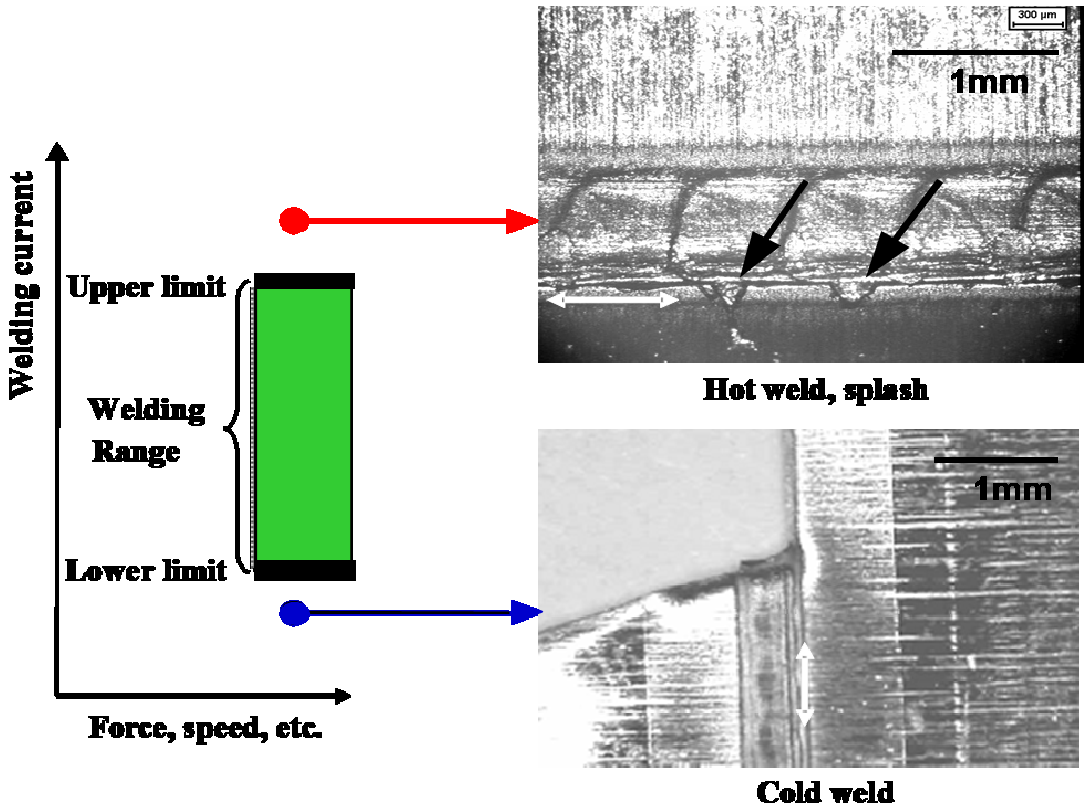

Figure 1.3 The left-hand side shows a schematic of the weld range and its associated welding operating window or welding latitude. On the right-hand side, the top picture shows an enlargement of an overheated or hot weld. Here, the arrows indicate the splashes; the welding direction is from right to left. The bottom picture shows a cold weld, which is broken by the tear test. In both pictures, the white arrows indicate the length of a weld nugget and the distance scales are 1 mm.

2 History & can manufacture processes

The usage of welded cans started to grow rapidly after the Second World War, replacing soldered tinplate can manufacture. The reason for this was to decrease the human lead intake from food, lead being present in the soldered side seams. As a reaction to the disappearing soldered cans, the alternative of welded cans was forced into the market and needed to fulfil the needs of can manufacturers and consumers, yet keep the desired output capacities.

The welding process compared to soldering, has a lot of other distinct advantages, such as speed and strength. First, typical welding machines, as made by the Swiss firm, Soudronic AG, provide flexibility with respect to can height and diameter changes. Secondly, the can body will consistently fail before a weld seam provided a seam of good integrity. Furthermore, a welded seam is lead free and uses less material; as typically, 0.5 mm material overlap width is required in contrast to the 5 mm for a soldered seam can. The narrow margin required in a welded seam also offers a wider scope for designs than soldered seams. Moreover, to provide the strength necessary for the axial and radial loading, the can walls are beaded (i.e. surface ripples are introduced), which is more difficult with soldered cans. The use and production process waste products, and the tinplate cans are easily recycled making welding an environmentally sound process for such a large volume-packaging product. As a result welding took over as the preferred production technique for three-piece can manufacture with food, aerosol and general line containers.

During the growth period of the welding process (1960s and 1970s) and over the years afterwards, different three-piece welded can manufacturing processes were developed, of which only a few found commercial acceptance. In America, the so-called Conoweld process was successfully developed for semi high-speed manufacture of tin-free steel (TFS) and hard coated containers. However, in Europe the emphasis was placed on manufacturing a wide range of tinplate containers, which was a remaining concept from traditional soldered cans and took advantage of the accumulated knowledge and experience in the use of tinplate-packaging applications over the past decades. Europe converted quickly and completely to a welded side seam for cans, and standardised cans and the production process found acceptance.

In the mid and late 1970s two-piece can manufacture started to grow in the European can industry in competition with the three-piece welding process, and in the early 1980s two-piece can manufacturing was adopted. For a two-piece can, a round metal blank, either steel or aluminium is stamped from a large piece of single reduced (SR) tinplate (i.e. temper rolled). From this, increasing degrees of cupping take place until a suitable wall is formed. The wall is ironed to the desired height (i.e. drawn and wall-ironed) and filled with the product, which is in the most

cases, are carbonated beverages. Today, two-piece can manufacture rivals three-piece can manufacture, because it eliminates the difficult to make small height can when welding, and reduces sterilisation times, giving better product qualities. It also needs less attention afterwards (e.g. better deformation behaviour, no weak spot corrosion) and harder; better adhering lacquers can be applied with higher cure temperatures. Furthermore, the material cost savings (thickness reduction) whilst still lending rigidity and the absence of a seam on the can make it an attractive rival.

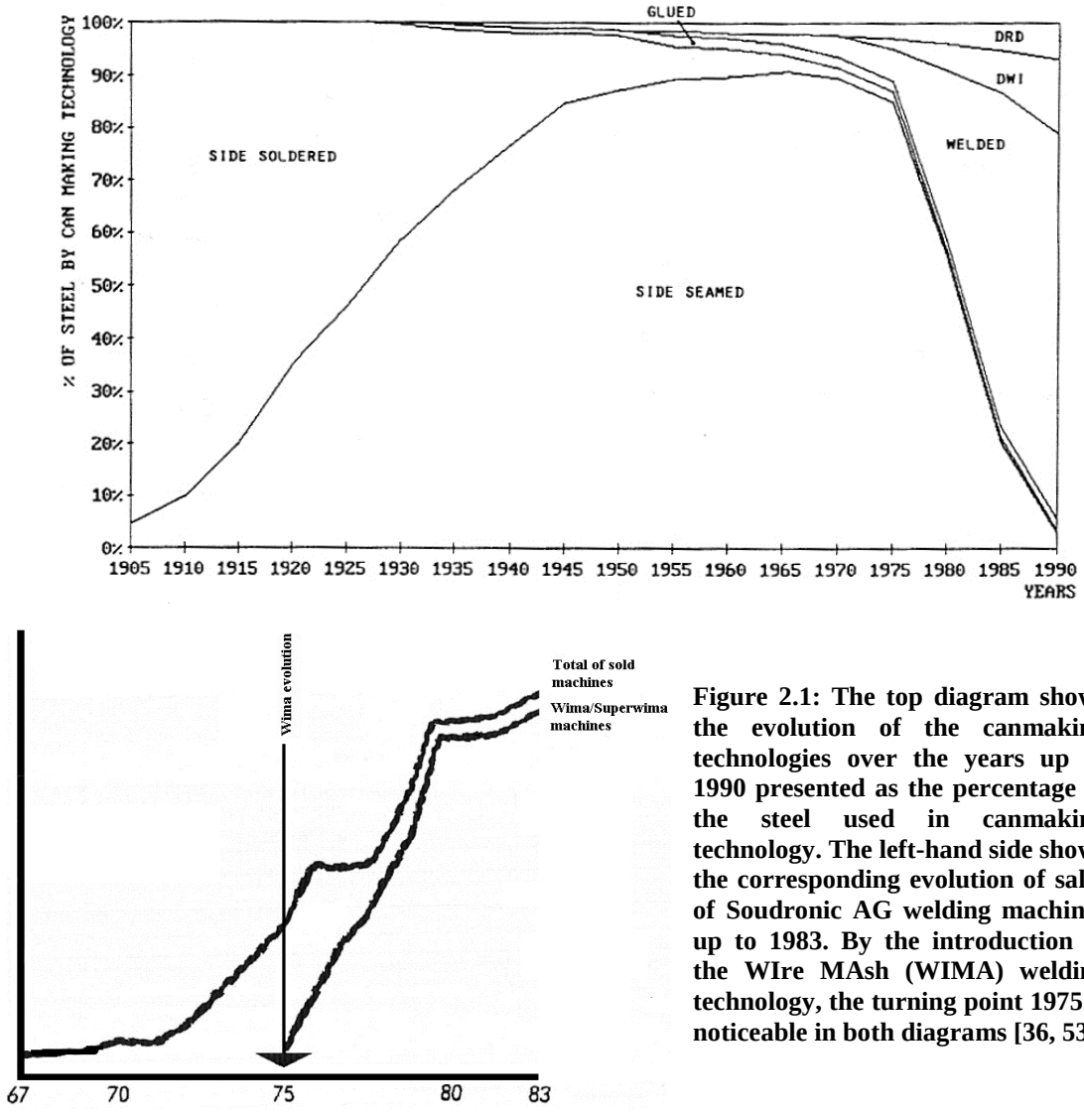

Figure 2.1: The top diagram shows the evolution of the canmaking technologies over the years up to 1990 presented as the percentage of the steel used in canmaking technology. The left-hand side shows the corresponding evolution of sales of Soudronic AG welding machines up to 1983. By the introduction of the WIre MAsh (WIMA) welding technology, the turning point 1975 is noticeable in both diagrams [36, 53].

In manufacturing three-piece tinplate containers, the extra requirement of a strong and airtight sealed seam is necessary. Besides welding and soldering, the use of special adhesives could be a

way of achieving such a tight seal. Nevertheless, the welding process, because of technical and commercial advantages, quickly overshadowed these other processes as shown in the diagrams of figure 2.1. The figure shows that the evolution in welding corresponds with a similar development in the sales of the welding machines. In the literature, the process of side seamed packaging containers is hardly mentioned. However it was replaced by welding because welding is faster and produces a stronger and leak proof seam. In side seaming the seam is purely a mechanical closure of the containers [3 to 5, 9 and 10].

2.1 Welding technologies of the three-piece can

2.1.1 Wire welding

For three-piece can manufacture, the resistance welding principal is based on a wire-feeding system to overcome electrode contamination and degradation during welding. This welding principal has a long history and is predominantly developed and still owned by one welding equipment manufacturer, Soudronic AG in Berdietkon, Switzerland. It is for this reason that the process is commonly named Soudronic welding. Can welding from the Soudronic point of view has evolved from a simple to a rather complex process in which today the small material overlaps create a solid-state continuous bond along the total can body height, consisting solely of repeating sequential-overlapping weld nuggets.

Around the early 1950s, the first wire welding principle called a butterfly or fully overlapped weld came into existence, as is schematically shown at the top of figure 2.2. The welds are named after their appearance. In the butterfly welding process can blanks with edge overlaps of 2.0 to 4.0 mm were required creating a weld nugget which only occupies a quarter of the overlapped area. The non-welded parts in the overlap were difficult to protect from internal crevices and corrosion, which was undesirable due to unsatisfactorily sealing with corrosion protective lacquers in food and drink containers. However, because of a wire-electrode feeding system the process was suitable for tinplate welding without the need of edge grinding and was typically used in hand feeding production, i.e. large volumes of pails, drums and other non-food specialty containers.

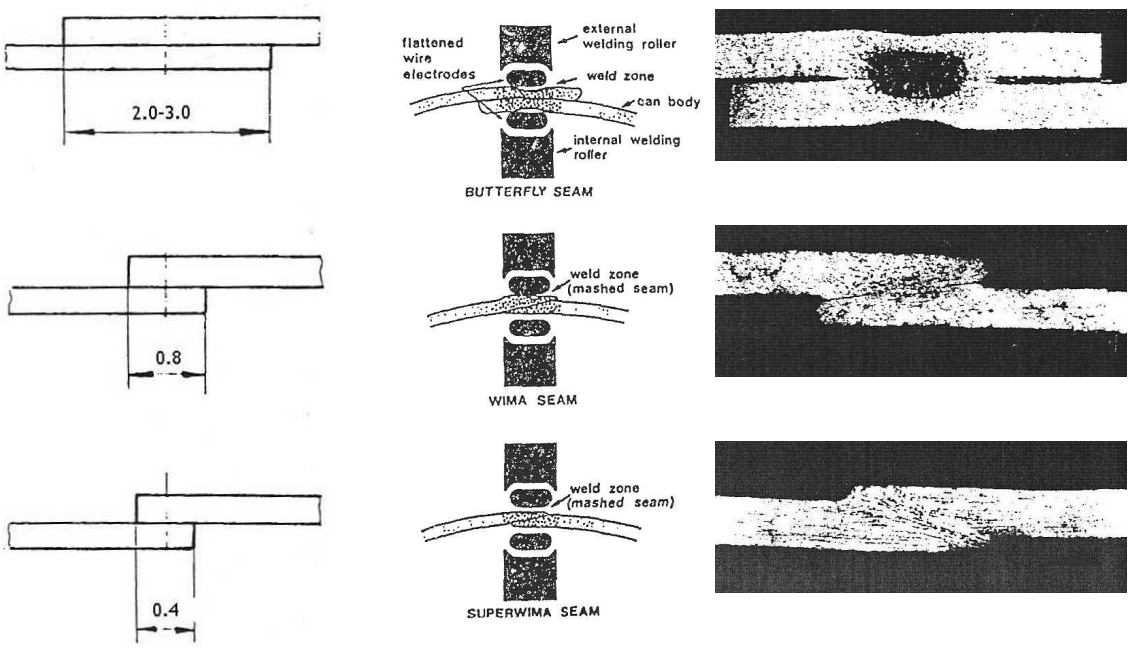

Figure 2.2: Historical developments of resistance wire welding. From top to bottom the butterfly, WIMA and super-WIMA welding principles are schematically shown. On the right-hand side associated photographs of the weld appearances are shown [6, 9 and 11].

The poor corrosion properties, the needs for higher production speeds and better material formability over the following years led to radical improvements in the mid 1970s. The next step in the line of the wire welding process evolution is called WIre MAsh (WIMA) welding. Mash meaning that the material is (highly) deformed and forged to join the materials together. The WIMA weld (see the centre features of figure 2.2) extended over the entire can blank overlap of 0.5 to 0.8 mm. The smaller overlap permitted welding speeds of up to 50 m/min making it possible to use tinplate for almost all beverage and food container applications. However, one side effect of this development is the considerably smaller tolerances it brought about on the process parameters.

The desire for reaching higher speeds and narrower overlaps led to the latest development step in resistance wire welding, super-WIMA welding. The super-WIMA weld (see the bottom features in figure 2.2) developed in the late 1970s. As with the former development it uses a material overlap, only smaller, typically 0.4 to 0.5 mm, and welding speeds of 80 to 115 m/min (1.3 m/s to 1.9 m/s) are not exceptional. However, the super-WIMA welding process further intensified the problems of process parameter tolerances and raised questions about mechanical and physical tinplate property variations that might affect the weld quality. Today, the super-

WIMA welding process is mainly used for aerosol and food can manufacture, within which weld seams need to be highly accurate, airtight and leak and pressure proof [3 to 5 and 9].

2.1.2 Edge grinding

The edge grinding process is based on the principle of surface cleaning the can blank edges before welding in order to avoid any electrode contamination and degradation. Although this welding principal did not prevail, it is important because the idea of surface cleaning has and still is being used in innovations on the existing container welding processes. As with the wire welding method, edge grinding before welding was predominantly developed by one manufacturer, Conoweld and therefore named Conoweld welding. As with Soudronic welding, the Conoweld welding process forms a continuous solid phase bond with sequential overlapping weld nuggets over the entire can body height.

From the 1950s to the beginning of the 1970s, the edge grinding process was a popular resistance welding process; it replaced the soldering processes and competed with the Soudronic process. In the edge grinding process, careful and complete automated mechanical removal of the steel blanks top, 1 to 2 µm and outer blank sides, 2.0 to 3.0 mm, was accomplished by machine grinding immediately before welding. This was done because of the large electrical resistance some top coatings or layers (e.g. chromium or iron oxide layers) cause, inducing poor weld operating windows and consequently poor weld qualities. Therefore, in the early years of solder replacement, factors such as coating hardness, weight, etc. made the edge grinding process competitive to wire welding.

However, because of the extra sensitive step in the line of production, the rate of production became slower than with the wire welding process, typically less than 50 m/min. Today, hard-coated containers (e.g. chromium coated) are lacquered after the welding process to make production more effective and faster, making edge grinding redundant [9 to 12].

2.1.3 Laser welding

The laser welding process is principally different from the resistance welding processes above. Laser welding of can bodies produces a fusion butt weld (see figure 2.3) instead of a solid-state overlap weld. Laser welding of cylinders is an innovative impending container making process that found its origin in the late 1980s. The idea came from tailored blank production, used in car manufacture, within which resistance and laser welding were already competitive processes from the early 1960s. Today laser welding is still a hot issue, and is of increasing interest as an alternative to resistance can welding. This is because of its technical advantages; better quality

performance with narrower welds and wider process and material operating windows with the same or even higher production speeds [13 to 19].

Figure 2.3: Schematic representation of the laser welding principle on the left-hand side with on the right-hand side an associated photomicrograph of a laser weld appearance [11 and 15].

The laser welding technique uses focused light from a high-energy laser beam. The high-energy laser in combination with the absorptiveness of the steel makes the edges of the steel blanks melt. When the melted edges of the cylinder are brought into close contact the metal can solidify and produce a strong fully connecting seam (see figure 2.3). Laser welding produces a very narrow weld area of 0.25 to 0.3 mm with only 5 to 20 % penetration into the can base material. The weld area because of the high cooling rates is stronger than the base material. In this way only a very narrow strip of the steel base is affected by the heat, which minimises unwanted mechanical property changes. The produced heat-affected zone (HAZ) is narrower than with resistance welding, also giving enhanced mechanical properties [13 and 14]. The heat affected zone is the base material microstructure immediately adjacent to the fused material, not molten but transformed by the temperature effects in this area.

In the literature [13, 17 and 18] it is found that several container and welding machine manufacturers have been operating can-lines with laser-welding machines for some time, to assess the outcome of this process. In the tests the laser beam was not switched on and off between the cans, but deflected into a copper heat sink to reduce time-feeding problems to maintain production speed and to keep a stable and focused heat input on the can bodies. After welding, the cans were guided through rollers to smooth (i.e. planish) the seam before downstream container completion.

According to some tests, differently produced tinplate steels with various tin coating masses and other, also harder coatings and lacquers can be welded with a high quality. Uchihara and Fukui [18] say that the reason for this is found in lacquers that are burned off before fusion occurs.

However, the process should have an applied gaseous shield to prevent oxidation of the material. It was also said by Schmitz et al [19] that in laser welding the only significant parameter is the sheet thickness, not the nature of the metallic coating that thereby offers attractive potentials for the joining of steel cans with outstanding metallic protections. However, Saito et al [13] stated that when coatings are too thick or have a high absorptive capacity, they could dissolve into the weld and create poor weld qualities (i.e. mechanical behaviour).

The advantage of laser welding is the minimisation of thermal damage to the coating and substrate and good formability and deformation properties after welding, ensuring an excellent cosmetic appearance and making the welds directly suitable for downstream lacquering. In addition, laser welding is the best welding process from a formability viewpoint because of the small heat input. As a result superior weld fatigue and forming operations compared to resistance overlap welds are achieved. The hardening degree of the material is governed by the cooling rate and carbon content and hence the use of low-carbon steels are a good way to increase the speed in laser welding whilst keeping the hardening degree constant [14 and 15].

Additionally, in all the research reported limitations on the process speed were found. Speeds of 20 m/min were easily achieved and even 30 to 35 m/min are reported whilst obtaining a satisfactory or good quality weld. When increasing the speeds above 35 m/min it was found that weld profiles start to ripple along the weld seam and blank edges started to loose material. It was concluded that the weld pool could not keep up with the weld speed. Sharp et al [17] said that in gaining faster weld speeds and better quality the use of pulsing techniques should be employed. In addition, in their long duration trials, pulsing techniques had eliminated undesirable metallurgical effects [13 and 18].

Beside the weld pool and speed problems, there is another crucial factor that is highlighted in the experiments, material guidance and geometry. Because the laser beam is a very narrow spot, it should be maintained around 0.1 mm from the centreline, leaving little space for movement or geometry errors. For instance clearance at the blank edges may only be a few percent because lack of penetration can give rise to incomplete bonding. However, as the leading and trailing ends of a can have a notch, there is no problem as long as the notch is not too long and does not propagate. In this case the notch is sealed off in the downstream container completion. The only defects of consequence, and which are more likely to occur, are the centreline cracks or defects as a result of steel plate inclusions [13 and 17].

As far is currently known, research on high-speed laser welding containers is still developing, predominantly to reach higher production speeds.

2.2 Two-piece can manufacture

For manufacturing seamless or two-piece cans there are two deep-drawing operations available:

- Drawn and Redrawn (DRD)
- Drawn and Wall-Ironed (DWI)

The DRD and DWI processes differ significantly despite the fact that deep drawing is the main forming operation involved in both processes. The formation of a can via one of the processes is a relation between material thickness and the limiting drawing ratio (LDR) (i.e. the can height/diameter ratio). This ratio is also strongly influenced by lubrication, lacquering and other material factors (e.g. texture). In for instance the DWI process peak loads with ironing decrease when tin coating levels are increased. [20 to 23]

In the DRD process cans are made by a series of press operations, the number determined by material type and LDR whilst the machined wall-thickness is nearly equal to the original material thickness. In the DRD process, different presses with smaller diameters are used to come to a final height/diameter ratio of the can (see figure 2.4).

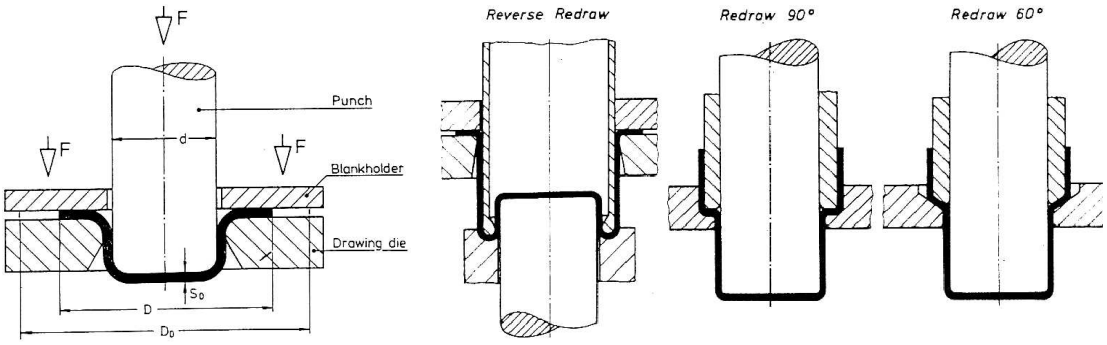

Figure 2.4: Schematic presentation of the drawn and redrawn process with on the left-hand side the first drawn step and on the right-hand side three different versions of a redrawn step. In all process steps, the wall-thickness is steady [20 and 23].

In the process the sheets are pre-lacquered to assists in fabrication (i.e. act as lubricant) whilst maintaining process (e.g. cohesion) and afterwards product (e.g. corrosion) resistance. The process is called clean, because washing after the process is not needed [20 and 21].

For many years shallow deep-drawn pre-lacquered cans and multiple deep-drawing post-lacquered aerosols were familiar in two-piece can manufacture. The two-piece can operations were used in small heights cans because it eliminated the more difficult to make soldered and welded side seams and because it reduced heating times with sterilisation operations, giving

better product qualities. On the other hand frequently encountered disadvantageous effects where seen. These involve damage due to lacquer abrasion by the tools leading to damage of the corrosive protection layer if not immediately cleaned and unavoidable sulphide staining at the drawn can walls.

By contrast, the DWI process does not require a pre-lacquered material. Several dies iron the material after a cup deep-drawing operation and, possibly also a re-drawing operation (see figure 2.5). The can is drawn from tinplate, because of favourable tin lubricating characteristics. The height of the can is achieved by drawing and ironing, not by multiple deep-drawing steps. Because this process involves high deformation strains and forces, several other lubricants can be used. In contrast to the DRD process, containers need to be washed and lacquered after forming [20, 21 and 23].

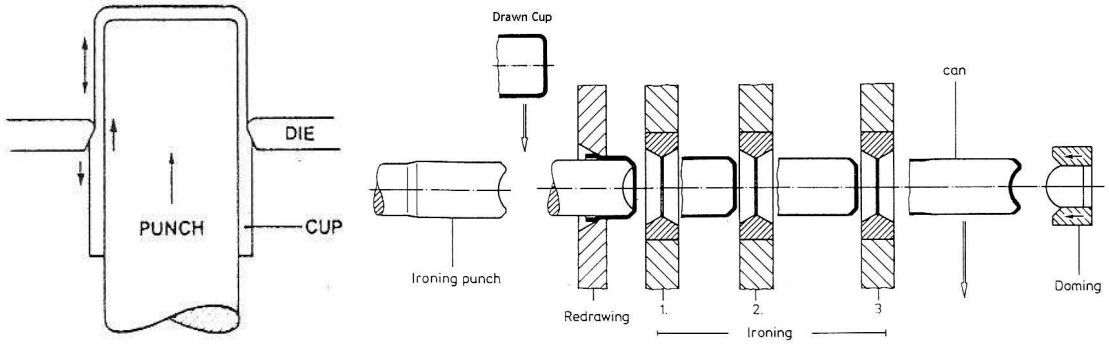

Figure 2.5: Schematic presentation of the DWI process with on the left the principal of height stretching and wall thickness reducing, and on the right the actual production in a DWI machine [21 and 23].

Without the weld seam, there is less attention required when the can is further processed and it is easier to come to a number of products. One reason for this is that there is a difference in the deformation behaviour of the weld seam, i.e. heat-treated and deformed material. Secondly, corrosion on the seam, which may represent a weak spot, is not present anymore and furthermore unattractive appearances in the can design are eliminated when no seam is present on the can body. The DWI can making processes also has the advantage of using harder better adhering lacquers that may be cured at higher temperatures through which satisfactory lacquered two-piece cans also keep the tastes of products better. The result of the wall thickness reduction, especially in double reduced materials, is the material cost savings in comparison to the three-piece can whilst still lending rigidity. This led to its use in the beer and beverage sector because, from a

practical point of view, the inside pressure holds the can rigid, with smaller wall thicknesses [18, 20 and 21].

If the deep-drawing processes were applied to the production of cans, which incorporate vacuum loads, i.e. outside pressures and reduced inside pressures (e.g. food containers), thicker walls, are required. Thicker walls make the deep-drawing processes more difficult because of the larger height/diameter ratios and associated problems with pre- and non-lacquered materials [20 and 21].

Over the years material and lacquer properties together with, shape design have developed, and both two-piece manufacture processes have compensated for their problems. Hence the use of deep-drawn processes, standardised containers and complicated commodity container designs are possible to meet the required properties whilst achieving considerable production rates.

2.3 Market and can manufacture

As described above the history and associated technical developments have a great influence on the resistance can welding technology today. However, the driving force behind these developments are greatly if not totally controlled by what is happening in the can manufacture markets.

It has been shown that the soldered side seam can manufacture converted quickly and almost completely to the welded side seam can. This was induced by the fact that lead intake had to be reduced. Although in America resistance can welding led to the development of the edge grinding process, Europe’s emphasis was on a wide range and tinplate container manufacturing took the lead in producing large quantities of standardised welded cans. Additionally, can welding better fulfils the needs of can manufacturers and consumers, such as enhanced can size flexibility, minimal costs, available materials, higher production speeds and automation of the commodity can manufacture. In relation, developments in the production of food, aerosol and general line containers pushed ahead by changing-over from butterfly to WIMA and later super-WIMA welding, characterised by high production speeds with low production costs, making resistance can welding a great success. These developments stemed from the traditional soldered container concept and are based on the accumulated knowledge and experience in the use of tinplate-packaging applications in the past decades.

Comparatively, the Conoweld process, initially used for beverage cans was quickly overshadowed by the DWI process in the aluminium industry because of better designs (i.e. no seam) and achieving significant material cost savings whilst still lending excellent can properties.

Secondly, the wire welding process with continuously increasing production rates lead the container welding market, pushing the Conoweld process aside.

Beverage cans that were introduced in Europe were immediately and only produced via deep-drawing operations, the two-piece can manufacture became commercially accepted, standardised and over the years more and more competitive with the three-piece can manufacture.

Today, three-piece can manufacture still holds a large share of the can market sector for aerosol, food, and general line containers. However, the DWI processes are also used for aerosol, food and speciality can applications. In Europe, deep drawing started off in the early twentieth century in the pet food canning industry in England because of the low height cans it produces. However, larger cans were predominantly soldered and because the aluminium industry, mainly in America, produced DWI cans, it was an opportunity to establish two-piece containers in Europe where a tinplate three-piece container dominated the market. Starting in the 1970s two-piece can manufacturing started to grow in the European can industry in competition with the three-piece container, but with tinplate rather then aluminium because of Europe's history and the tinplate availability. Today, the DRD process is still used for parts of the markets involving small heights or special dimension cans.

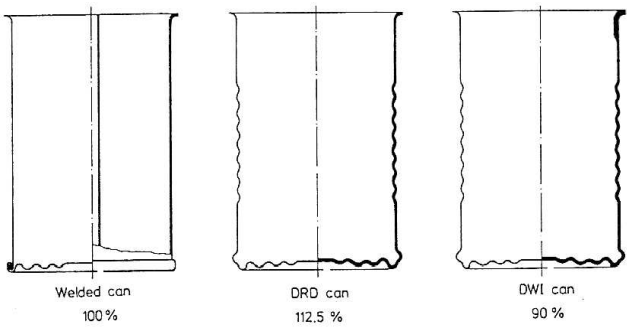

Figure 2.6: Schematic overview of the different can cross-sections with the relative costs displayed below the cans [22.].

When comparing the cans relative costs as schematically shown in figure 2.6 it seems distinctive that the market stays balanced between the two processes. The reason for this is probably found in capital investment costs, in which not only can height or material weight, but also the number of cans and can size is of importance in choosing the manufacturing process. The market and its strategic factors, place continuing significant demands on the packaging industry, requiring constant response and resulting in improved process and material requirements [10, 11, 22, 24 and 25].

During the technical developments, downscaling the can gauges for tinplate became a driver imposed by the can manufacturers because of the material weight or costs savings. Eventually limits of 0.10 to 0.12 mm and 0.13 to 0.15 mm where reached for respectively deep-drawn cans and welded cans. Today, these production limits are not used in mass production, because of failure risks in combination with increasing forming demands involved in producing the cans.

In can welding manufacture, future steps are found in several fields. First, can manufacturers in cooperation with steel suppliers are trying to search for a way to weld without any necessity of

edge grinding or the use of wire-feeding systems whilst still achieving sound and deformable can bodies. Secondly between all the processes that currently operate, can manufacturers are also trying to achieve process optimisations (e.g. copper-wire configurations). In these ways adjustments on the can manufacture lines are minimised whilst costs are reduced and production rates are increased. Because of the optimisations, a constant increase in the complexity takes place and canmaking becomes more and more engineering rather than a manufacturing problem and hence the optimising rigidity is stagnating even larger innovations, such as laser welding. [10, 11, 24 and 25]

Nevertheless, laser welding is developing for the manufacture of three-piece cans, but because it is not yet able to compete with the present three and two-piece can production speeds and manufacturing technologies, it has yet not found commercial acceptance. Despite this, the technique has better quality performance with narrower welds; better process operating windows with equal production speeds, and uses less energy than with a dispensed copper wire-feeding system.

3 Can-line production sequence

Welding or body seaming containers is a process step with major influence in three-piece can manufacture. Before and after welding, limitations and restrictions such as yield strength, Young's modulus and coating layer specification influence what is happening to the can body material and its properties in the final product. Although welding is a major influencing process step, the process of making three-piece cans consist mainly of forming operations. The can-line production sequence is constructed by:

1. Lithography and cutting roll-sheets into can body blanks
2. Forming individual blanks into can bodies
3. Closing and joining to form can bodies
4. (Heat treating or forming weld seam)
5. Lacquering and curing can bodies
6. Flanging and beading can bodies
7. Lock seaming the bottom, filling and topping can bodies
8. Sterilising and packing containers

The fourth process step is not performed at all times, depending on quality requirements and usage of the produced containers. The can-ends are produced by another production line to be seamed onto the can body in one of the last production steps in the can-line sequence. Within the production line, the following two operations largely influence the material choices:

1. Rounding or body forming of the can
2. Welding of the can body

The above-mentioned steps directly influence the entire container forming operation and necessary material alterations are only applied after checking the materials behaviour at the rounding and welding stages. Because the production of cans is a continuous production process, variation in steel grades needs to be kept to a minimum to ensure a stable and continuous production speed, which ensures that adaptation of the processing machines should be minimised.

3.1 Lithography and blanking

Before the steel sheets are slit into can body blanks, the coiled bare steel sheets (tinplate) from the steel manufacturers are unrolled and subjected to a painting process (i.e. lithography) for the outside appearance of the can body. When paint colours are applied, several layers could be applied depending on the design. Secondly, up to three protection layers can be applied to gain optimum protection properties between the paint and environment (i.e. corrosion).

The paint is applied in stripes on the sheet material and thereby sets the dimensions of the can blanks for subsequent slitting and welding as shown schematically in figure 3.1. The non-painted strips are necessary for the welding operation. The rolling direction of the material is also labelled because this also influences the welding and forming processes. The paint is spray-coated onto the tinplate and cured by moving the material trough a furnace. Alternatively, the paint can be dried and hardened by a ultra-violet light source, which is faster and provides better and harder protective layers.

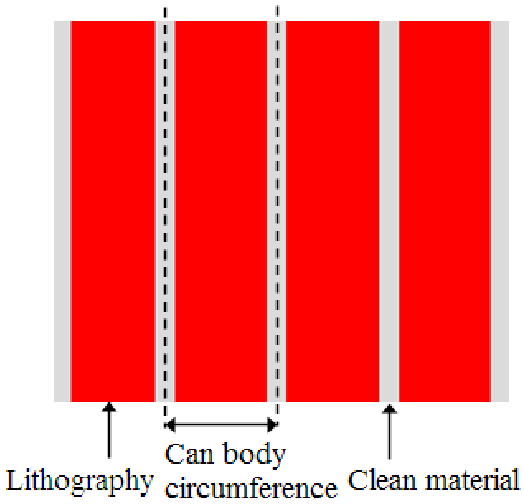

Figure 3.1: Schematic of the packaging-material after the outside design is applied. The dashed lines indicate the cutting outline. The clean material indicates unpainted tinplate.

After the lithographic process, shearing and stacking of the large uncoiled sheet into square plates with a size of 950 mm x 950 mm (dependant on the container end dimensions) is performed. The sheets are unloaded into an automated cutting machine; also called a slitter, to cut the sheets into can body blanks. The slitter determines the size of the can blanks with accuracies of around 0.05 mm. The initial can blanks have a dimension of for example 75.2 x 165.2 mm. First, the larger tinplates are guillotine–cut into long strips of 75.2 mm wide, after which the strips are roll-cut to obtain the initial blanks with a width of 165.2 mm. The principle of the cutting operations is shown schematically in figure 3.2.

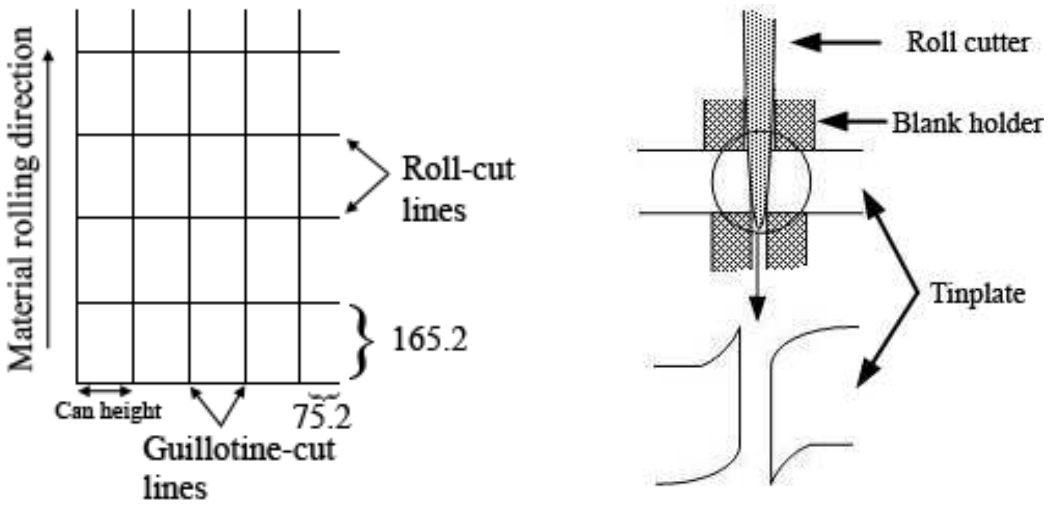

Figure 3.2: Principles of the cutting operation: on the left–hand side a schematic of the cutting scheme from the large 950 x 950 mm tinplates is shown for c-grain oriented containers, the sizes are in mm. The picture on the right–hand side shows the schematic of the roll-cut mechanism introducing sharp tips at the bottom or top of the blanks.

As a result, the dimensions of the blanks determine the height and diameter of the containers. After the blanks are cut, they are fed, all having the same orientation, into a hopper. The hopper is a part of the can body maker that extracts single can body blanks by a suction head and feeds them forward into a rounding or flexing unit. A sensor component operates a deflector to divert incorrectly and multiple fed can body blanks.

3.2 Roll-forming

For rounding of the can body blanks into can bodies, roll-forming operations need to be carried out. The reason for using roll-forming operations instead of bending operations is that roll-forming has the advantage of reacting better to material variations. At the rounding unit of the body maker, the can body blanks pass through a set of flexing rolls and steels to reduce the internal material stresses and to enable the formation of the can body cylinder as shown in figure 3.3.

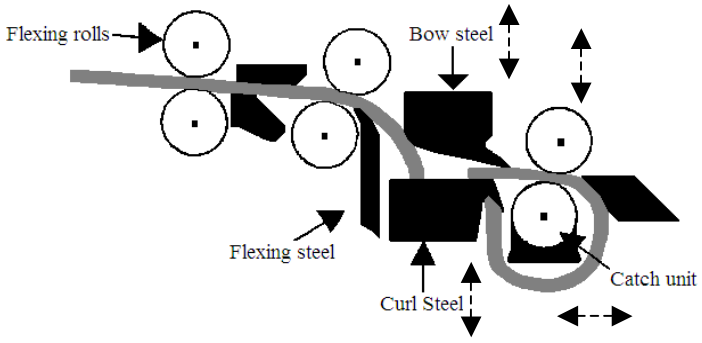

Figure 3.3: Schematic of the rounding unit within the body maker prior to welding. The picture shows the blanks being formed with flexing rolls and steels. The dashed arrows indicate the movement of the rolls and steels

The sharp tips created by the cutting machine are situated at the outside when roll-forming, as shown in figure 3.4. Consequently, during welding, the sharp tips are positioned at the electrode wheel sides and therefore smooth contact of the tinplate surface is achieved at the weld interface line. For research purposes this also gives the advantage to see the material extrusion (i.e. deformation measurement) at the weld seam edges [1].

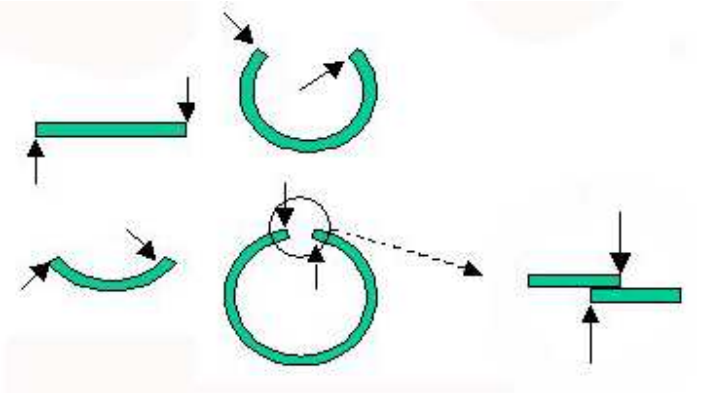

Figure 3.4: From top left to bottom right, the roll-forming process is shown in steps. In this way it is able to see where the sharp tips of the cutting operation finish up. The arrows indicate the sharp tips of the cut edges, which finally show up at the outside of the material overlap and are exposed to the electrodes.

For transport and actual welding of the can bodies, a suitable constant over-rounding/material overlap width, $B_{ü}$ is required. As a result, material property variations, without changing the settings of the body maker will lead to unwanted overlap variations. As shown in figure 3.5 the rounding operation depends completely on the materials yield point, R_{el}.

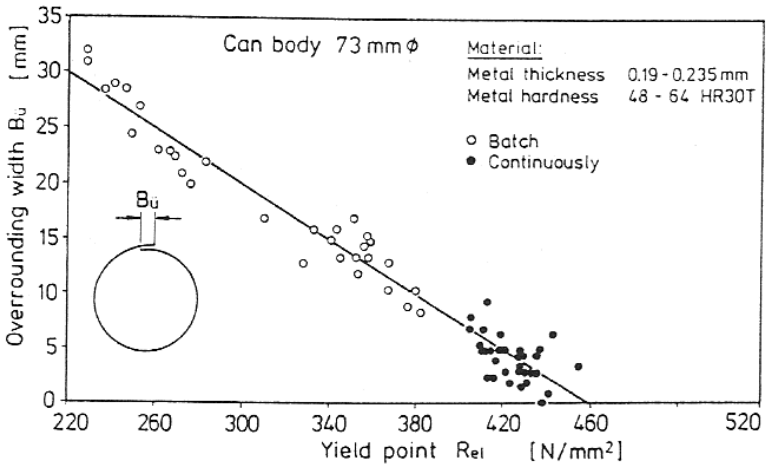

Figure 3.5: Rounding/material overlap width, $B_{Ü}$ behaviour for batch and continuously annealed tinplate experimentally found by [4].

Sodeik et al [4] found that the main significant rounding differences are found between batch and continuous annealed (BA and CA) steel sheet, because these processes give the largest difference in the yield point of the material. The large scatter will not overlap the material tolerances, as shown in figure 3.5. For this reason batch and continuous annealed material should not be mixed in one can production line. Apart from this, the figure also shows that a too large a difference in the yield point of different batch annealed material also creates negative overlaps in the material tolerances and hence should not be combined in one can production line. The practical results substantiated the theoretical

work by Gardner [26] using the springback test, and in essence indicate that the body size, metal strength and thickness can be integrated into the relationship:

$$\frac{R}{r} = 4\left(\frac{RS}{Et}\right)^3 - 3\left(\frac{RS}{Et}\right) + 1 \tag{3.1}$$

where R is the radius of the mandrel in [mm], r the radius after springback in [mm], S the yield strength in [MPa], E the Young's modulus in [MPa] and t the thickness in [mm].

Too large a difference in the material overlap, associated with excessive over- or under-curl of the rounding process, will also cause a block of the cylinders, by which proper feeding to the welding unit is halted. To minimise problems in rounding, tinplate with thicknesses and temper tolerances for one specific container production line should be welded in one batch.

As mentioned above the steel sheet rolling direction in relation to the can cylinder formation direction is also of particular importance as shown schematically in figure 3.6.

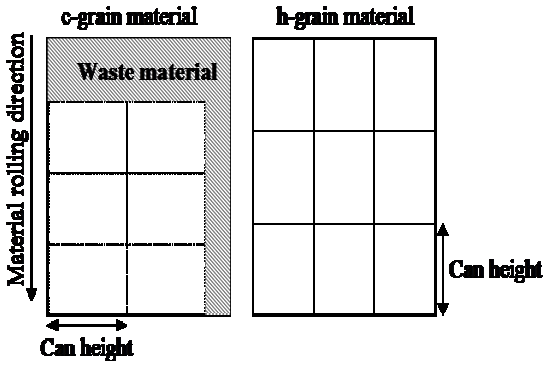

Figure 3.6: Schematic of the two different rolling direction in relation to the can body welding direction, C-grain on the left-hand side and H-grain on the right-hand side. The application of C-grain material imposes more waste material.

Elzinga [27] showed that too large a difference in the overlap width with the rolling direction parallel (H-grain oriented) and perpendicular (C-grain oriented) to the forming process is found. This will also create can cylinder feeding problems or poor weld qualities when combining the two rolling directions. Reasons for the large differences were found in the anisotropy and the internal residual stresses of the steel sheets after rolling.

Adaptation of the body maker to the specified materials before the welding operation is the best solution. The automated feeding from the lithographic machine to slitting and the body maker takes care of the materials direction to ensure consistency within the first can production processes. Besides material properties, the body maker is also a criterion that is important when roll-forming. Different body makers give different overlap values [5]. The roll-forming machine is integrated in the welding machine and hence roll-forming is established just before welding (see figure 3.7).

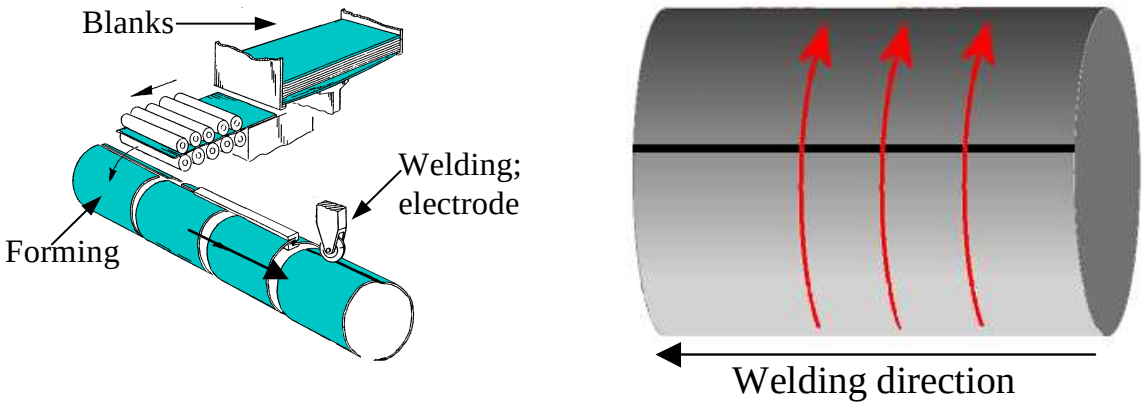

Figure 3.7: The left-hand side shows the roll-forming process just before welding. The right-hand side picture shows the welding direction of the can cylinder in contrast to the rolling direction of the material, C-grain orientation.

From the rounding unit the can blank is transferred onto a z-bar [3], which controls the non-welded can bodies by means of a spring-loaded guidance cage. The can is forwarded along the z-bar by a set of feed chains and bearings along the outer cylinder walls. The feed chains have a variable drive to match the speed of the electrode wheels to ensure no damage occurs at the trailing end of the can. After the z-bar just before the electrode wheels, the calibration component (i.e. Diablo Rolls) control the can body material overlap width.

3.3 Welding

The non-welded can blank cylinder is fed through two electrode wheels which perform three main tasks:

1. Take over the transport of the can body cylinders from the feeding chains
2. Pass a current through the material overlap width
3. Apply an electrode force to mash the overlap width together

The welding unit closes the material overlap width and creates a solid-state continuous bond along the total can body height consisting of repetitive non-overlapping weld nuggets. The welding process as mentioned before is a wire welding process and based on the principle of resistance (pressure) welding. The process uses a sine wave alternating current power supply, which passes between two copper alloy electrode wheels. The electrodes are dissimilar in size rotating copper alloy wheels situated above each other. The can bodies move in such a way that the smaller lower electrode is inside the can body (see figure 3.8)

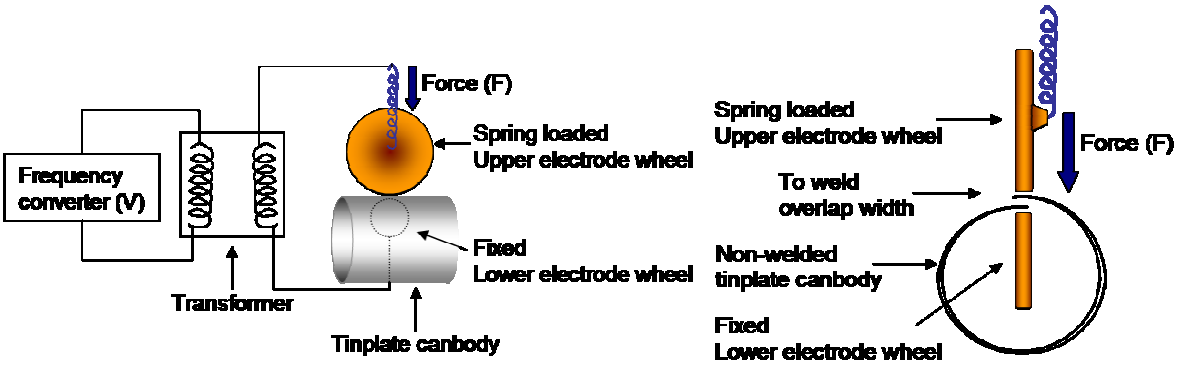

Figure 3.8: Schematic of the HSRW process. The left-hand picture shows a side view of the welding process and the right-hand picture a front view. In both pictures the spring-loaded upper electrode wheel and smaller but fixed lower electrode wheel supply the current (AC) to the can body overlap width.

During the welding process a controlled amount of pressure is applied to ensure optimum contact on the weld interface to achieve the desired weld seam shape. Supplied by the electrodes, the welding current is passed through the steel sheets by which the resistance between the materials interface generates the essential heat. The pressure, current and speed determine the amount of resistance being generated. The can body production is continuous with a gap of approximately 1 mm between the individual can body cylinders. The gap is set to avoid collision of can bodies at the welding unit and subsequently joining of the separate can bodies to each other.

To account for the change in conditions when electrodes run on and off the can bodies, the welding current at the start and end of each can body can be changed with respect to the mid-section of the can body. This production feature is also the basis for the integrity of the weld seam in the flanging stage of the can-line production sequence [3, 5 and 28].

3.4 Lacquering and curing

Most of the time within the can manufacture the products in the cans are very aggressive or in any case deterioration with iron sensitive products and cut edge oxidation takes place. Consequently, the importance lies with the product with which the can will be filled. Different types of lacquer are used for different (specific) products. For example, baked haricot beans in tomato sauce react with the tin inside the can. Yet, white fruits, such as pears and apples, are packed into un-lacquered cans because the oxygen is absorbed keeping the fruit inside free from oxidising and colouring brown. For this reason it is important to protect the base material, and

especially the seam made during welding, with a protective layer by the lacquering (i.e. spraying) process.

A magnetic conveyor transports the welded can bodies to the lacquering stage where a powder or spray-coating is applied onto the inside of the can and weld seam. The latter process is also known as side-striping. The coating prevents interaction of the product with the inside, especially the weld seam of the container. The outside of the can body may be side-striped to protect the container from environmental conditions. Curing of the sprayed lacquers takes place in a large furnace oven to remove solvents and harden the lacquers.

When lacquer is used, up to three layers are applied to act as a barrier between the tinplate and the product in the can, preventing corrosion, tainting of the food and to protect the outer surface. Lacquering and side-striping have two important aspects in conjunction with the welding process:

1. Effective protection to avoid serious corrosion and contaminants on the inside and outside of the container
2. Application of the right coating types and weight levels for accurate welding

Lacquering processes are developed to support these two points. Although the methods are common knowledge in can manufacture, it is still a point of attention in welding cylinders for can manufacture, because contamination during welding can produce sparking and welding failures and eventually corrosion after lacquering of the can bodies.

Normal tinplate quality is satisfactory to weld cylinders in an effective manner and lacquer afterwards. Standard tin passivity films are applied rather than chromium/chromium oxide. The choice of (tin) coating weight is governed by the requirements of corrosion resistance, lacquerability and weldability. Over the years the tin coating thickness has been lowered significantly for two reasons:

1. The change from soldered can manufacture to welded cans, which requires considerably less tin to join the material
2. The high tin prices, which caused a conversion to very low and different coating types without employing any different process steps within the can production lines.

The latter point led to the investigation of coatings such as nickel and chromium or combinations of these with tin. In the end, a decline of the tin prices and the developing WIMA welding process caused the can making industry to concentrate only on tin and associated coating weights.

Corrosion or good lacquerability is tested on the evaluation of iron pick-up by certain products inside a can after a certain storage period at a controlled temperature. These results for different coating types or weight levels can be displayed in a star-profile diagram as shown in figure 3.9.

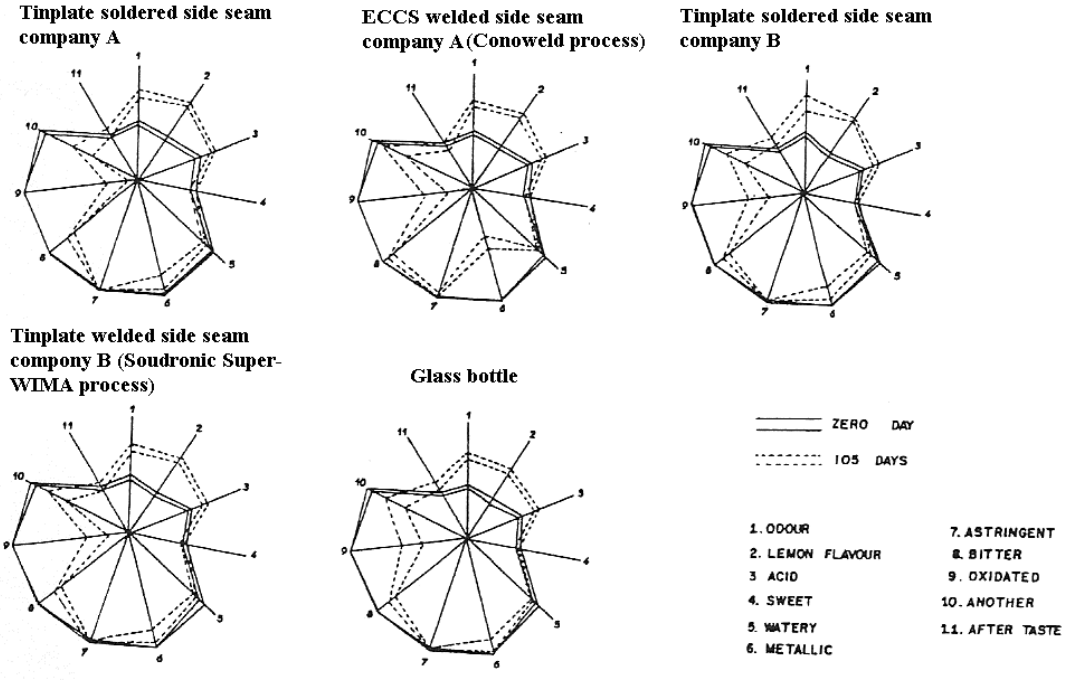

Figure 3.9: Star-profile diagrams show how differently layered and produced cans react to the different contents at the start and after 105 days storage at 35°C [29].

The rings in a star-profile diagram represent the iron pick-up in which the outer ring is the one with the least amount of iron pick-up. The star-profile diagrams and iron pick-up diagrams (see figure 3.10) can be used to compare different coatings and coating levels, but also different production processes and packaging applications. In all methods it is easy to give a critical iron pick-up value and determine whether the corrosion values or lacquer performance is acceptable.

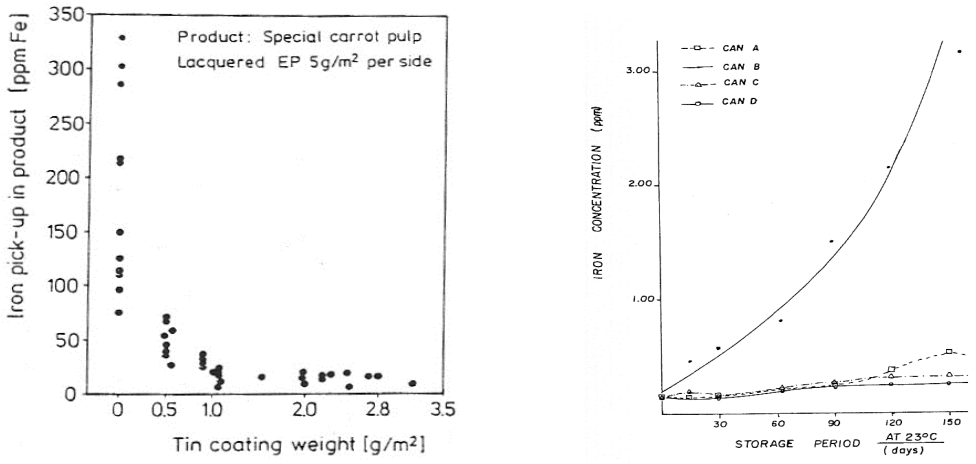

Figure 3.10: The effect of iron pick-up after a three months storage at 50°C for a special carrot pulp with different lacquer levels on the tinplate [4] On the right-hand side the iron concentration or pick-up in a lemon soft drink as a function of the period of storage at 23°C is shown [23]. The capitals correspond to the descriptions given in the star-profiles of the different produced cans in figure 3.9.

3.5 Flanging and beading

After lacquering, side-striping and curing the necking or flanging is performed. Both necking and flanging are forming operations of the can bodies' top and bottom edge. Necking can even be considered as part of the same operation as flanging. This indicates that necking has relatively the same disadvantages and advantages as flanging. The forming operations can be performed in different ways. Figure 3.11 shows the two standard methods, used in flanging. Die flanging is a process in which a static die from the axial position of the can bodies forces the can body edge into its new shape. With spin flanging the flange tools are separately spinning whilst forcing the edge into the right shape. Although spin flanging requires more sophisticated machinery it also provides superior results when comparing it to die flanging since less internal stresses are created.

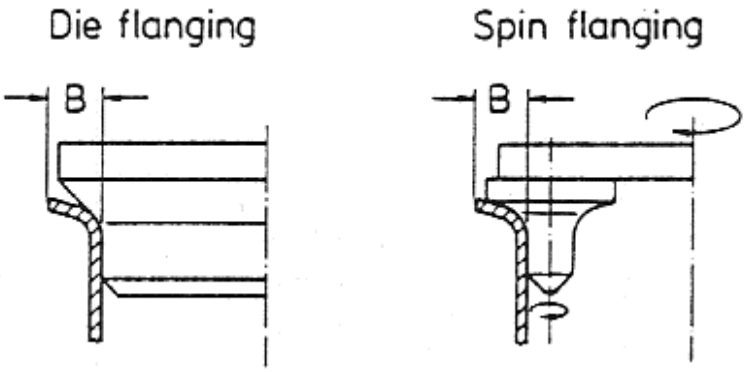

Figure 3.11: Schematic of the methods used for flanging of the can edges. The left-hand side shows a cross-section of the static die flanging process. The right-hand side displays a cross-section of the spin flanging process with the separately rotating flange tools. The capital B stands for the flange width created by the flange methods.

Because flanging is performed after welding, lacquering and curing (i.e. heat-treated and deformed material) the use of materials with higher strength and smaller dimensions can lead to problems such as, material failure (e.g. cracks and surface abrasions).

Figure 3.12 shows the relative elongation of a flanged can body edge for various can diameters. The linear relation between the flange width and the relative strains in the flange are visible. The figure also shows that the elongation values from the tensile tests are not comparable with these phenomena.

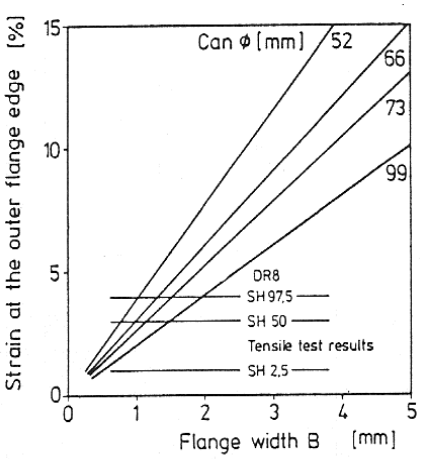

Figure 3.12: Diagram of the relative elongation of the flanged canbody edge, B for various can diameters. DR and SH stand for double reduced material and respectively [4].

In testing the flange or necking behaviour, over-flanging or necking of the edge is used as a test method. Based on a certain number of samples, the cumulative frequency of cracked cans is stated as a criterion. With over-flanging or necking the diagrams in figure 3.13 show the influences of flanging method, rolling direction, can diameter and annealing process when processing certain can diameters.

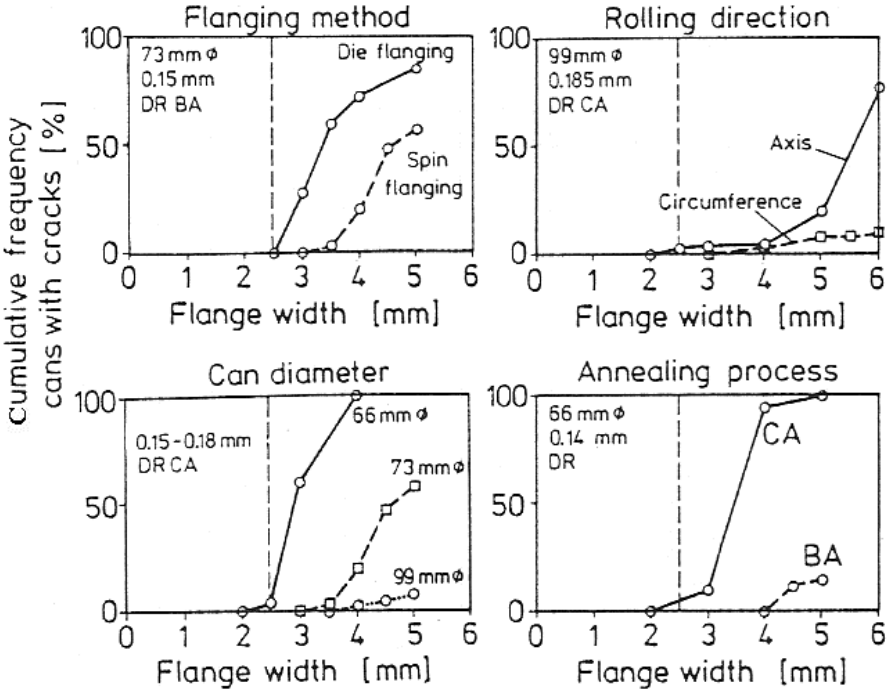

Figure 3.13: Diagrams presenting the influence of flanging method, rolling direction, can diameter and annealing process on the flanging stage enforced by over-flanging of the welded cans. BA, CA and DR represent batch annealed, continuous annealed and double reduced material respectively [4].

The rims on the outside of a can body, as shown in figure 3.14, are embossed before applying the can-ends and is known as can beading. The dimensions and number of rims depend on the dimensions of the container and its application (see section 3.7). Suitable beading (i.e. relevancy of the rims) is applied for increased strength of the can body to endure the stresses which are encountered during pressure cooking (i.e. sterilisation), generating radial stresses of the container and during storage generating axial container stresses.

Figure 3.14: Picture of a food can, showing the rims/beads on the can body.

3.6 Filling and seaming

The beaded and flanged can bodies are double-sealed to the can-ends of which figure 3.15 shows the detailed operational features.

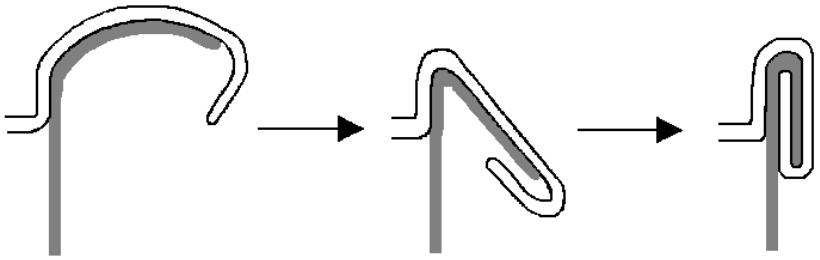

Figure 3.15: Schematic cross-section of the double-seaming stage of the can-ends on the can body. The picture shows a double-seaming of the can body and can-end.

The double-seaming of the can-ends to the can body is performed by a so-called seamer. First an open topped can, ready to be filled with the product is made. Before being stacked each can is tested for the smallest possible leaks. The reason for this is that the products are placed raw into the can and sterilised at high temperatures in large pressure cookers. After testing the open topped cans are stacked and sent to the filling plant. The ends are pressed from flat sheet steel within a can-end production line. The type of ends can be a plain end to open with a can opener or easy open end with a ring pull, as shown in figure 3.16.

Figure 3.16: The left-hand side shows a easy open can-end and the right-hand side a few plain can-ends all to be seamed on to the can body

Dependant on the applied lacquers as mentioned before the containers are matched with the correct product. The open topped can is filled and the final end of the can is also double-seamed onto the can body forming a tight pressure seal. The closed container is transported to the large pressure cookers where the product in the closed containers is sterilised. Finally, the cans are labelled, dated and re-palletised to send to the distributor for sale to the customers.

3.7 Can Stability

3.7.1 Can bodies

Within the can making industry welding of can bodies requires research on minimal practicable metal thicknesses for optimal durable and economical reasons. For instance, the weld seam allows relative good forming behaviour of can body beads compared to a soldered seam [5 and 23].

The sterilisation process for cans subjects the can bodies to a high load due to hydrostatic outside pressure within the hydrostatic retort of the sterilising process (see figure 3.17). To withstand hydrostatic inside pressures the can bodies are provided with beads.

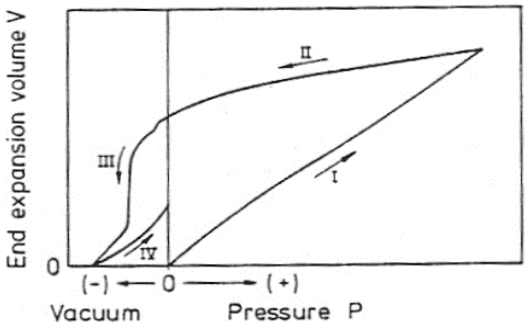

I: Pressure increase
II: Pressure relief down to can inside pressure = 0
III: Vacuum increase up to $V = 0$
IV: Vacuum relief down to $P = 0$

Figure 3.17: Pressure-volume diagram as the sterilisation process of for instance food cans applies to the container. In the diagram four stages are characterised during the temperature cycle with sterilisation, each stage imposing a pressure and volume change in the container and evident stress features within the material of the containers.

Beads will withstand increasing pressure with the increase in depth of the rims. However the axial pressure (i.e. for stacking the cans in storage) is reduced. A certain radial and axial load is specified through which the optimum bead depth can be calculated. Figure 3.18 shows a picture in which the bead depth is plotted against the can body wall thickness at constant axial and radial loads. It shows that the strength of the material only influences the axial and not the radial loads (i.e. Youngs modulus).

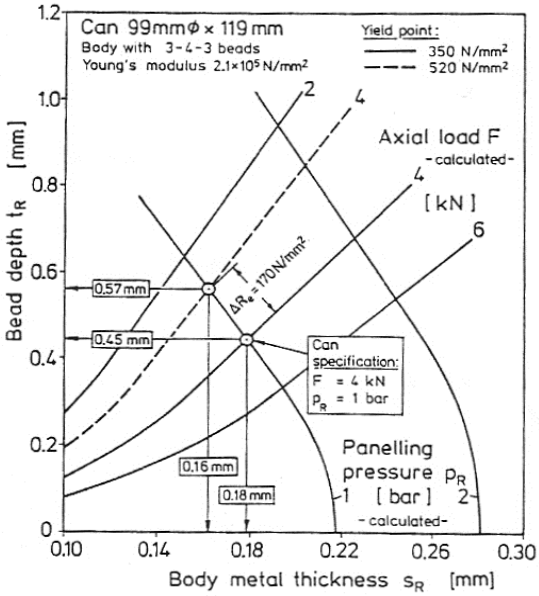

Figure 3.18: Diagram displaying the stability of beaded can bodies. The bead depth, t_r is plotted as function of the metal thickness, s_r at constant loads and panelling pressures. The load and pressure lines are theoretical values dependant on process and material properties. The diagram shows that with an axial load of 4kN and a pressure of 1 bar a bead depth of 0.45 mm is required when having a material thickness of 0.18 mm.

Consequently, if the wall thickness is reduced by increasing the material strength the stability will only be maintained when the bead profile is increased. This can be crucial as the new material may not be capable of having deep profile beads [30 and 31].

3.7.2 Can-ends

In developing a low cost welded food can, the possibility of saving costs for the end material must also be considered. Especially during the sterilisation process of containers, the can-ends are subjected to high strains. In the sterilising process the can-ends may even be subjected to plastic deformation and start to buckle. Buckling of can-ends should be prevented because poor appearance and low strength after sterilisation are detrimental. Figure 3.19 shows the parameters, which are responsible for the influence on buckling of the can-ends. The figure also shows that the can-end diameter is the most important parameter when trying to influence the can-end stability. Metal thickness and hardness also influence the buckling phenomena but to a lesser extent than the diameter. As found in the literature, buckling is only one factor in the can-end stability [32].

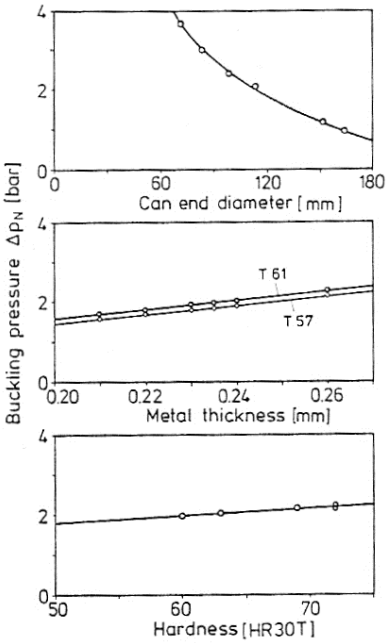

Figure 3.19: Overview of the parameters that influence the occurrence of buckling of the can-ends. The diameter of the can is the most influential parameter.

Flexibility is a second important factor that influences the

can-end stability and is apparent by the increase of the volume under the can-end because of the inside pressure as shown in the left-hand diagram of figure 3.20. The figure is a description of the strain when the can-end is subjected to the sterilisation process or heat treatment after seaming the top and bottom. The figure presents the pressure-volume curve (hyperbola for the product) over which the can-ends will not fail. Whereas below the curve, buckling should be expected with eventually can-end failure. With a thicker can-end the reliability increases and with lower thicknesses the ends could fail if the hardness of the material becomes too low. Further details concerning this relation diagram are given by Sodeik and Sauer [33].

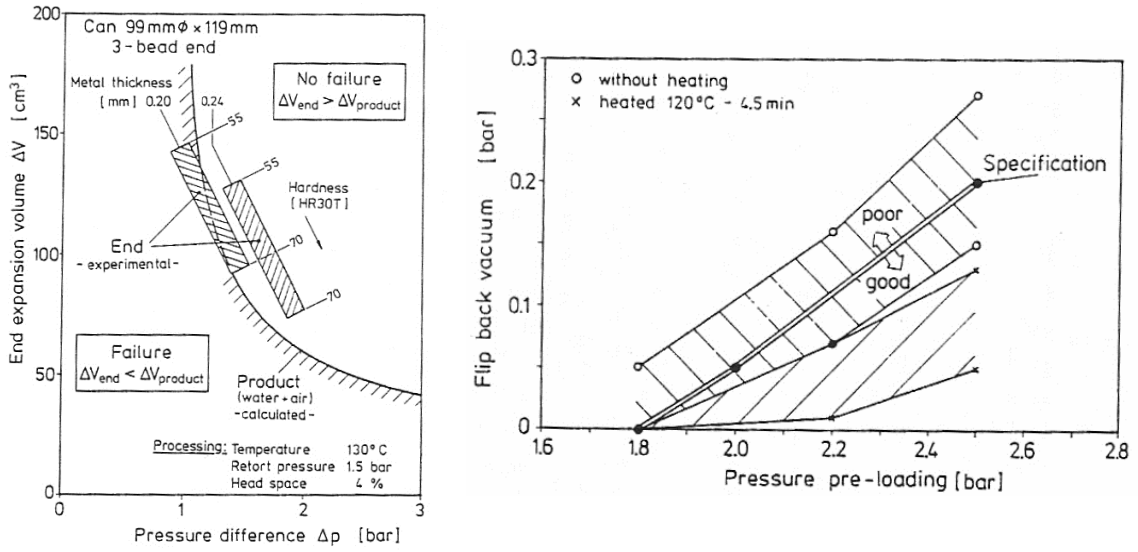

Figure 3.20: The diagram on the left-hand side shows the stability criterion for a container having certain dimensions and filling consisting of water and air (i.e. the hyperbola). Above the hyperbola the can-end will not fail whereas below the curve, buckling should be expected. The right-hand side diagram shows the specification for the flip-back phenomenon. The flip-back after pressure pre-loading as a standard (i.e. a particular value of the vacuum necessary to return to the original state).

Finally, flip-back after pressure pre-loading of the can-ends is also an assessable factor for the stability of a can-end. This means that a certain vacuum value is necessary to return the can-end to the original state, which is set at certain pressure pre-loading values caused by the internal pressure. The right-hand side of figure 3.20 shows the relation between the pressure pre-loading and the flip back vacuum [23].

4 Power supply

Within high-speed resistance welding many different current wave shapes are utilised to supply power, for different reasons. In addition, delays and significant changes in the current amplitudes over the can body height may for instance reduce the possibility of defects and/or contribute to the integrity of the weld seam in the flanging stage of the container production [3, 5 and 28].

Schaerer and Weil [36] compared the characteristics of direct current (DC) and full sine wave seam welding (i.e. AC). The difference between alternating and direct current power supply is that DC flows in one direction, whereas AC flows back and forward in a wire at regular time intervals. They found that amplitude control of the current is the main factor linked to the power supply. Amplitude control is used to provide optimal waveforms, which improve the weld quality at welding speeds above 50 m/min. With improved weld quality Schaerer and Weil combined higher strength with defects-free welds, using commercial available tinplate. The results showed that a full sine wave creates an energy input, Q in [J], determined by:

$$Q = \int_0^t I^2(t)R(t)\ dt \tag{4.1}$$

in which R is the resistance in [Ω], I is the current in [A] and t the time in [s]. With the aid of equation 4.1 Schaerer and Weil discussed how two current types, AC and DC influence weld quality. They noted the following aspects when welding 0.19 mm thick tinplate at 50 m/min with a direct current (see also the left-hand side picture of figure 4.1):

- The surface and centre of the weld seam are subjected to similar temperatures
- A joint as a whole is not produced
- The heating effects on the surface are so powerful that a rough surface emerges
- Surface oxidation due to high surface heating occurs

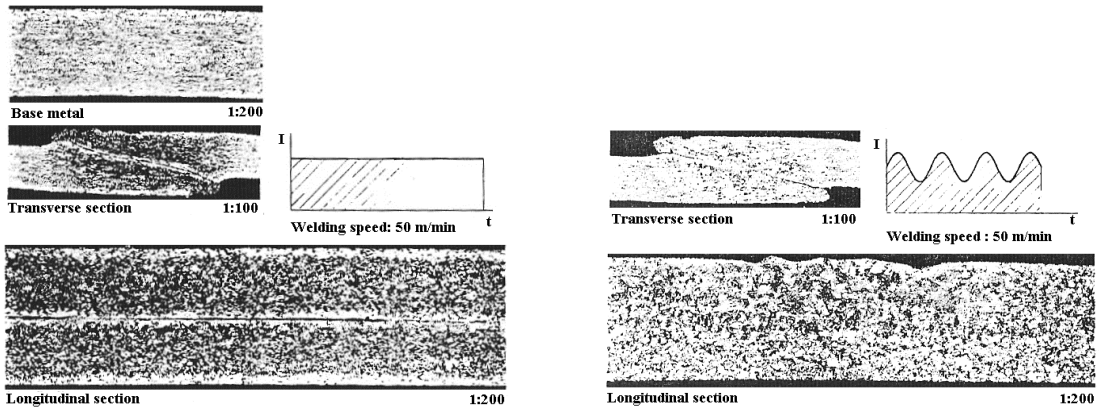

Figure 4.1: On the left-hand side the form of a DC power supply is shown and the effect it has on the materials. On the right a super-imposed DC waveform is drawn with the associated effects on the materials. Below the microphotograph scales indicate the enlargement. All welds were made with a welding speed of 50 m/min.

Applying a superimposed DC oscillation (see the right picture of figure 4.1) the heat penetration into the centre of the weld seam compared to normal DC welding ensures a suitably welded joint at the centre. The following aspects are notable:

- Surface and centre of the welded seam are heated to the same extent
- Considerable surface oxidation on the welded surface occurs
- A rough surface is generated as a result of the strong heating effect

In DC welding due to high thermal activation over the entire material thickness, brittleness is encouraged. Essentially, an abrupt microstructural development in the small heat affected zone (HAZ) enhances the risk of cracking near the weld seam when deforming, especially with thinner materials. It also diminishes the smoothening operation and adhering properties, required for the lacquering process.

Employing a full sine wave with thicknesses of 0.15 mm and 0.12 mm at speeds of 60 m/min, Schaerer and Weil found the necessary interplay between cold and hot stages needed for a satisfactory weld quality (see figure 4.2):

- A total coverage of the joint
- The seam being produced remains elastic
- Double reduced and thinner tinplate sheets retain the same features
- Relatively slow heat transfer from centre to periphery, because the weld interface line is subjected to a larger thermal activation than the outside of the weld seam

- Gradual microstructural development as the base metal microstructure extends into the centre of the weld seam

For this reason applying a pulsing power input (minimum current amplitude) obtains an optimum weld quality, therefore AC is the best option for high-speed resistance mash seam welding [36]. As mentioned before delays (i.e. phase angles/shifts) and significant changes in the amplitude of the current and shape of the wave are excellent tools to handle the heat distribution in the can body weld seams. The main wave shapes are: sine wave (or scatter sine wave), square wave and triangle wave.

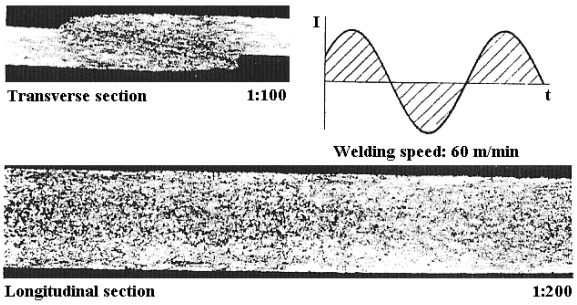

Figure 4.2: In the upper right corner the waveform applied in an AC supply is shown. Below the microphotographs, which display the effects of the AC, the scales indicate the enlargements. The weld was made with a welding speed of 60 m/min.

The waveforms as used in practice are represented as curves depicting a gradual change in the current as it increases and decreases for each direction of current flow. A sine wave is the most common and in-practice simplest of the waveforms as the frequency can easily be changed to provide a continuous current flow to the work-piece. For a sine wave cycle, the continuously changing current value proportionally indicates the heating and cooling of the material.

The sine wave shape within high-speed welding is attained with the use of a rotary transformer, because the turning motion of this transformer can produce the exact shape of a sine wave. However, if a solid-state transformer is used (as on most welding machines), the sine wave is approximated by sectioning the frequency within certain limits of the polarity. Elzinga [34] showed with the approximation of the sine wave and an element of scatter, a slight trend towards increasing defects, as there is no gradual rise in the current per se. In this case, the sine wave displays a jagged stepped rise and fall. However, the resolution at which the separate elements are applied (i.e. how often do the approximating elements cross the exact sine wave) is so small that the approximation is taken to be commercially viable. On the other hand, this does not diminish the likelihood of irregular spikes (i.e. larger values as the upper and lower limits of the exact sine wave). The spikes appear within the current pattern and cause an irregular temperature effect for a certain time period. The reasons for this might be an inconsistency in the power generator or temperature fluctuations in some other part of the welding machine.

Square waves as shown on the left-hand side in figure 4.3 are rarely used in high-speed welding [36]. The square wave takes on the form of an AC wave, except for the gradual increases and decreases in current.

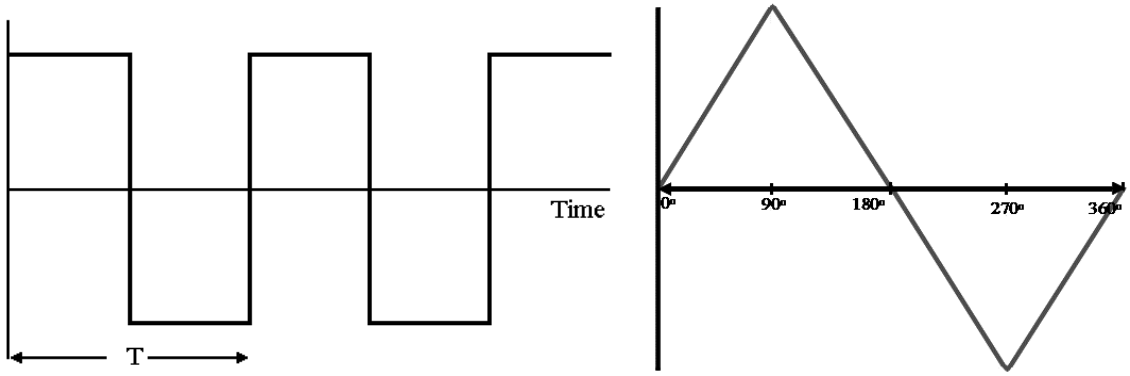

Figure 4.3: Schematic of a square waveform on the left-hand side with T as one waveform period and on the right-hand side an illustration of one wave period from a triangle waveform is shown.

Although a square wave is seldom used in practice, since it is a difficult to accomplish instantaneous change of current, work has been conducted which outlines the apparent difficulty of using it as a commercially acceptable method [125]. Simulations using a triangular wave as shown on the right-hand side of figure 4.3 were similar to those of a perfect sine wave, except for the lower temperatures, produced due to a slightly smaller area underneath the half-cycle [35].

Since older welding machines were not equipped with systems to solve frequency problems, phase angle control (see figure 4.4) with increasing frequencies was employed. Phase angle control proved to be the best approach in solving these problems. The phase angle is defined as the difference between the phase of one sine wave varying quantity and the phase of a second quantity, which also varies sinusoidal at the same frequency. This phenomenon is also known as phase difference (t in figure 4.4) and normally expressed in degrees.

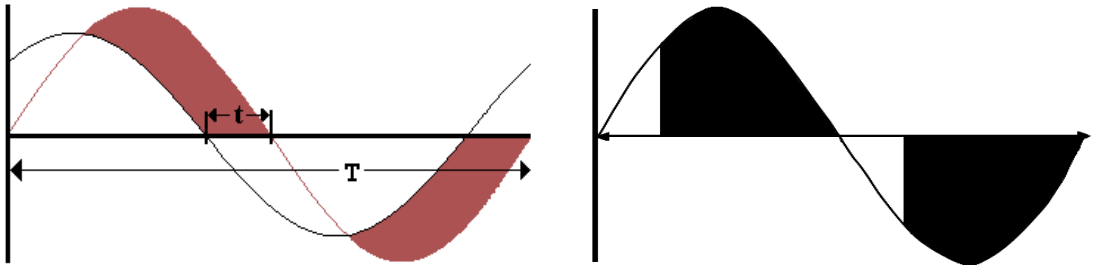

Figure 4.4: On the left-hand side a phase angle/shift is seen with t (i.e. coloured parts) being the difference in the angle and T the period of the waveform. The right-hand side picture shows the mechanism behind phase cutting.

The continuous alternating current restricts the conventional resistance welding heat control method of phase cutting (the illustration on the right-hand side of figure 4.4). Phase cutting is a form of pulse width modulation (PWM) applied to AC voltages for limiting the power supply. As in all forms of PWM, phase cutting works by using a solid-state switch only allowing current to flow for a fraction of the time. Phase cutting makes use of the AC voltage variations to control the duty cycle, the switch turns on when the voltage reaches a certain level and turns off when the voltage reaches the ground level; this allows easy and economic alteration of the duty cycle. Unless a shift of at least 80% is used the off period (i.e. no current period) becomes excessive and lack of bonding on the weld interface line can appear between the weld pulses [5 and 36]. Over time phase angle control readily took the form of an uninterrupted full sine wave with amplitude control, proving to be a suitable welding technology for can bodies in industry today.

5 Welding electrodes and wires

A disadvantage of resistance welding of tinplate is the presence of low melting temperature tin on the tinplate surface, which results in alloying when using copper electrode wheels and consequently rapid contamination and deterioration of the welding conditions (electrical and thermal transition rates) and severely diminishes the quality of the welds. This problem can be overcome by the use of a continuous copper wire feeding through a groove in the copper electrode wheels, providing a continuous clean electrode surface to the can bodies and keeping the contact resistance within the acceptable quantity and variation. The wire-feeding system guides a copper wire between the electrode wheels and work pieces (i.e. an intermediate electrode) [3 and 5].

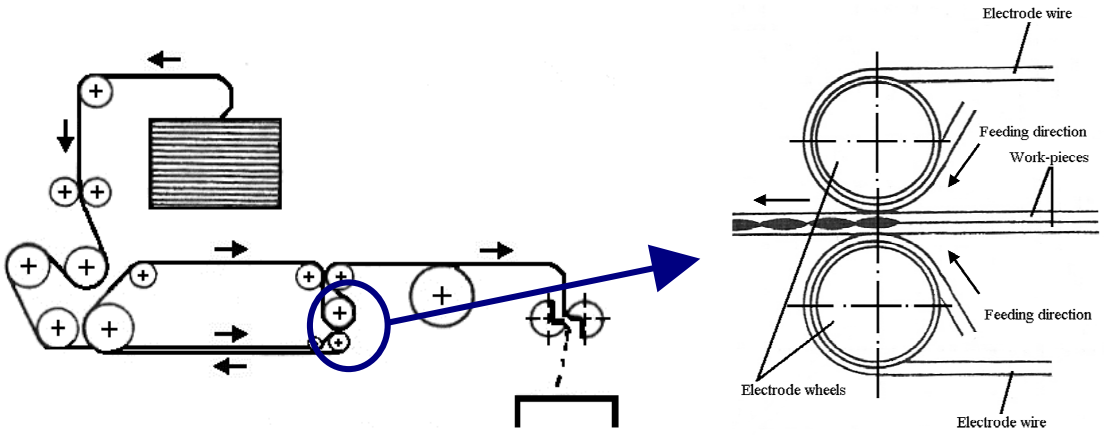

Figure 5.1: Overview of the copper wire-feeding system employed with wire welding, which incorporates the profiling rolls, guiding rolls, flattening rolls and chopping mechanisms at the end. On the right-hand side an enlargement of the actual welding unit is shown [37].

The copper wire is made of electrolytic copper with a diameter of typically 1.38 mm or 1.50 mm, which has an electrical conductivity of $5.9 \times 10^7 / \Omega m$. The wire itself starts off with a circular cross-section and is guided by a series of pulleys to a series of flattening profiling rolls where it is formed into a rectangular or elliptical profile. Profiling is followed by double sided feeding, using top and bottom of the copper wire once at the bottom and top electrode in order to bring contamination to a minimum and copper wire usage to a maximum. For this reason the wire firstly circumscribes the bottom electrode wheel followed by a twist for a fresh surface to circumscribe the upper electrode wheel. An evenly distributed wire tension is achieved by a variable drive system. After welding the contaminated copper wire is chopped into small chips

and collected for recycling via melting or refining. Figure 5.1 schematically shows an overview of a wire-feeding system. [37]

The use of a copper wire-feeding system with copper electrode wheels is a result of the prominent alloying mechanism between tin and copper at the elevated temperatures within the welding process [37]. Inertia and friction characteristics of the electrode to tinplate and the deformation of the intermediate welding wire can, in additional role to tinplate properties, influence the weld integrity, especially at higher temperatures and the subsequent physical material alterations [5]. Additionally, the electrode wheels must align correctly, the welding wire should have the right cross-section and the position of the z-bar must be accurate in order to get an optimal heat generation and development on the weld interface line.

Figure 5.2 from [38] displays the thermal and electrical conduction with increasing tin concentration. The graphs show a significant reduction of both material properties when the tin percentage is increased. Also, when the surface of the copper wire alloys with tin, the electrical and thermal conductivity alter significantly, whereby on top of the complex contact resistance patterns, temporary but large temperature variations occur, which contribute to poor weld qualities.

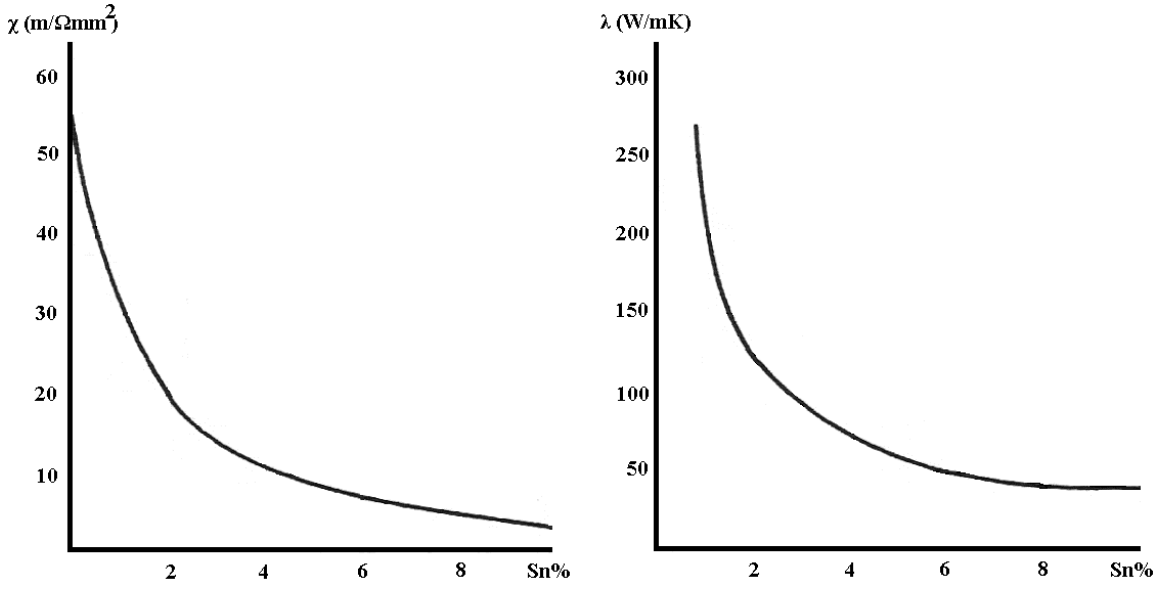

Figure 5.2: The left graphic shows the electrical conductivity in [m/Ωmm^2] of copper with rising tin concentrations. On the right-hand side the graphic shows the thermal conductivity in [W/mK] of copper with increasing tin concentrations.

In addition to the wire-feeding system there are different solutions available to obtain a satisfactory weld without contamination and deterioration of the electrodes. Other alternatives are

also significant since usage of copper wire is a substantial disadvantageous. For instance, welding with a 1 mm^2 diameter copper wire at 50 m/min, 0.5 kg of copper per minute of operating time is consumed. In addition, an increase in the welding speed requires more sophisticated and rapidly forming, tightness and feeding of the copper wire without decreasing the weld quality. Consequently, research is performed on the use of non-reactive copper alloys containing tungsten and molybdenum. Furthermore, titanium-zirconium-molybdenum (TZM) electrodes where investigated try to dispose of the wire-feeding system [37].

Using TZM electrodes gave good welding results and the non-deteriorating behaviour of the electrodes could make it commercial attractive. However, TZM electrodes should be reworked after certain process times since irregularities originated on the electrode surfaces. A linking roll-body device made of electrolytic copper with an electrode ring made of TZM material could therefore be employed (see figure 5.3).

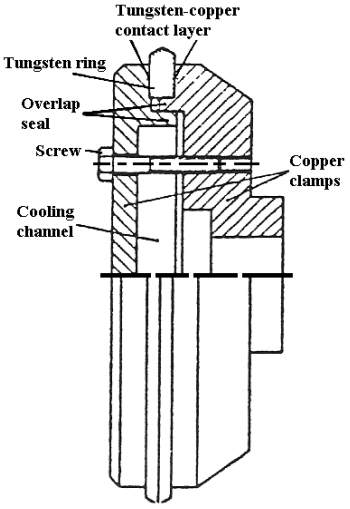

Figure 5.3: Principle of a linking roll-body electrode with an electrode ring of tungsten or titanium-zirconium-molybdenum alloy.

The main difference between the two methods is the higher electrical conduction when using a copper wire-feeding system, even though undesirable alloying and mechanical stiffness on the weld seam come into existence. On the other hand, with TZM electrodes tin remains on the tinplate and copper is not deposit on the weld seam whereby TZM electrodes result in greater mechanical stiffness and lead to a superior corrosion protection. Since TZM electrodes are around 50 times more expensive. For this reason TZM linking roll-body electrodes are not yet commercially adopted.

The first welding machines worked with a round shaped copper wire. Over the years, developments resulted in the rectangular or elliptically shaped wires of today. Changing the shape of the wire influences the production capacity by means of wider welding ranges (i.e. more tolerances), which has advantages when for instance downscaling the thickness of the tinplate. Large tryouts were performed on trapezium shaped copper wires. Trapezium wires have narrower contact widths on one side of the wire and hence compensate for the temperature variations caused by the differences in the diameter of the electrode wheels. Weld symmetry is improved resulting in superior weld quality. With differently shaped wires, especially a trapezium wire, the welding range in its optimised condition can be increased by a factor two compared to conventional round copper wires. Mutually, increasing upper and decreasing lower welding limits, cause the increase in the welding current range. However, raising the upper limit is more

profound [37]. The research of Elzinga et al [39] aimed to raise the upper limit by studying the possibility of substituting the classical rectangular and elliptical profile with a trapezium-profiled wire. The trapezium copper wire would give a more balanced temperature distribution, thereby reducing the possibility of splash on the inside of the can body. The reason for this is a similar contact area of the upper electrode wheel and the lower electrode wheel to the tinplate as shown in figure 5.4. The lower electrode wheel with the smaller diameter results in more heat generation (i.e. a higher current density), which is compensated by the wire shape resulting in greater flexibility production, as in some cases the welding current could be increased by twice as much [40], without observing hot welds or splash.

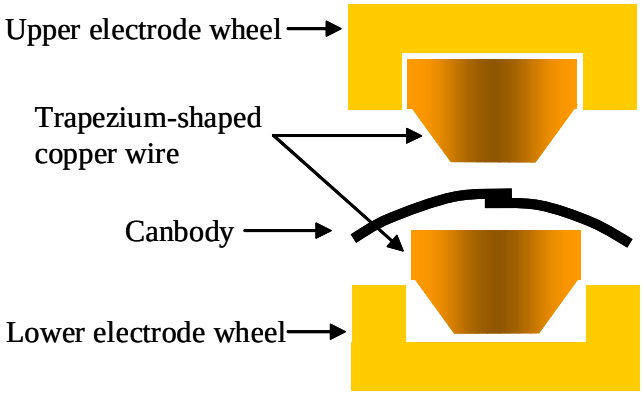

Figure 5.4: Schematic of trapezium-shaped copper wire when welding the tinplate. The picture clearly shows the difference in the contact areas that should compensate for the difference in heat generation over the material overlap thickness.

The main feature behind reshaping the copper wire is to get a better and more symmetrical heat distribution in the welded material by which the control of the process will improve. Electrodes having the same diameter in the process thereby inducing the same contact lengths fail in accomplishing a symmetrical welding process [97]. An advantage of wire shaping is that most wire geometries can easily be introduced in can body welding machines by replacing the profiling rolls.

The quality and geometry of the welding wire affect the integrity of a weld seam. Imperfections in the copper wire, such as grooves or blemishes affect the electrical resistance and consequently the copper wire needs to have a bright finish and smooth surface after profiling. The tolerance of the profile of the copper wire is 0.02 mm and should be consistent to allow a maximum contact area on the can body overlap width. Additionally, the tension of the copper wire should be maintained because in combination with the temperature conditions, the copper wire experiences an elongation. The elongation of the copper wire can be measured by the tin removal (i.e. alloying) from the surface of the tinplate onto the copper wire. The length of the alloying onto the copper wire is set to allow the length of the welded seam plus 3%. The gap between the two wires (which circumscribe the electrode wheels) is also an important setting and should lie between 0.5 and 1 mm. When the gap becomes smaller joining of stretched wire at the gap and fishtailing (see chapter 13) at the trailing end of the weld seam can occur.

Besides the other welding parameters, which determine the welding range, alteration of the copper wire has a significant influence on the welding process; most notable within the research of electrode influence is the effect of the change in wire shape. Changing the wire shape leads to variations in temperature balance, which still needs to be examined further, with respect to other welding parameters (e.g. coating levels thickness, speed, and etc.). Although the margin of symmetry in the welding process with conventional wire is not significant, stronger welds may be offered by changing the copper wire shapes as materials become thinner and are subjected to ever more severe deformations afterwards. Other materials or alloys for the creation of the electrode wheels seem unrealistic considering the weak commercial viability.

6 Resistance welding phenomena

With resistance welding it is important to understand the concept of electricity and its relationship to the process. When a voltage, V, in [V], is applied to a resistance, R, in [Ω] in a circuit, a current flow, I, in [A] results. The relationship between these properties is given by the equation:

$$I = \frac{V}{R} \tag{6.1}$$

The effect of current and resistance in a circuit is heat generation due to collisions between the moving electrons and the lattice structure of the metal. Heat generation is a product of current, resistance and time, t in [s]. If the resistance is invariable, a descent in the measured amount of current will result in less heat and oppositely a higher current will result in more heat being generated. Similarly, if the measured current is kept constant and the resistance changes, a higher resistance will result in higher temperatures. Conclusively, if in a system a particular temperature is required, then a current should flow through the resistance for a period of time.

The basics principles of electricity applied to the HSRW process in a simplified circuit, as shown schematically in figure 3.8, can be presented by:

- The frequency converter supplying voltage to the transformer applied over the electrodes and work-pieces
- From the transformer, current flows through the current bar, the upper electrode wheel, the can body, the lower electrode wheel and the welding arm back to the transformer, closing the electrical circuit
- Resistance, which is proportional to the type of material and its cross-sectional area at the welding unit

The electrode wheels, the copper welding arm and current bar have considerable cross-sectional areas in comparison to the can body overlap width. For that reason the welding arm and current bar have very good electrical and thermal conductivity and a relative low resistance. The tinplate can body with a smaller cross-sectional area has a comparatively high resistance. As a result, the welding current is subjected to the highest resistance at the interface line of the material overlap. If the current can flow through the material overlap width for a sufficient amount of the time, heat is generated. During this the material is heated to the state of plasticity and the applied electrode force, F, in [N] on the material overlap width, joins the two surfaces to form a weld seam. The heat due to resistance at the interface of the can body outer sides and the electrodes is kept to a

minimum by the use of the copper alloyed wire and wheels; dissipated by an integrated water cooling system. However, rapid heat development by a large contact resistance is important because it can result in a lower welding current necessary for welding. Yet, the rapid heat development at the electrode wheels results in interfacial splash before sufficient weld strength can be established.

With resistance or resistance welding excess energy or heat is generated in each element of an electrical circuit. This is done in proportion to the electrical resistance, time and the square of the (welding) current:

$$E \sim I^2 Rt \tag{6.2}$$

within which E is the energy in [J], I the (welding) current in [A], R the resistance in [Ω] and t the time in [s]. For simple examination of heat generation during resistance mash seam welding, the resistance, R can be approximated through the conducting volume of the work pieces, defined as:

$$R = \frac{\rho h}{A} \tag{6.3}$$

where ρ is the material specific resistivity in [Ωm], h is the thickness of the work-piece in [m] and A is the contact area in [m^2]. As the contact area consists of the initial overlap b and d in [m], a heat generation term can be defined and used in conjunction with the 2-D Rosenthal solution [41]. This solution can during welding at a certain place in the weld approximate the thermal cycles by:

$$T - T_0 = \left(\frac{I}{A}\right)^2 \frac{\rho A}{2\pi k} K_0\left(\frac{vR}{2\alpha}\right) \exp\left(\frac{-vx}{2\alpha}\right) \tag{6.4}$$

where $T\text{-}T_0$ is the rise from the base temperature in [K], K_o is the 0^{th} order Bessel function, k and α are the thermal conductivity in [W/mK] and diffusivity in [m^2/s] respectively, v is the welding speed in [m/s], x and R are the distances in [m] along and radially from the heat source. Similarly, peak cooling rates in [K/s] are approximated by:

$$\frac{dT}{dt} = -\frac{2\pi k^2}{\alpha}\left(\frac{v}{\rho A\left(\frac{I}{A}\right)^2}\right)^2 \left(T - T_0\right)^3 \tag{6.5}$$

In the HSRW process the heating and cooling is generally very rapid. For this reason, the time above a specific temperature for a metallurgical reaction is important and can be estimated by integrating equation 7.5 to:

$$\Delta t = \frac{\alpha}{2\pi}\left(\frac{\rho A\left(\frac{I}{A}\right)^2}{vk}\right)^2 \frac{\Delta T}{T_p^{\ 3}} \tag{6.6}$$

where Δt is the time in [s] above the critical temperature, T_p-ΔT. T_p is the maximum temperature in [K] for joining, and ΔT is the difference between the maximum temperature and critical temperature. The more time above the maximum temperature the better the weld quality [7]. Higher heating rates evidently establish higher cooling rates by means of conduction via the electrode wheels and tinplate and heat conduction from the weld zone. The equations above show the reaction on welding current, welding speed and overlap variations, of which the welding current is the most sensitive parameter [7]. Additionally, an energy or heat balance can be constructed to estimate what happens during the rapid heating and cooling. The balance is shown schematically in figure 6.1. In the HSRW process the electric field and current density induce a thermal field, whereby contact algorithms are needed to calculate the heat penetration and gradients. However, with a moving intermediate copper wire, special attention is also needed for surface frictions and stress analysis (i.e. deformation). The asymmetry of the process brought about by the dissimilar sizes of the electrode wheels greatly intensifies the complexity of the problem. This indicates that for continuous developing factors the evaluation of the energy balance requires a complicated 3-D thermal and mechanical analysis or numerical solution.

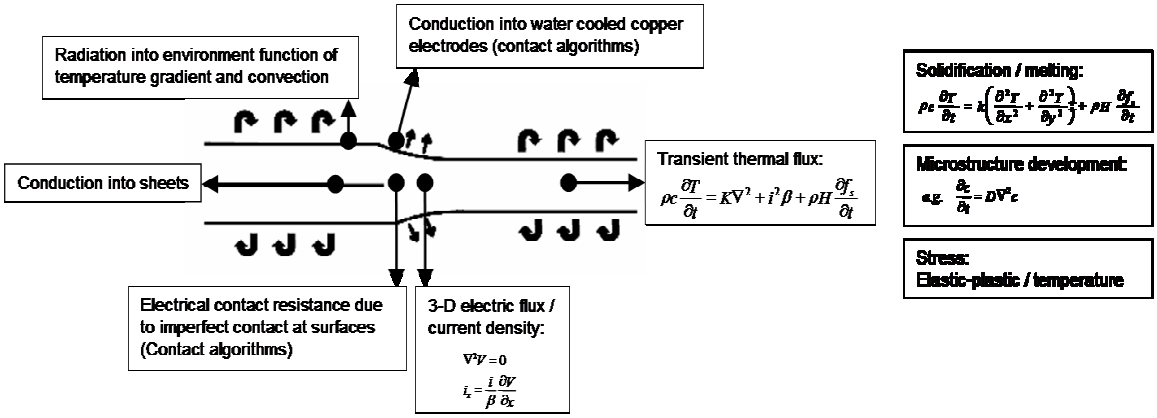

Figure 6.1: Schematic of the energy balance in the HSRW process. Each box indicates which factors could be accounted for during welding.

When taking a closer look at the resistance, two types of electrical resistance should be distinguished:

1. Volume resistance: property of the bulk material
2. Contact resistance: generated by the interface between two materials

The volume resistance is little affected by external factors, is uniform and varies with for instance the carbon content and linearly with the thickness of the material. Contact resistance is strongly dependant on interface contaminants, external pressure creating an as intimate contact as possible and the contact area. To make a sound weld in the HSRW process, contact resistance is the main indicative parameter and should dominate the volume resistance. The contact resistance is coupled to factors, such as speed, current and force and can thereby alter the ratio of volume to contact resistance and hence the possibility to make a sound weld [94]. Resistance welding is also influenced by the total resistance path (i.e. sum of the volume and contact resistances) between the electrode wheels. Figure 6.2 displays the five resistance elements that are generally taken into account when studying the welding of two overlapping work-pieces.

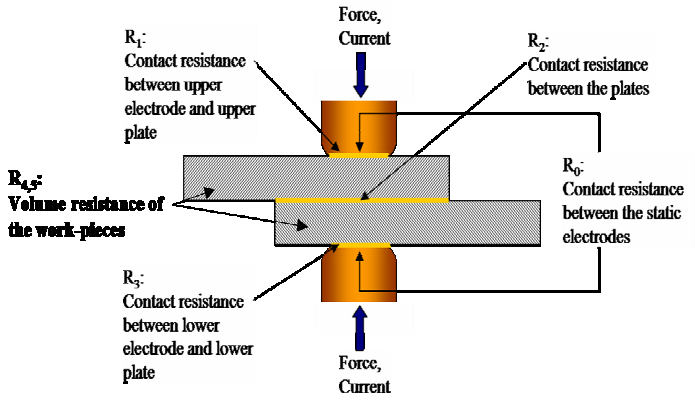

Figure 6.2: Schematic presentation of a static welding process, whereby the resistances that come across are classified by R_1 to R_5. R_0 is the summation of all resistances in series connection.

Can makers [42] have conducted a lot of research to characterise the static contact resistance between the electrode and work-piece. Sodeik [9] talked about how problematic it is to measure individual resistances in a static setting, yet the sum of resistances is measurable as a function of electrode pressure. This measuring technique also indicated that welding of a variety of materials, such as nickel-coated steels could easily be accomplished. The work of Ichikawa and Saito [43] was conducted to find an optimum welding current by use of mechanical weld testing and observation of the weld appearance. They found that an optimum welding range for tinplate could be categorised using static electrode contact resistance measurements by determining that $R_0 \approx R_1+R_2+R_3$. The results show that the level and range of optimum welding currents decreases with an increase in R_1 and R_3. Secondly, as the contact resistance at the overlap width increased, the upper welding limit reduced quicker than the lower welding limit, resulting in a narrower or no welding current. Conclusively, wire-welding tinplate with a low contact resistance at the outer

surface provides appropriate weld conditions. In addition, it was found that the contact resistance reduced the current path during welding. According to Ichikawa and Saito microscopic surface asperities and insulation layers on the surface such as oxide films governed the contact resistance, therefore the following characteristics have to be considered:

- Coating-electrode contact at the outer surfaces
- Coating-coating contact at the weld interface line (i.e. the inner surfaces)

Waddell et al [28] qualitatively suggested that contact resistance influences the heat developed in terms of the heat being proportional to current density and resistance, and its effect on the path of current flow as shown in figure 6.3. They considered that the effect of contact resistance on current path was only prevalent at higher welding speeds, whereby sufficient heat generation takes place at the exit of the electrode wheel to tinplate contact area. Higher contact resistance would have the same effect since the current path at the weld interface would then be concentrated at the exit.

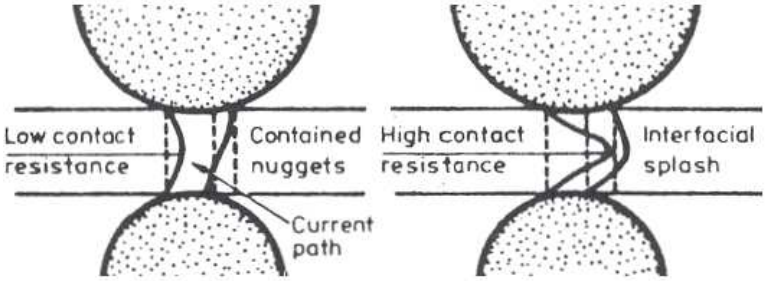

Figure 6.3: Weld formation mechanism in high-speed seam welding and how the contact resistance affects this. The effect of contact resistance on the region of maximum heat development: increased contact resistance increases the heating rate and influences current path and therefore the region of heat development.

It should be emphasised that static resistance tests measure only one of many factors involved in successfully high-speed resistance welding can bodies. However, it might serve to guide what materials and surface conditions are to be utilised. Shimizu et al [44 and 45] stated the limitation of quantifying the effect of static contact resistance in the HSRW process. Since the process has a dynamic character Shimizu et al discussed that the dynamic electric resistance could not be divided into contact and bulk resistance and introduced the equivalent contact resistance; determined by subtracting the calculated bulk resistance from the measured total resistance during the welding process. By a consideration of the main factors affecting the weld quality, tin coating weight, tinplate thickness and welding speed to the equivalent contact resistance they found that the welding range is adversely affected by:

- A reduction in tin coating weight and tinplate thickness due to an increasing contact resistance
- An increase in welding speed due to the smaller nugget size and intermittent HAZ pattern as a consequence of the reduced contact time between the electrode wire and work-pieces

Tan et al [46] also looked at the dynamic resistance yet with a small-scale resistance spot welding process of Ni. They found that variation of the welding current waveform and material surface condition, and correlation of electrical measurements with observed material surface changes indicated complex physical phenomena occurring during welding. They stated that the dynamic resistance R in [Ω], between two sheets follows the equation:

$$R = R_C + R_F + R_B \tag{6.7}$$

where R_C, R_F and R_B are the constriction resistance, film resistance and bulk resistance, respectively. All three are to be measured, can be calculated separately and are the result of changes in bulk and contact resistances. Tan et al showed that as welding progresses, the breakdown of the surface film causes a decrease of the dynamic resistance. The resistivity of the bulk material and asperities (i.e. surface ductility) will increase because the temperature increases, which results in an increase of the dynamic resistance. Followed by softening of asperities, the contact area increases thereby decreasing the dynamic resistance. With melting the solid to liquid phase transformation of the material during weld nugget formation will subsequently decrease the dynamic resistance because there is a (large) resistivity difference between the phases. Changes in the dynamic resistance were divided in the following stages: asperity heating, surface breakdown, asperity softening, partial surface melting, weld nugget growth and expulsion. Comparatively, large-scale resistance spot welding of steels shows that the onsets of melting and maximum weld nugget length vary due to the difference in electrode force and (specific) material resistivity. Nevertheless, figure 6.4 demonstrates the dynamic resistance stages and time instants (i.e. development) for steel in LSRSW, constructed by Dickson et al [47] and which corresponds to the results found by Tan et al.

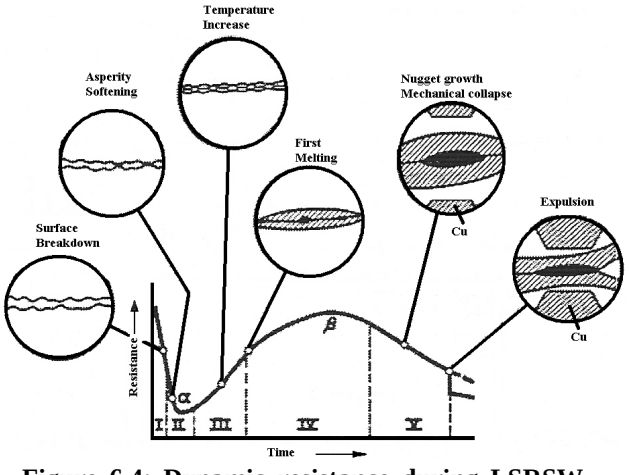

Figure 6.4: Dynamic resistance during LSRSW of steel, showing the different dynamic contact resistance stages with the evolution of time [47]

7 Weld quality

The quality and integrity of a weld highly depends on the process criteria. A sound bond without any weak areas is for instance required in aerosol containers, although for general applications less critical demands are allowed. With respect to processing, the weld shape and quality dictate the production speed, and quality is important to maintain high process efficiencies. As a result, the following three issues, which can also be seen as the post-weld criteria for the weld formation during the welding process, are important in respect to the weld quality:

- Strong weld seam: strength above a certain threshold
- Absence of defects: comma and splash
- Good deformational behaviour for post processing

When welding, the formation of a good quality weld constitutes the following two desirable features [50, 71 to 80]:

- A continuous and permanent joint supported by similar material composition
- Similar material and surface properties in the joint and base materials

To accomplish these features, the metallic atoms which are joined should be brought together as close as possible, but at least within a distance of ten times their atomic diameter [78].

7.1 Weldability

The term weldability is in essence material related. In the literature weldability is directly related to weld quality and commonly defined as a measure used for assessing a qualitatively good weld. The weldability very much depends on material requirements, processing conditions, and weld machine restrictions. With coated steels weldability is firstly related to be the lifetime of the electrodes and how much this influences the welding process. Secondly, weldability is determined by the correct welding schedule necessary to give an acceptable weld quality. The weldability does not necessarily need to reflect the best possible weld quality, because a balance between quality, economic operation and acceptability for specific components in the application is as important. Since electrode lifetime is not considered a problem with the HSRW process, the weldability is best defined in terms of the welding schedule (i.e. weldability ranges or welding ranges), which can be introduced for all types of coated and uncoated can body materials. Metallographic techniques and inline tests are used to obtain the welding ranges, which are valuable for the assessment of the overall welding situation. The reason for this is that it directly reflects alterations in weld quality when varying process parameters and material properties.

The welding ranges are the operating frames for making sound welds, and weldability is directly associated with these ranges. The intention of a satisfactory weld quality is set by a minimum and maximum limit. Generally, the point where it is not possible anymore to produce sound welds is called a cut-off point or welding range limit. Beyond these limits, detectable weld defects are encountered (see chapter 12).

7.2 Welding range

Welding ranges are by definition: "*a plot of two of the major welding parameters in which it is possible to guarantee weld quality as defined by arbitrary limits*". The parameters used to define a welding range are chosen to give realistic controllable production margins. The welding range is mostly a mapping of the welding current and one other main governing welding factor or parameter (e.g. welding speed, weld nugget length, electrode force, etc). However, the types of parameters, which are chosen for the welding range, are dependent on material, application and type of welding machine. The reason for taking the welding current is the close relation with contact resistance; hence heat generation and temperature phenomena. Consequently, as welding parameters are varied to see what happens to the welding range, current gives a reasonable and understandable explanation of what occurs to the material during welding. According to Sodeik et al [4] experience shows that 400A (at 50 /min and a flow-melted tin coating) is a threshold value necessary for the welding current range to produce a sound weld within the process and tinplate normal variations.

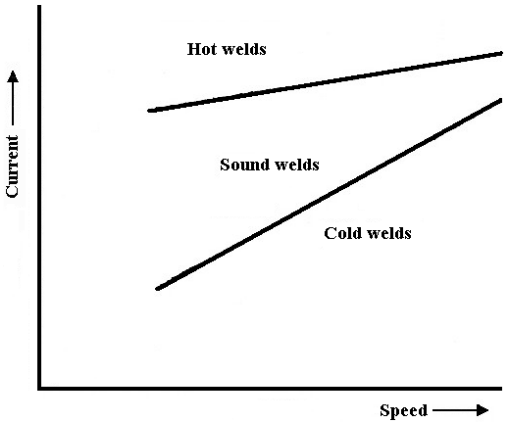

Figure 7.1: Typical example of a welding current range for low-carbon steel established by the welding current, welding speed and fixed electrode force. The range shifts upwards and becomes narrower with an increasing speed.

Despite the choice of parameter, as in most literature the welding ranges are best situated on the relation between welding speed and current at a constant electrode force [3]. A typical welding range is represented in figure 7.1. The figure shows a welding current range for low-carbon steel. With an increasing speed, a higher welding current is required that induces less heating variation to produce a sound weld. In order to guarantee the weld quality the limits of a welding range are defined by:

- Lower limit determined by a stuck weld condition (i.e. cold weld)
- Upper limit determined by formation of splash (i.e. hot weld)

The wider the welding range, the broader the variable parameter limits and hence the greater the control over acceptable and sound welds. Consequently, when welding can bodies, focus should be on setting a maximum range to give welding optimal freedom for compensation of (normal) variations in the material properties. [8, 48 and 49]

7.2.1 Lower limit

Coherent to the lower limit of the welding range is the assessment of the weld strength. With the determination of the lower limit an objective and meaningful value needs to be obtained to meet the essential (mechanical) properties to facilitate the service requirements (e.g. sufficient ductility and adequate strength). Since metallographic examination can be complex, and in particular time consuming, requirements for the lower limit ought to be tested in a simple and effective test. For that reason, mechanical testing (destructive testing) is the best option. Although some tests are more severe than others, the following generally accepted tests methods are utilised for lower limit determination:

- Inside out tests (i.e. flange test): the welded can body is turned inside out
- Ball tests: a steel ball is forced along the inside of the welded can body at the weld seam and base material
- Cone testing: the welded can body is pushed on a cone-shaped mandrel
- Tear tests (i.e. peel test): a tab at the end and begin of the weld is notched and pulled along the can body height

These test methods give a qualitative indication of the actual strength of the weld seam. The pulling direction of the tear test can be under a 0º or a 45º angle with respect to the welding direction. The difference between the two methods is the criteria for a cold weld, which will be stricter for the 45º-tear test. Tear tests could also be used to detect hot welds. In most tests the imposed criteria require that a number of welds (e.g. ten, five from the leading to tailing end of the can body and five vice versa) do not to fracture in the weld seam, which indicates that the failure may only occur in the base material or HAZ.

The test methods are also fairly subjective since most tests are performed with human involvement. For this reason there can be a great difference in obtaining the lower limit with similar parameters settings and the same test method. Between the different manufacturers and

researchers there is lack of agreement over which test should be used in accordance with reproducibility, objectivity and applicability.

7.2.2 Upper limit

The upper limits of the welding ranges are determined by visual inspection of a particular number of welds. The criteria in this inspection imposes that on sight of material ejection from the weld seam (i.e. formation of splash), the upper welding limit is passed. Visual inspections are conducted under a light microscope, normally at magnifications of 10 to 40 times the original size. Determination of the upper limit is done by cutting the weld and a part of the base material along the entire can body height and inspecting it from the leading to the trailing end. The inspection takes place at what is assigned as the inside of the can since formation of splash is first encountered at this side due to a higher current density (i.e. higher temperatures).

A more severe criterion is that surface cracks and roughness, and porosity (e.g. commas) are the limitation in obtaining the upper welding limit. For example, many can manufacturers classify commas as an upper limiting condition, because of the poor mechanical properties encountered upon deformation of the weld seam. Consequently, the examination method for the determination of the upper limit becomes more sophisticated and time consuming, since formation of these defects can occur at the surface and on the weld interface line.

7.3 Weld quality classification

In the published literature, one criterion of the microstructure was suggested for the determination of the lower limit [50]. This criterion is defined as a percentage of incomplete bonding across the weld interface line, as given in table 7.1 and later discussed in chapter 12.

Table 7.1: Overview of the weld quality-rating scale defined by 50.

Rating	Quality	Description
1	Cold	No grain growth across weld interface; slight tin bonding
2	Slightly cold	More than 25% tin bonding; some grain growth
3	Fair	Less than 25% tin bonding; 50% grain growth
4	Good	Minimum of 75% grain growth across weld interface
5	Slightly hot	100% grain growth; evidence of martensite transformation
6	Hot	Extensive martensitic transformation; metal expulsion

Williams et al [52] say that from an ideal point of view, weld quality should be determined by detailed metallographic analyses. However, this is a complex and time-consuming operation,

because weld quality is very dependant on the heat generation and development; hence the microstructural evaluation. Consequently, a wide range of metallurgical features can be used to categorise the welds. Williams et al tried to use metallographic features as shown in figure 7.2 to define the integrity of the high-speed resistance welds. Based on practical analyses they divided the weld quality into the following six criteria:

A. Overlapping weld nuggets, each consisting of columnar grains
B. Barely touching weld nuggets, each consisting of columnar grains
C. Large weld nuggets consisting of columnar grains, separated by a region of acicular ferrite or acicular ferrite and coalesced carbide region
D. Medium sized weld nuggets consisting of columnar grains, separated by a region of acicular ferrite or acicular ferrite and coalesced carbide region and with an additional region of equiaxed ferrite
E. Smaller sized weld nuggets separated by acicular ferrite and a region of coalesced carbide, a region of equiaxed ferrite and a region with a visible (non-bounded) interfacial line
F. No defined weld nugget, just a visible (non-bounded) interfacial line

The welds as defined by the classification above mainly describe microstructural phenomena, (see chapter 12) which evidently can be used as a basis for determination of the welding range.

As mentioned before many different factors affect the quality of the weld. The main factors are shown in figure 7.3, which also indicates some scientific basis for the complexity within the HSRW process. Figure 7.3 is a translation of the energy balance, shown schematically in figure 6.1. In order to comprehend the weldability and weld quality form this diagram, the physical phenomena and evolution behind the welding process need to be considered.

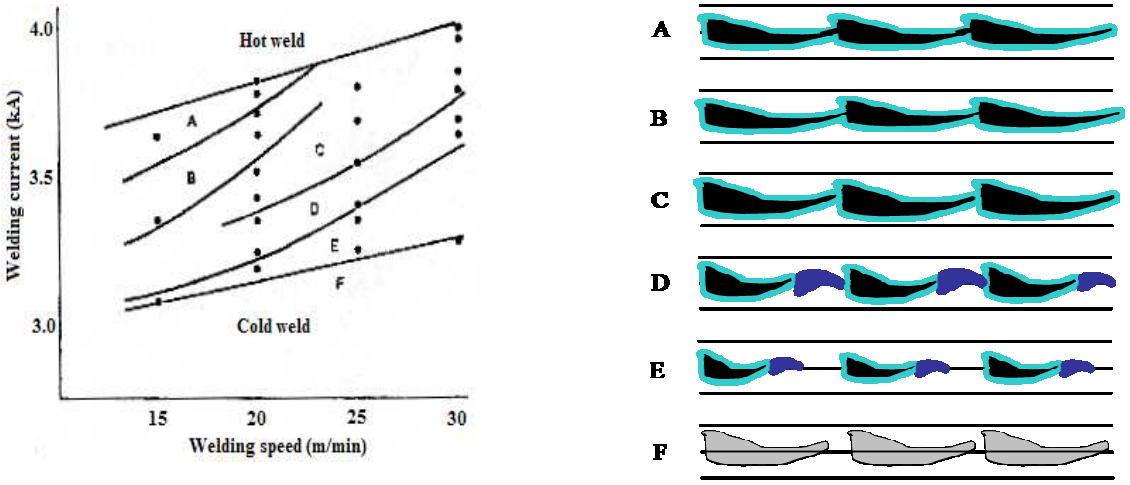

Figure 7.2: Schematic classification of the weld quality grades on the right-hand side. From top (A), fully welded to bottom (F), non-bonded. The left hand-side shows the corresponding welding current range for the low-carbon steel established by the welding current and welding speed. The straight linear lines give the lower and upper limits of the range. The lines in between indicate the areas of the six classifiable criteria. [52].

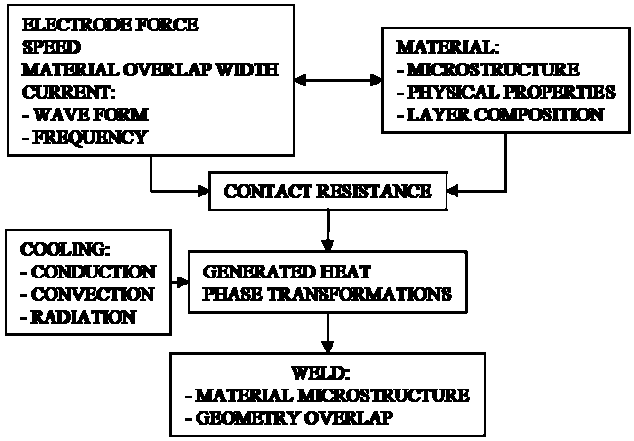

Figure 7.3: Schematic overview of the physical and thermal factors showing how they affect each other and the integrity of a high-speed resistance weld.

8 Process parameters

8.1 Current

The first significant process variable is the welding current applied to the system, which is controlled and fixed by a potentiometer. When maintaining a constant welding current and varying other process parameters and material properties, the form and integrity of the weld changes, possibly introducing poor quality welds and defects. An increase in the welding current whilst restraining the other parameters will increase the length of the weld nugget and make the weld thinner (in the through thickness direction), and wider as a consequence of higher temperatures and larger temperature gradients. With an increasing welding current the weld nugget size alters since more heat is applied to the materials. Eventually with a too high a welding current there is a risk of creating a hot weld with extremely large weld nuggets.

Generally, as the welding current is increased the extent of weld nugget penetration into the sheet increases, whereby the growth of the weld nugget mostly extends to a greater part of a theoretical weld nugget size (see section 8.3), until a certain welding current level reaches the theoretical length. The theoretical weld nugget length is not always attainable since the capacity of the sheet to carry the welding current could be exceeded, whereby the steel sheet can be burned (i.e. overheated).

The relationship between contact resistance and the minimum welding current required to produce a weld of good quality is for example shown in figure 8.1; both tinplate grades have a small tin layer thickness and show that as the contact resistance increases, the minimum required welding current decreases [28].

Within the literature a division is sometimes made between primary and secondary welding current. Primary current is the welding current that the welding machine delivers to the work-pieces. Secondary current is a temporary current induced by the primary welding current, which passes through the electrical circuit at the start and end of the primary welding current employment.

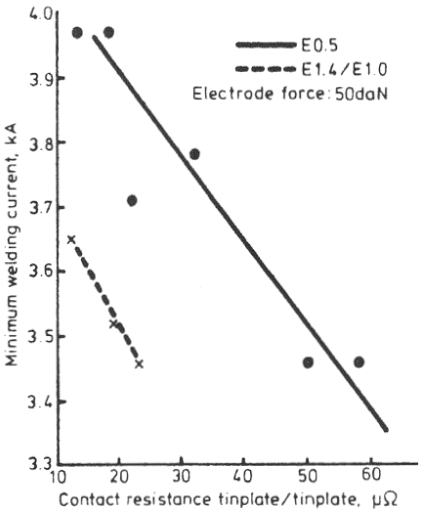

Figure 8.1: Effect of contact resistance in [μΩ] with a minimum welding current in [kA] required for a satisfactory weld nugget formation of E1.4/E1.0 and E0.5 tinplate grades when applying an electrode force of 500N.

8.2 Electrode force

The spring-loaded force on the electrode wheel influences the contact resistance as shown in figure 8.5. The essential positive effect of the electrode force is to lower the difference in contact resistance between different tinplate material grades and thereby promote the growth of weld nuggets and contain the formation of any formed liquid material.

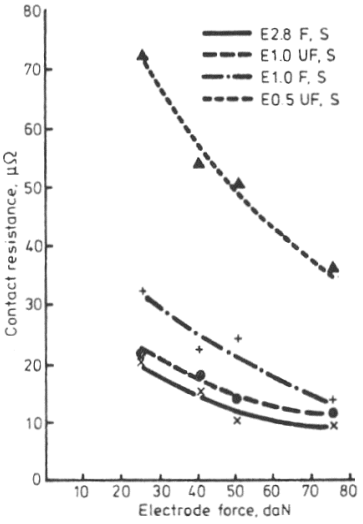

Figure 8.2: Effect of the electrode force in [daN] in the range of 250 to 750N on the contact resistance in [µΩ]. F and S represent flow-melted and stoved, respectively.

Figure 8.5 shows that as the electrode force increases the contact resistance decreases. For tinplate with a relative low initial contact resistance, the contact resistance tends to have a minimum at electrode forces between 500 and 750N. Application of different tin coating weights (i.e. E-numbers) shows that the difference in contact resistance reduces when increasing the electrode force. However, the relative difference in contact resistance between the different tin coating weights remains quite similar.

The values for the contact resistance obtained with tinplate-electrode and tinplate-tinplate configurations are identical. Higher tinplate-tinplate and tinplate-electrode contact resistances are associated with flow-melted tin layers and tempered sheet steel (i.e. heat-treated).

Figure 8.4 shows the dependence on the available welding current range with an increasing electrode force. As expected from the contact resistance, lower tin coating weights require the electrode force to be increased in order to get a sound weld within a reasonable welding range.

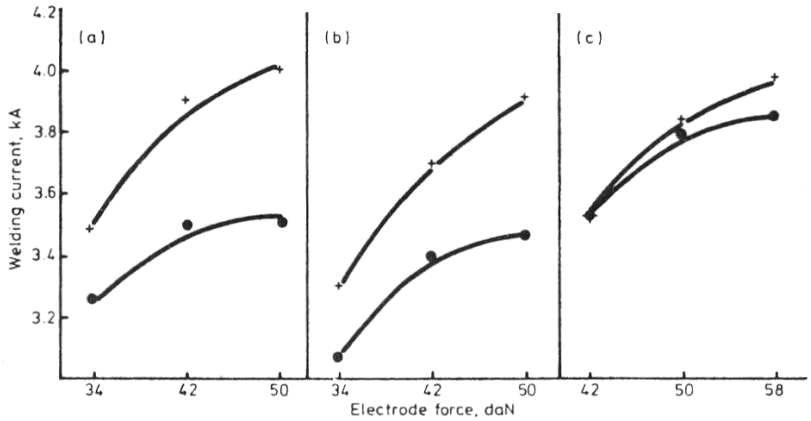

Figure 8.3: Diagrams of welding ranges for a) E1.4, b) E1.0 and c) E0.5 tinplate material grades with respectively a contact resistance of 19, 23 and 32 µΩ on the basis of an increasing electrode force in [daN].

An increase of the electrode force establishes better contact (i.e. less resistance) on the weld interface line and on the tinplate-electrode interface; hence less heat development, lower temperatures and less steep temperature gradients. However, more electrode force also induces more deformation of the weld seam. With a higher electrode force, the lower contact resistance creates the possibility of a cold weld; therefore a higher welding current should be applied to give a sound weld. The welding range can be twice the range when increasing the load from 400 and 700N (see figure 8.4).

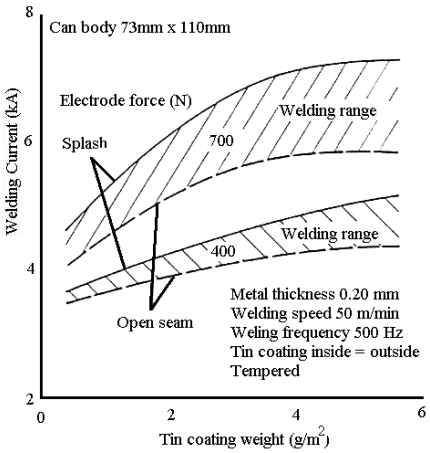

Figure 8.4: Diagram of the welding current range at different coating weight showing the difference with two electrode forces.

8.3 Speed and Frequency

The influence of welding speed used on weld formation is expressed in the extent of overlapping weld nuggets to produce a gas tight seam. In this respect there is a limit to welding speed at any given welding current frequency, "*the achievable welding speed by alternating current welding is restricted by the available current frequency*" [51]. This indicates that the frequency can be altered to meet higher speeds. However, a maximum possible weld nugget length is still governed by the frequency (i.e. pulse width) and the speed (i.e. travelling distance). The maximum theoretical value for the weld nugget length, d in [m] can be obtained for a given frequency, f in [s^{-1}] and speed, v in [m/s] by [52]:

$$d_{\max.nugget} = \frac{v}{2f} \tag{8.1}$$

Generally, as the welding current is increased, weld nugget growth extends to a greater part of the theoretical maximum nugget length (figure 8.5). The limiting speed at each frequency arises from the inability to apply sufficient heat to the weld interface without overheating the material. As a result, at lower speeds a minimum number of weld nuggets per length of material is easily set for pressure-tight seams. However, to keep the minimum weld nuggets criteria at higher speeds the following issues are essential:

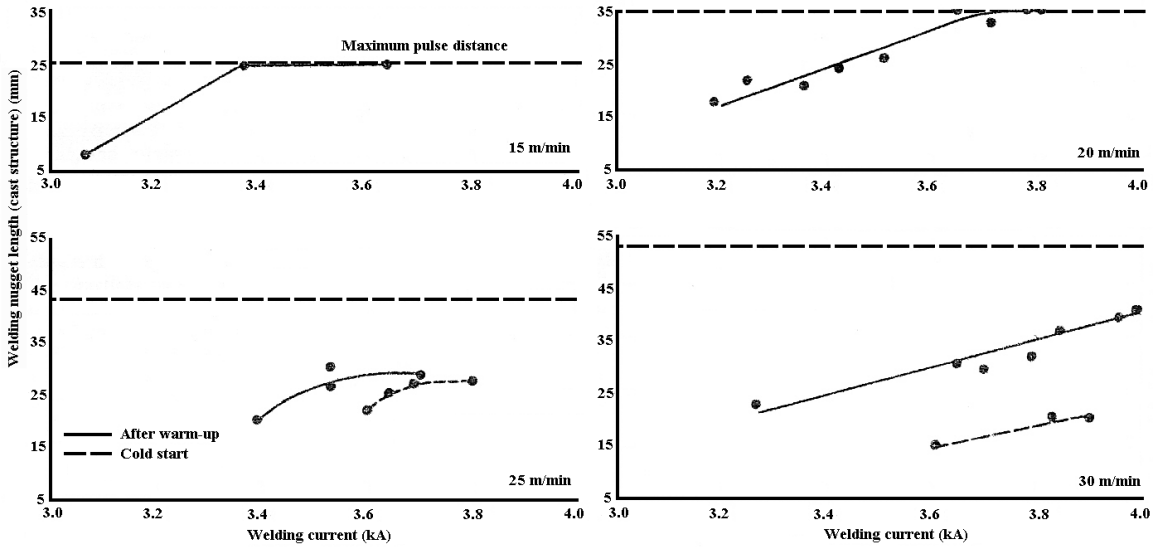

Figure 8.5: The four diagrams show the influence of the welding current on the weld nugget size for different welding speeds. The dashed horizontal lines are the maximum theoretical value for the weld nugget length. The dashed curves in the two bottom diagrams come from tinplate that has been welded after a heating stage. The solid curves were welded from room temperature (i.e. cold start) [52].

- Higher degree of the oval shape of the weld nugget
- Higher heat penetration into the surrounding material
- Decrease in gap width between the weld nuggets
- Lowering the promoted wedge shape of the weld nuggets

Alteration of the welding speed and frequency is mostly translated to temperatures and temperature gradients between weld centre and surface and their influence on the formation of the weld nugget (i.e. microstructure). If the welding speed is low, the high thermal and electrical conductivity of the copper electrodes and the increased contact time of the electrode wheels and the overlap width allow more time for heat generation followed by heat loss. As shown in figure 8.5 the maximum weld nugget length is easily attained. In addition, lower welding speeds also offer a more effective temperature balance with the majority of heat produced at the weld interface line.

Conversely, high speeds induce less time for heat generation and cooling of the weld area; providing inferior temperature balances and the possibility exists that the tinplate or electrode wire could burn by overheating. Finally, the welding current does not flow in a simple path between the electrodes as it does with lower speeds.

Figure 8.5 also shows that a heating stage before welding requires a higher current (i.e. more heat input) to obtain the same weld nugget length, as this creates a lower temperature gradient.

To reduce the weld nugget separation distance, an increase of the welding current could provide longer weld nuggets. From the work of Williams et al [52] figure 8.6 shows the effect of an increase in welding speed when displaying longitudinal weld cross-sections. They found increasingly larger and more separated weld nuggets at a fixed frequency and speeds of 30 m/min, and slightly thinner and overlapping weld nuggets at the speeds of 15 m/min and concluded that lower speeds are more suitable for gas-tight seams. Shimizu et al [44] also found as shown in figure 9.7 the effect on the nugget development; increasing the welding speed influences the quantity and quality of bonding on the weld interface line.

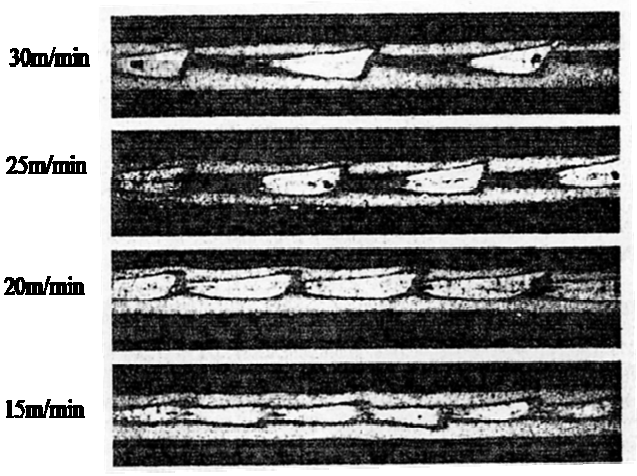

Figure 8.6: Influence of the welding speed on the formation of weld nuggets. Etching with 4% picral and a magnification of 18x [52].

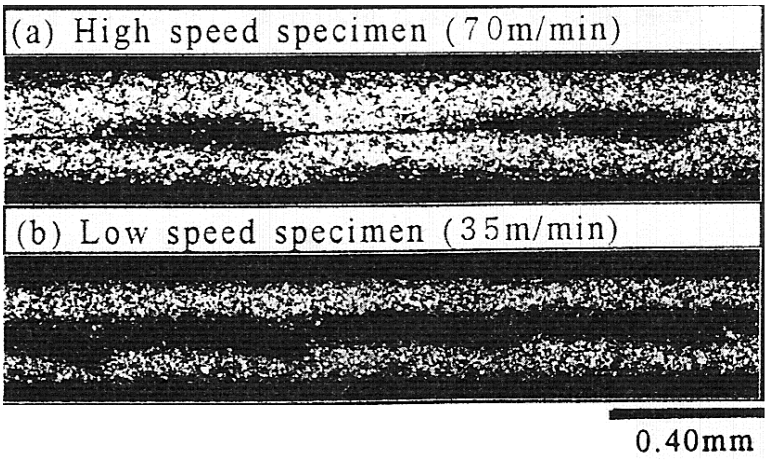

Figure 8.7: Longitudinal cross-section of the weld seam, showing the effect of two different welding speeds, (a) 70m/min and (b) 35 m/min on the nugget formation, microstructure and hence the weld quality. The distance scale on the bottom is 0.40mm [44].

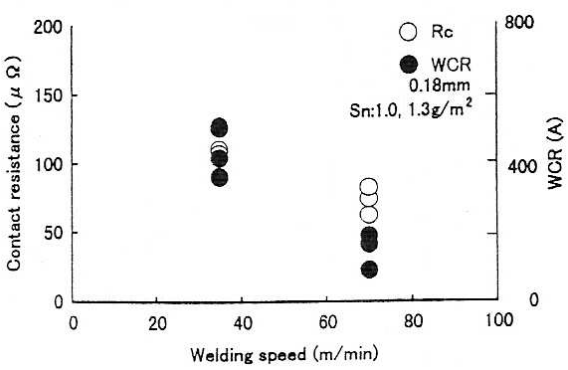

Figure 8.8: Diagram with the effect of the welding speed in [m/min] on the contact resistance, Rc in [μΩ] and welding current range, WCR in [A]. The thickness of the tinplate was 0.18mm and the tin coating weights were 1.0 and 1.3 g/m^2 on one side of each sheet [44].

Finally, Shimizu et al also displayed the welding speed and welding current range in relation to the contact resistance (see figure 8.8). They found that both parameters decreased with an increasing welding speed.

To date, for high welding speeds there is a frequency alteration, which compensates for the poor temperature balances thereby allowing speeds of up to 115 m/min with a sound weld seam.

8.4 Contact surfaces

Maintaining an accurate overlap width along the can height is one of the main process variables. An accurate overlap width is affected by the size of the overlap, thickness of the tinplate, thickness of the tin coating and contamination of the welding area from initial and weld-created surface layers. Contamination of the weld area by oxides, varnishes, inks, etc. can result in gross sparking and weld defects [3]. It is therefore important that the dimensions of the can blank and the matching overlap width are within the correct limits.

Over the years the capacity to reduce overlap widths changed, thereby reducing the amount of material. Today, the overlap width for three-piece containers is 0.5 to 0.7 mm, given that the weld needs to be gas tight and withstand (cooking) pressures during the sterilising process. If the overlap width is reduced, higher temperatures are observed during welding, followed by thinner welds and excess of weld edge extrusion. Between the overlap width and tinplate thickness there exists a trade-off in terms of welding speed, frequency and electrode force to provide a sound weld. Typical mash seam welding is done with relative overlaps in the order, 1 to 2 times the base material thickness, and relative joint thickness in the order of 110 to 130% of the base metal thickness. This range of overlaps and final joint thickness corresponds to strains on the weld interface line from about 120 to 175%.

Shimizu et al [44] also discussed the contact length between the tinplate and the electrode wheels, which correlates with the welding current range (WCR) as shown in the left-hand side diagram of figure 8.9. It shows that the welding current range increases when with greater contact

length. They also found an effect of the contact length with different coated tinplate sides, as shown on the right-hand side of figure 8.9. This diagram shows the welding ranges and the contact length. The contact length demonstrates a parabolic character with increasing tin coating weights. At higher welding speeds the applied effective force (contact length between electrodes and welded sheets) is relatively low. As a result the dynamics of the process significantly reduce the welding range. Therefore, at higher welding speeds the weld nuggets do not overlap due to reduced contact times between the electrode wheel and on the weld interface area.

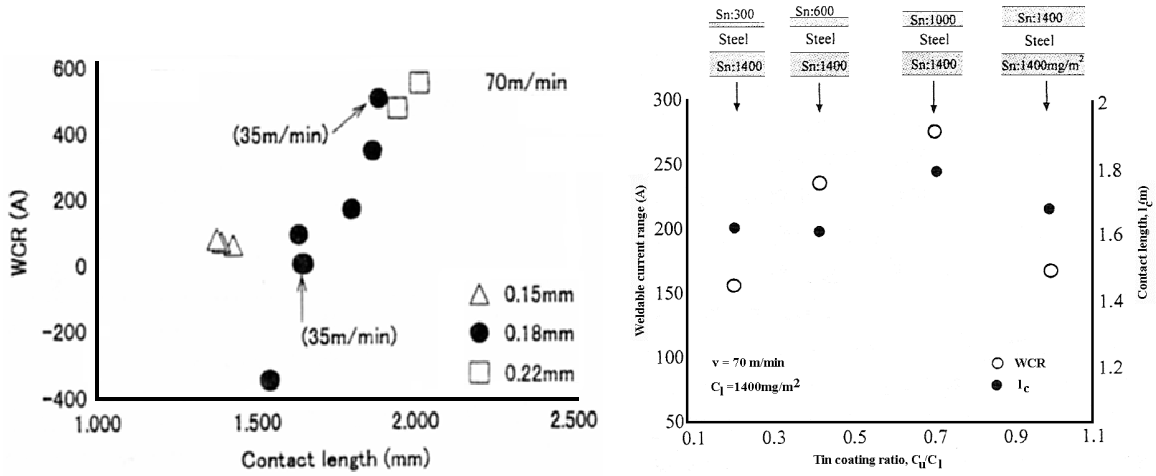

Figure 8.9: On the left-hand side the effect of contact length in [mm] on the welding current range, WCR in [A] with respect to a welding speed of 70m/min and three plate thicknesses is shown [44]. The right-hand side shows a relation between the contact length in [mm] and the welding current range, WCR in [A] with different applied tin coating ratios; visualised above the diagram [45].

9 Tinplate and material properties

Since the welding process is susceptible to slight changes in the operating conditions. It is also sensitive to the majority of the tinplate properties (e.g. plate dimensions, tin coating weight, steel chemistry). Some examples of the broad and remarkable relationship between the process parameters and the material are shown in figure 9.1.

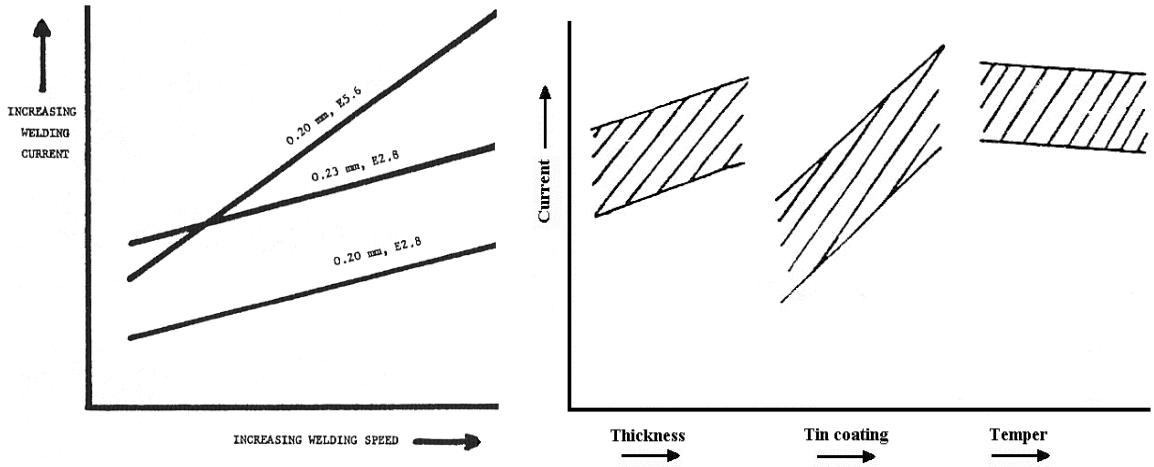

Figure 9.1: Representation the left-hand-side of the effect of gauge and tin coating weight variation on the welding parameters welding current and speed [3]. The right-hand side shows the effect of tinplate thickness, tin coating and sheet temper with the welding current and hence the welding ranges [5].

Consequently, by means of the contact resistance most tinplate properties affect the weldability. For this reason the basic tinplate specifications are of great importance to minimise welding failures of the can body and to optimise the welding range.

Conventional tinplate has very low and consistent contact resistance therefore most resistance is generated in the tinplate. For example spot welding promotes uniform and reproducible heating to the desired welding temperature, within which surface roughness, degrees of passivity, or oil levels have no essential effect on contact or total resistance under pressure, "*Tinplate has almost ideal surface for resistance welding because the tin is so readily deformable under only moderate load, that oxides, oil and surface contaminants are easily displaced by physical movement of the deforming tin layer, and by subsequent melting of the tin when it is heated to just 232°C*" [9]. However, tinplate parameters such as coating level, thickness, tempering and hardness (i.e. carbon content and distribution) are critical with respect to the HSRW process.

9.1 Production process

Before proceeding with the tinplate properties, it is important to describe the tinplate production. The production route for tinplate by electrolytic tinning in a coating plant is shown schematically in figure 9.2. Starting with hot-rolled sheet steel entering the pickle line, surface scale and oxides formed after hot rolling, and during transportation and coil storage are removed. Typically, 0.6% of the weight of the steel coil is removed during the pickling process.

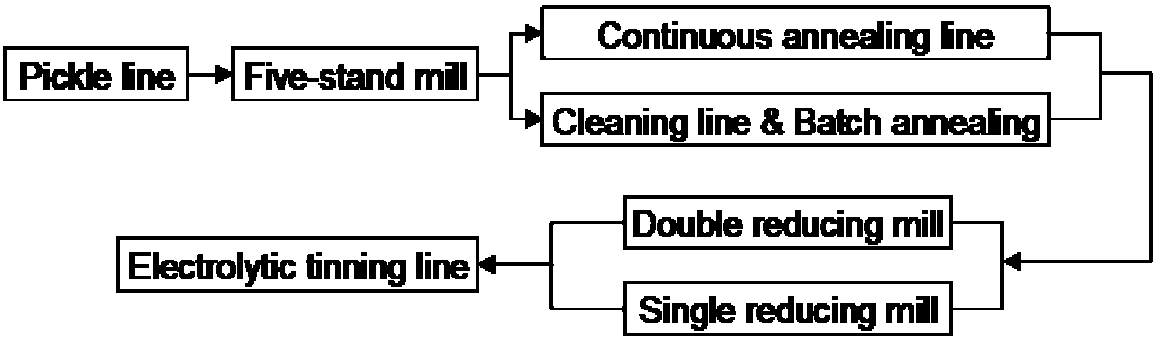

Figure 9.2: Schematic overview of the final steps in the production line for making tinplate-packaging steel.

After pickling, the sheet is sent through a cold mill, which employs a continuous cold reduction. The mill reduces the gauge of the sheet to get a sufficiently thin steel sheet, which forms the basis for electrolytic tinplating. The steel coils are cleaned to remove all traces of oil and grease, and annealed (batch or continuous) to remove the work hardening and stresses introduced by the cold rolling. The steel sheet is reduced further in the double reducing (DR) mill, to get the correct sheet dimensions and to provide a smooth steel surface. During annealing, some scale may have formed on the surface, therefore in the tinning-line, the strip is pickled and washed with an alkali solution to remove oil and grease traces. This is followed by passage through a series of electrolytic cells, of which one is shown schematically in figure 9.3. Two bars of pure white tin are closely situated on either side of the steel sheet. By connecting the tin bars to the positive terminal of a DC generator, they become

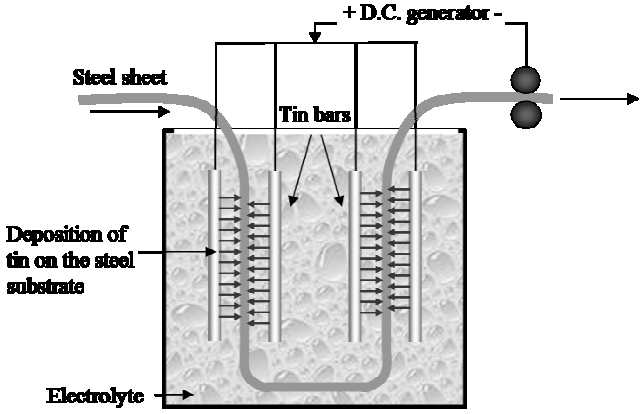

Figure 9.3: Schematic of the principle of electrolytic tinning of packaging-steel.

anodic whilst the steel connected to the negative terminal becomes cathodic. A current will flow through the system by which tin is extracted from the solution and deposited on the steel sheet. To remove excess electrolyte solution, the sheet is washed. At this stage, the surface of the strip has a dull, matte white finish. A smooth surface is achieved by flow melting the tin. This is done by passing an electric current through the sheet. Immediately after flow melting, water sprays to prevent oxidation cool the tinplate. Spraying the sheet with a weak chromic acid and steam drying it prevents discolouration. For subsequent processing, the sheet is sprayed with an emulsion. After this, a measuring system ensures the thickness of the tinplate within the customers' tolerance. Before passing a pinhole-detector, the sheet also passes a series of rollers to relieve internal stresses. The sheet is cut by shear into the required dimensions, depending on the application [53 to 55].

9.2 Iron-tin binary system

Considering the electrolytic applied tin, many stable inter-metallic compounds can be formed under equilibrium conditions of temperature, pressure, etc. Up to 910 °C in the phase diagram (see figure 9.4) compounds, like FeSn, $FeSn_2$, Fe_3Sn, Fe_3Sn_2 and Fe_5Sn_3 exist [56 to 59].

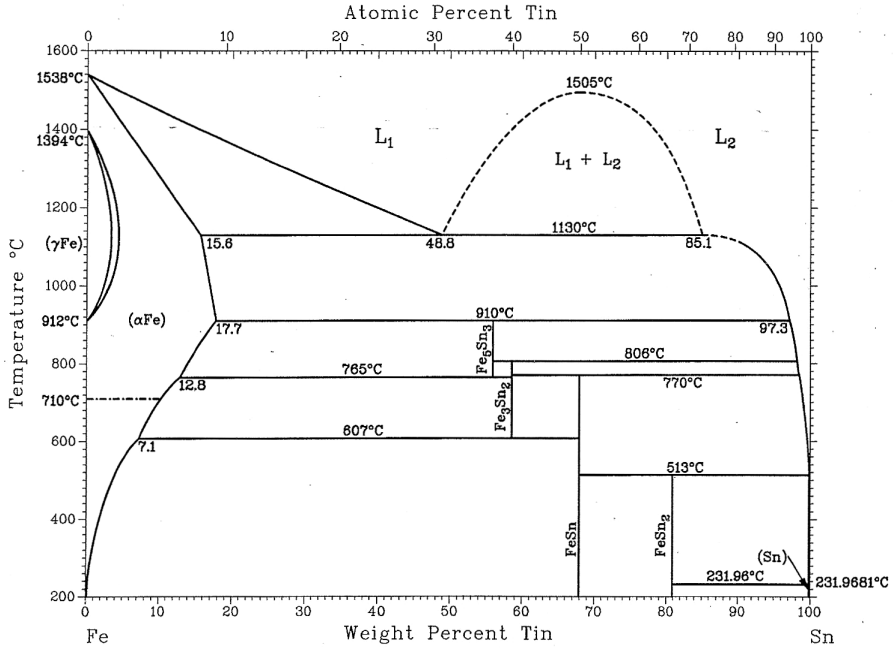

Figure 9.4: Iron-tin phase diagram. On the bottom and top, the tin composition in weight and atomic percentages respectively are shown. The temperature on the vertical axis is in degrees Celsius. The temperatures and percentages in the phase diagram indicate the values at which certain phase transformations take place [58].

Between 607 and 910 °C Fe_3Sn_2 and Fe_5Sn_3 form at 56 and 59 wt% tin respectively. These phases are created at elevated temperatures and therefore unstable and absent at room temperatures. The compounds, FeSn and $FeSn_2$, which contain 68 and 81 wt% tin respectively, are the only two inter-metallic compounds that are stable under ambient conditions and found at room temperature. The phase diagram does not show the formation of Fe_3Sn, at 42 wt% tin at 770 to 880 °C. However, Fe_3Sn is an oxygen stabilising compound and richest in iron content [56 to 58].

The iron-tin phase diagram shows that iron and tin significantly affect each other's transformations and physical factors. The effect of tin on polymorphic transformations of iron shows only 1 wt% tin raises the transformation temperature from $\alpha \leftrightarrow \gamma$ by about 40 °C whilst lowering the $\gamma \leftrightarrow \delta$ transformation temperature by 140 °C, this loop closes at 2.5 wt% tin and 1150 °C. On the tin rich side, the melting point rises to 650 °C, 800 °C and 910 °C by additions of only 0.3 wt%, 1.7 wt% and 2.3 wt% iron respectively. At the higher temperatures, iron and tin show a range of immiscibility or metastable phases in the liquid stage from 50 to 85 wt% tin. Finally, it should be mentioned that the melting point of tin is 232 °C, whilst its boiling point is 2602 °C, which indicates that tin has a large molten range compared to other metallic compounds, ~2370 °C [57 to 59].

9.3 Sheet gauge

The thickness of the tinplate has a considerable influence on the contact resistance and hence the welding range. By obtaining thicker tinplate, higher current levels are necessary to give sufficient weld qualities. This indicates that large variations in tinplate thickness can cause inconsistent and even poor weld qualities. The welding ranges become smaller with thicker sheets, whereby at too thick a sheet, the upper and lower welding limits surpass each other, and no welding range is left for a sound weld. A higher welding speed even intensifies the effect of larger sheet thicknesses. As a result, the weld nugget development decreases with increasing sheet thicknesses as shown in the right-hand side diagrams of figure 9.5.

The cut-off point of the welding range allows thicknesses above that point to have a particular tolerance without varying other welding parameters. Consequently, welding machines can be set to have a certain material thickness tolerance. Yet, welding parameters need to be altered when going beyond the cut-off point. The variations in the tinplate thicknesses are optimally controlled when varying the welding speed.

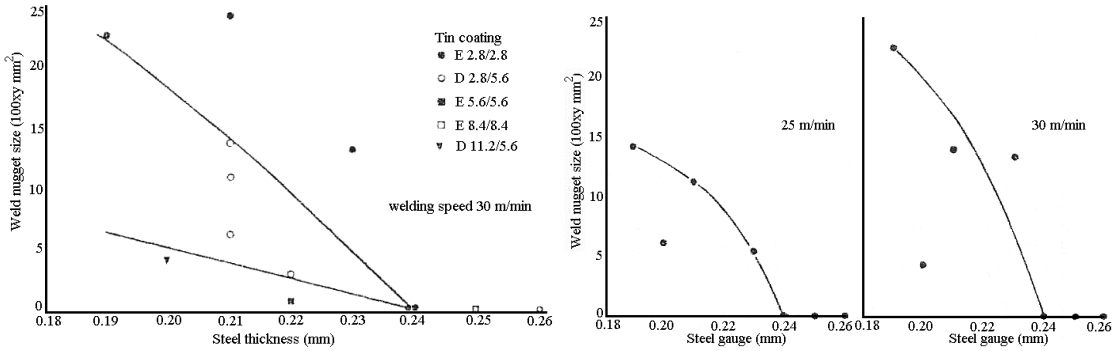

Figure 9.5: The left hand-side picture shows the relation between the tinplate thickness in [mm] and the weld nugget size in [mm^2] with different tin coating weights. The right-hand side shows a similar relation only with various welding speeds in [m/min].

Gregory et al [5] also indicate that control of the tinplate thickness is a prime material factor in the HSRW process. They found a rapid change in thickness tolerance when going to higher welding speeds whilst a minimum of 10% tolerance in µm should be maintained. They also mention that at maximum welding speeds, 5% tolerance is still required for satisfactory welding, which can be attained by high precision upstream processing.

If the weld quality needs to be maintained, higher levels of weld current can also be applied for thicker tinplate. Williams et al [52] also found that the welding range decreases between the lower and upper limits as shown in figure 9.6. Essentially, when welding thicker tinplate and obtaining a good quality weld, standard practice would be a slower welding speed with an increased welding current.

Shimizu et al [44] looked at the thickness of low-coated tinplate at welding speeds of 70 m/min and found the contact resistance being adversely affected by thicker sheets and the welding current range becoming effectively larger, as shown in figure 9.7.

Decreasing tinplate thickness and higher carbon levels promote the effect of splashing because increase in bulk resistance causes more heating in the bulk of the material. With these features weld nugget penetration becomes larger and the temperature gradient between interface and surface decreases and so higher temperatures at the surface will occur.

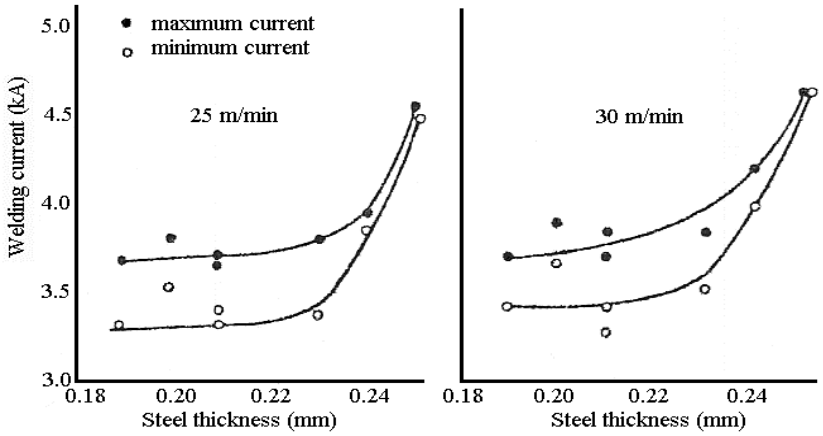

Figure 9.6: Welding current limits in [kA] in relation to the tinplate thickness in [mm] at two different welding speeds in [m/min] at constant carbon content [52]. Both diagrams show a smaller welding current range with an increasing tinplate thickness.

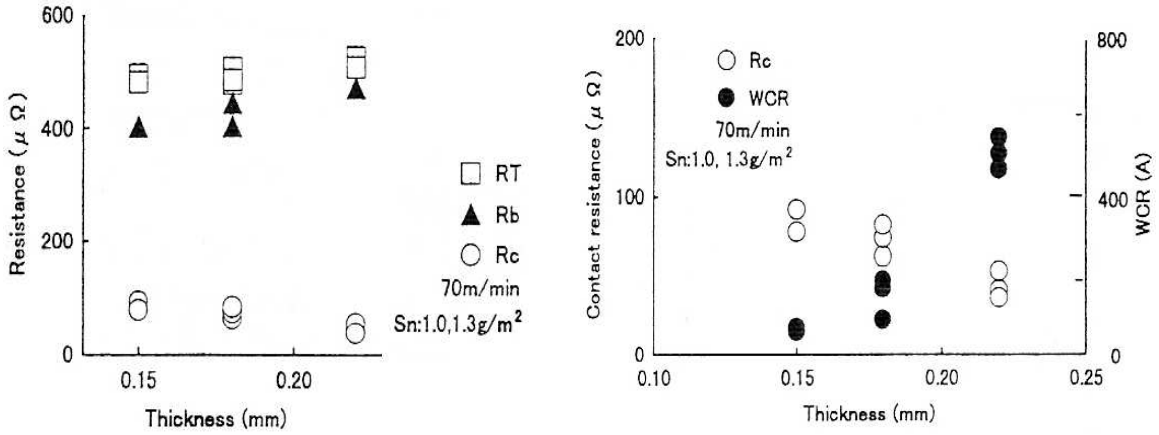

Figure 9.7: The left-hand picture shows the effect of the total resistance, RT, bulk resistance, Rb and contact resistance Rc in [μΩ] when increasing the tinplate thickness. The right-hand side picture also shows the effect of the thickness increase on the welding current range in [A]. Both picture were made with a welding speed of 70 m/min and a tin coating weight of 1.0 and 1.3 g/m^2 at one side of each tinplate container and with thicknesses of 0.15, 0.18 and 0.22mm.

9.4 Sheet coating layer

Over time several weldable tinplate grades with as low as possible tin coating weights were developed. To date, tin coatings with 2.8 g/m^2 of tin on each steel sheet side (i.e. E 2.8/2.8 grade) are used. Even though tinplate is commonly used, the following materials are also set in three-piece containers since production and economical reasons make them more viable:

- Chromium/chromium oxide (ECCS) /Tin Free Steel: low-carbon steel that is coated equally on both sides with a complex metallic coating by electro deposition
- Blackplate and full hard: low-carbon and uncoated steel
- Polymer coated steel: blackplate covered with a polymer produced by either film coating or direct extrusion

The type and thickness of the coating influence the contact resistance and hence the absolute temperature and temperature gradients. Sodeik [9] measured a static electrical contact resistance at different electrode forces, of which the results are shown in table 9.1. One-side coated tinplate increases the contact resistance by a factor 50 wherein the non-coated side becomes the predominant source of heat generation and whereby the total resistance variation leads to inconsistent heating. Low-coated tinplate gave welding troubles whilst blackplate, with a several day old surface and TFS also showed high static contact resistances. However, blackplate freshly cleaned before welding displayed much lower and more consistent total resistance phenomena, yet the surface deteriorates after several hours of exposure to room atmosphere, creating an iron

Table 9.1: Measurements of the total resistance in [mΩ] and its variation for a series of identical samples providing an indication of the ease of welding of various materials and tinplate coating weights in [g/m^2].

Plate	Coating	Resistance (mΩ)	Steel part of resistance (%)	Remarks
Tinplate	E 5.6/5.6	0.028 ± 0.002	70	−
TINPLATE	E 0.5/0.5 to E 5.6/5.6	0.025 ± 0.004	50 to 80	−
Tinplate	E2.8/0	0.4 ± 0.2	5	Large scatter
Tinplate	E0.5/0.5 Fully alloyed	0.7 ± 0.2	3	−
Blackplate	−	18 ± 5	0.1	Large scatter
TFS	Chromium	22 ± 5	0.1	Large scatter
TFS	Nickel	0.5 ± 0.1	5	

oxide layer. The Nippon Steel corporation reports on the development and the properties of light nickel coated steel (i.e. Canwel) and light tin coated steel (LTS) [43 and 60], of which were both electrically treated with chromic acid, and found to have a good weldability for high-speed can manufacture. They made a comparison between static and dynamic contact resistance, which is shown in figure 9.8. The static contact resistances corresponded with the results from Sodeik. However, for most materials in contrast with the static contact the dynamic character induces better weldabilities. According to Asano et al [60] the reason for the good dynamic resistances is found in the steel sheet resistivity, electric current path, surface contact state, and their mutual relation before and during welding. They determined that metals with high contact resistance coatings would likely involve expulsion of a liquid phase due to abnormal localised generation of heat. Asano et al concluded that tin, due to its low melting point was the most effective coating to improve weldability and attain satisfactory corrosion resistance compared to blackplate. Elzinga and Bisel also verified this effect of the weldability with the application of different metallic coatings on packaging-steel [61].

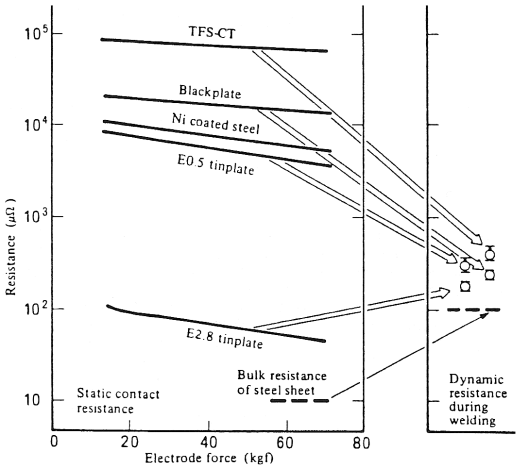

Figure 9.8: Difference between the static contact resistance at different electrode forces in [kgf] and dynamic contact resistance both in [μΩ] presented by [43].

The tin coating thickness is generally specified by the application, contents and lifetime of the container. Various literature sources indicate that weld nugget formation is most effective and provides optimal welding ranges with an E 2.8/2.8 tinplate grade. Norman et al [3] even said that in contrast with the welding parameters there is no problem in achieving a good weld quality when welding tin coating weight levels of up to 5.6 g/m^2. Lowering tin weight levels, the minimum required welding current progressively decreases since the contact resistance becomes higher. At medium tin coating levels the significant contact resistance forms conventional weld nuggets as a result of liquid formation [28]. Williams et al [52] found that with higher coating weights; up to 11.2 g/m^2, smaller weld nuggets were formed. Yet, to attain a certain weld nugget size, the material needed to be welded at slower speeds. The reason for this was said to be the greater shunting effect (i.e. moving) of the welding current around the weld nugget, in accordance with the temperature distribution. The thicker tin coatings also require higher welding currents to create sound welds, as shown in figure 9.9 [3, 5, 45 and 62]. Figure 9.9 indicates that the amount

of tin coating on the steel surface specifies the welding current range, which becomes smaller with a decrease of the tin coating weight.

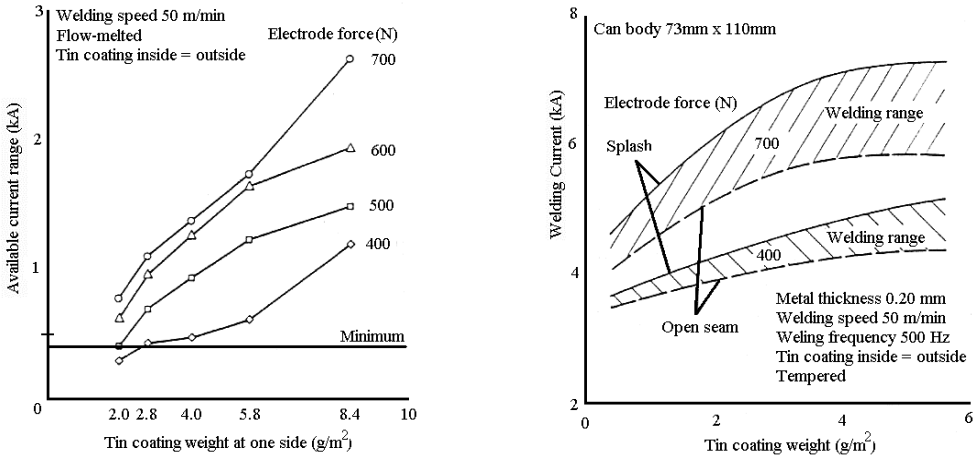

Figure 9.9: Two diagrams showing the welding current range in [kA] as function of the tin coating weight in [g/m^2] at one side of the tinplate for different electrode forces and a welding speed of 50 m/min [4].

Besides speed and current other welding parameters are said to provide less variation in order to achieve a good quality weld. Fluctuations in the tin coating weights are a major issue when the welding speed is increased; because of rapidly formed poor weld qualities. Shimizu et al [44] investigated the weldability with different coating weights on each tinplate side at different welding speeds (see figure 9.10). They also found, as mentioned in section 9.3 a smaller welding range with higher welding speeds. The effect of the weld nugget development with different tin coating weights is shown in the figure 9.10 and on the right-hand side picture in figure 9.11. Gregory et al [5] mentions that to prevent any problems with tin coating weight variations, the weight levels should be as low as possible.

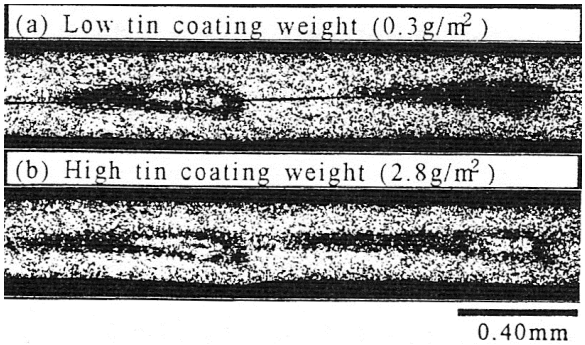

Figure 9.10: Longitudinal cross-sections showing the effect of (a) 0.3 g/m^2 and (b) 2.8 g/m^2 tin coating weight on the weld nugget formation; microstructure and hence weld quality at a welding speed of 70 m/min. The distances scale on the bottom is 0.40 mm [44]

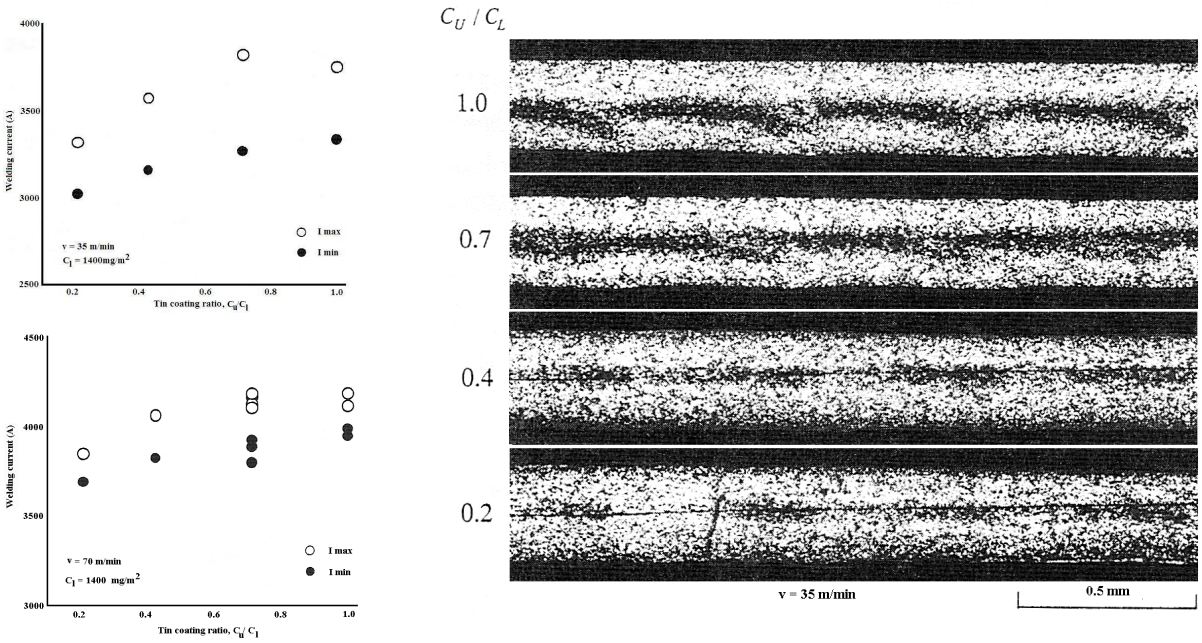

Figure 9.11: The left-hand side shows two diagrams displaying the welding ranges for different tin coating ratios when applying a welding speed of 35 and 70 m/min. The value of C_l is 1.4 g/m^2. The right-hand side diagram shows the effect of the tin coating ratio on the nugget development with a welding speed of 35 m/min. The distance scale of the photomicrographs is 0.5 mm [44].

The works of Waddell et al [28], and Ichikawa and Saito [43] both found a reduction of the electrical contact resistances with an increase of pure (white) tin on the surface, and that higher contact resistance from less pure tin on the surface resulted in poor welds. They considered that presence of the pure tin improved the contact conditions since pure tin is softer than the steel substrate and copper electrodes. Alloying (i.e. the ratio of iron-tin and pure tin) is influenced by heat treatments, such as flow-melting, steam drying and tempering. For a coating weight with a larger iron-tin alloy to pure tin ratio, a higher contact resistance, as shown in table 9.2 [28], was found, whilst conventional analytical techniques did not indicate the presence of pure tin over the entire surface, the results did suggest pure white tin in the overall coating. Table

Table 9.2: Typical contact resistance values in [μΩ] obtained, using a digital micro-ohm meter (APT-Model DMO 400) for tin coating weights in [g/m^2] on both tinplate surfaces [28].

	Contact resistance (μΩ)	
Tin coating weight (g/m^2)	**Range**	**Average**
2.8	7-14	11
1.4	16-25	19
1.0	10-27	17
0.5	10-81	37

9.2 also shows the better consistency in the contact resistance values at the higher tin weight levels. With respect to each tin weight in table 9.2, the following was observed:

- E 2.8: wide welding range (up to 15% of the welding current)
- E 1.4: acceptable welding range (10-15% of the welding current)
- E 1.0: acceptable welding range only at lower welding currents in contrast with E 1.4
- E 0.5: significantly narrow welding ranges, especially if the coating resistance is high

Low tin weights that were flow-melted, produced good weld qualities over relative wide welding ranges, more than 250A. The welding ranges even increased 330 to 500A (10%-15% of the welding current) with higher electrode forces. Low tin weights without temper have a low contact resistance and can only be welded with high electrode forces resulting in welding ranges of 100 to 300A (2% to 8% of the welding current). Conversely, with temper low-tin coated steels induce high contact resistance and hence cannot be satisfactorily welded, even after reducing the welding speed. Nevertheless, low-tin coating grades with a DR steel substrate could be welded when applying a sufficiently high electrode force. The work of Ichikawa and Saito [43] concluded that electrical contact resistance could even reduce when applying 0.2 g/m^2 tin extra on each side of the tinplate. Elzinga [62] concluded that pure tin between 0.43 and 0.86 g/m^2 on an un-flowed tinplate grade are readily weldable and that the lowest amount of 0.43 g/m^2 pure tin (i.e. the lowest amount of free tin) is even more weldable. Elzinga than relates this free pure tin layer behaviour to the determination of the welding ranges.

Ichikawa and Saito [43] also considered that pure tin on the material surface enlarged the area of the current path as shown in figure 9.12. Since pure tin is softer than the steel substrate and copper electrodes a larger current path area can be realised.

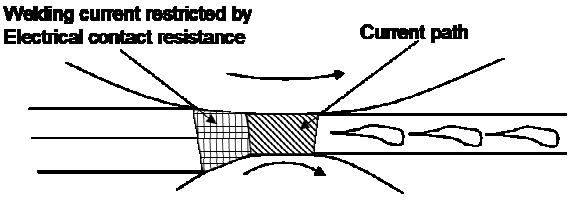

Figure 9.12: Region of current path and restriction to current by contact resistance.

Williams et al [51] mentions inter-granular cracking (i.e. micro-cracking) in the heat-affected zone when a high-tin coating is applied and welded above the upper limit of the welding range. This was clarified by the fact that from tin rich areas tin would penetrate along the ferrite grain boundaries and might even be considered at lower welding currents.

Simon et al [50] attempted to determine the influence of surface characteristics with wire welding by statistical analysis and discovered that no single parameter tested, including tin coating weight level, profile surface roughness, and annealing conditions directly related to the weld quality. Tin layer thickness by itself did not significantly affect weld quality, but provided

information on the influence of surface characteristics on the final weld quality with respect to the electrical contact resistance. Surface characteristics were found to be the most significant determinants when predicting weld quality by the number of rough peaks per unit area and peak height.

9.5 Steel chemistry

Tinplate is low-carbon steel that consists of iron, up until 0.3 wt% carbon and small quantities of alloying elements. The largest category of this steel class, like with tinplate, is a flat-rolled product, usually in a cold-rolled and annealed condition. The high-formability steels consist of an even lower carbon content (below 0.1 wt%) and have very few alloying elements (i.e. Mn up to 0.4 wt%).

The amount of carbon in the steel base material has a profound influence on the HSRW process. When increasing the content of carbon the bulk resistance of the steel will increase. Because of hardening reasons the quality of the weld becomes poorer when increasing the carbon content. Consequently, the welding current necessary to produce sufficient weld nuggets needs to increase with higher carbon contents. As shown with the thickness of the material an increase in carbon content narrows the welding range, certainly when the welding speed is increased (see figure 9.13).

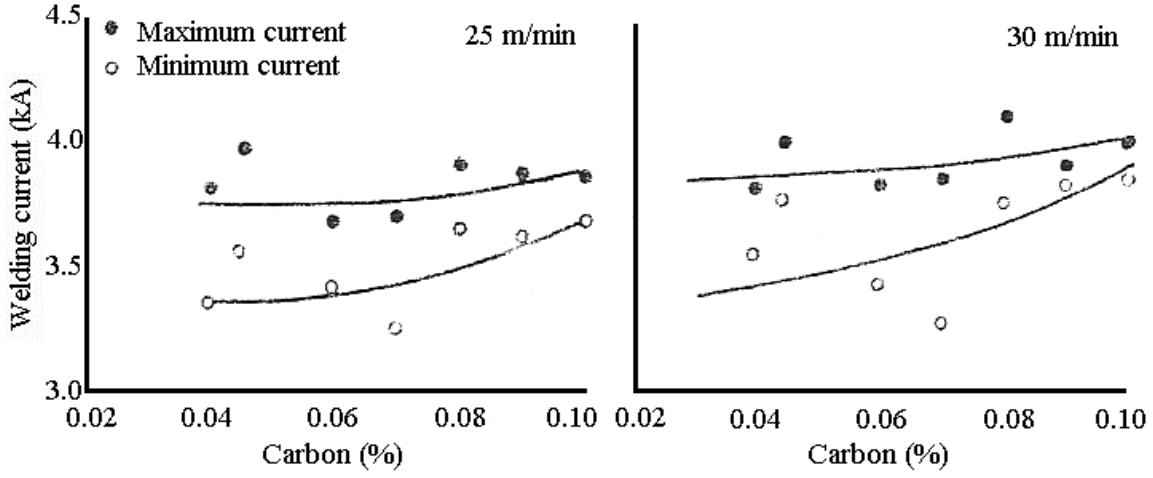

Figure 9.13: Relation between the welding current in [kA] and the carbon content in [wt%] at constant thickness with two different welding speeds in [m/min].

For fixed welding conditions the amount of carbon produces weld nuggets separated by acicular ferrite to regions of coalesced carbides as the carbon level increases from 0.06 wt% to

0.10 wt% carbon. Although more carbon is commonly experienced to give better welds, tinplate with low-carbon levels allows an increasing safety margin (i.e. tolerance) with the HSRW process conditions.

Directly related to the carbon content is the heat input and thereby the finally obtained microstructure and hardness. Small increases in the amount of carbon lead to hardness increases of 200 to 250 Hv over the initial hardness of the base material. Carbon contents of 0.09 wt% to 0.10 wt% provide an increased tendency for surface splash explained by the following phenomena [52]:

- Higher welding currents with more carbon because the bulk resistance results in higher heating effects
- Higher heating reduces the temperature gradient between interface and sheet
- Higher amounts of carbon offer more surface roughness (i.e. asperities)

These features also account for a narrower welding range at higher carbon levels. In addition, high carbon levels result in a rougher surface, indicating that higher surface temperatures were attained, which cause surface softening. Soft material will tend to pile up ahead of the electrode wheels in the direction of welding, causing a wavy surface on the weld seam. A too large excess of the wavy surface will cause burning because the reduced section is unable to carry the welding current, or failure at pressure testing because of the high brittleness.

The resistivity of the steel is increased with higher carbon amounts, whereby a higher current is necessary to maintain a good weld quality because a higher resistivity results in a lower current density. Williams et al [52] found that the weld limits decreased with increasing carbon content, in particular at higher speeds. Essentially, a poorer weld quality was observed as an increase in carbon level from 0.06% to 0.10%, which caused weld quality to range from barely touching nuggets, to small nuggets separated by zones of acicular ferrite and regions of coalesced carbides. The corresponding hardness values observed increased with increased carbon content and lower temperatures with the extent of hardness depending on the heat input to the weld area and the resultant quicker cooling rates. A lower heat input resulting in much slower cooling rates, after curing gave a bainitic structure, which was softer. The combined effect of carbon content and tinplate thickness was such that although an increase in carbon would increase hardness, an increase in tinplate thickness would reduce cooling rate, thus reducing the extent of hardening. It was also found that lower alloyed steel does not significantly create larger welding ranges as standard and higher alloyed steels. The lower carbon and manganese quantities only provided a softer weld, which can be beneficial when deforming the weld after welding [63].

9.6 Steel texture

The production of cans, the high speed welding process in terms of grain orientation or texture yields pronounceable results when varying the material rolling direction in relation to the can cylinder welding direction (see figure 9.14). The welding process produces more favourable results if the rolling direction is perpendicular (c-grain) to the welding direction since there is grain growth across the weld interface line. If the rolling direction is parallel (h-grain) to the welding direction, then there are problems (to high internal stresses) with splitting during the flanging process to seam on the can-ends [27], which leads to cracking of the weld seam. However, improved h-grain cans could reduced the number of coil widths both made by steel suppliers and stocked by customers and the application of stripped lithography would be easier as shown in figure 9.14.

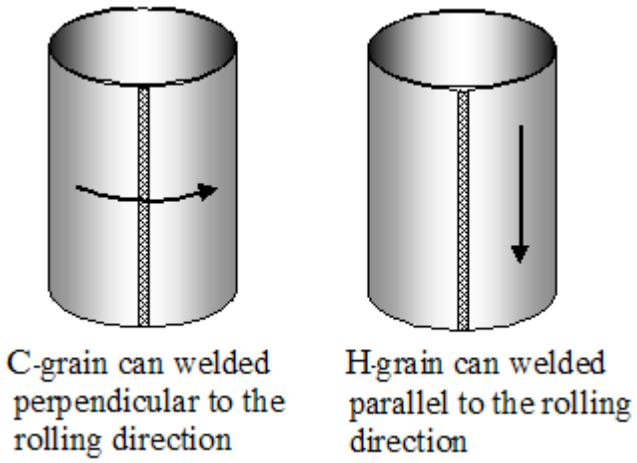

Figure 9.14: The c-grain and h-grain cans with respect to welding direction.

To decrease the risk of splitting flanges, especially with smaller and more critical can diameters, which in itself already develop more stresses, the rolling direction of the tinplate should run circumferential around the cylinder (c-grain orientation). Notching either sides of the weld seam can even further relieve the internal stresses [3].

9.7 Heat treatment

Between annealing and electroplating, tempering is used to improve the sheet shape and to impart surface finish in order to enhance the final mechanical properties (i.e. the internal stresses) of the tinplate. However, heat treatment also has an important influence on the optimum welding range because it influences the contact resistance by the consistency of the steel chemistry. Variation in the element distribution induces difference in the heating of the material and in the mechanical properties. Minimising the element distribution, having an as homogenous as possible material, is sometimes hard to accomplish, because of initial steel and can-line production processes.

Continuous annealed material has better-controlled heating and cooling conditions over the sheet dimension than batch annealed material, which results in more consistent heating of the weld.

The narrowing of the welding range is more pronounced with thickness changes than with carbon levels and thickness and carbon level has the opposite effect in hardening. More carbon increases slightly the hardening but increasing thickness reduces the cooling rates and thus the hardening more significantly.

Since low tin-coated sheet steel significantly reduces the welding range, Waddell et al [28] concluded with respect to surface treatment by heat and the effect on welding range that:

- Flow melting only had a significant effect with low tin coating levels yet the electrode force had to be raised to get a sufficient welding range
- Heat-treatment increases the contact resistance and reduces the welding range with declining tin coating weights

10 Weld formation

The primary joining classification (e.g. welding, soldering) is generally based on the characteristics of the joining process. However, the process determines the bond category (e.g. metallic, ionic) and together they make up the bonding mechanism of the process [65 to 67].

10.1 Atomic level

The use of tin coated low-carbon steel makes a joint of this material consisting entirely of metallic bonds, wherein strong electrostatic forces hold the individual iron and tin atoms together. Metallic atoms cannot fill their outer electron shells; therefore the valence electrons are not tightly bound to the nuclei and are free to move in a metallic structure or compound (i.e. delocalisation or electron sharing). Thereby, as illustrated in figure 10.1, metallic compounds or bonds establish a net flow of electricity and rapid transmission of kinetic energy (e.g. temperature) [65 to 70].

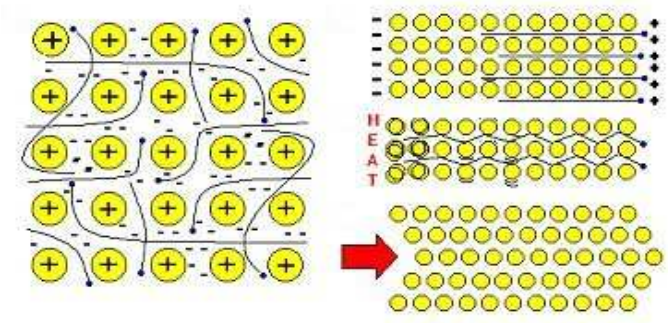

Figure 10.1: On the left, the figure shows a schematic of the metallic bond principle and on the right the corresponding metallic properties: electric field, thermal field and slipping of planes by applying a force are shown [70].

Inter-metallic compounds of iron and tin, which can be formed, are not purely metallic. The structures of the inter-metallics may be directional and less dense as for instance non-metal elements (e.g. oxygen or hydrogen) are entrapped, whereby an ionic or covalent character is formed. As a result more brittle, less dense, but stronger bonds, and different thermal and electrical conductivities arise compared with pure tin and iron [65 to 70].

10.2 Process classification

The joining of the metallic sheets is accomplished by heating in combination with forging. To achieve a cold pressure weld the surface strain should be in the order of 400 to 500 % [7]. The strain achieved on the weld interface line experienced in the HSRW process is much less than the strain required for cold pressure welding. This suggests that forging plays a minor role in the formation of the welds [64]. As a result heat is the major aspect, and thermal bonding (i.e. welding/soldering) is the primary process classification [71 to 75]. Although the heat can be generated by different heat sources in different ways (i.e. place, work-piece size and shape) with

welding and soldering, welding in contrast with soldering employs a higher (maximum) temperature to join materials [71 to 78].

At lower heat inputs (i.e. below the welding range), most of the literature discusses soldering phenomena in the seams. Soldering is based on creating an inter-metallic bond or alloy via a molten solder (low melting point metal), such as tin on the initial tinplate, which connects the interfaces. In soldering some diffusion into the substrates and solder, which is more pronounced with higher process temperatures, might occur. Nevertheless, the bond is characterised by a layer system as shown schematically in figure 10.2 [73 to 77]. The inter-metallic layers imply that the base materials will alloy at the interface line to form a connection layer over the entire height of the can body. Dissolving small amounts of base material in the solder can enhance the bonding of the sheets.

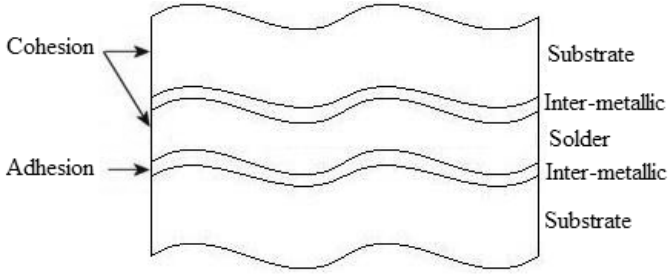

Figure 10.2: Schematic of the layer system when soldering is the primary joining classification within a joining process. The figure shows the important bond features next to the image.

Nevertheless, Gould [7 and 79] indicated that, when properly forming, resistance mash seam welding is a solid-state joining process showing no evidence of melting and exceptions to this are typically observed when excessive welding currents and/or low welding speeds are used, where theories suggest grain growth across the weld interface line [50 and 78 to]. Solid-state welding is defined as a process that produces coalescence with or without the application of pressure at a temperature essentially below the melting temperature of the base metal whereby time, temperature, and pressure individually or in combination produce coalescence. Since the base metal does not melt, solid-state welding can offer the advantage of metals retaining their original properties without HAZ problems. With solid-state welding, the process time can be extremely short, in the microsecond range or exceptionally long, in the order of several hours. As the process temperature increases time is usually reduced.

With solid-state welding a high intimate contact is essential as the atoms on the surfaces should attract each other to form inter-atomic solid bonds therefore it needs excellent interface conditions to join the materials [83 to 86]. However, surface barriers hinder the intimate contact, namely asperities (differences in surfaces elevation), oxides, and surface contaminants, which can be reduced significantly using stress and heat [58, 79 and 83 to 86]. Brick [87] found that surface texture was the main issue influencing the required temperature.

In solid-state welding, a threshold deformation exists below which no weld is made, as shown in figure 10.3. McEwan and Milner [88] discussed that heating reduces the yield strength and residual elastic stresses between surfaces (threshold deformation), which facilitates the solid-state bond mechanism.

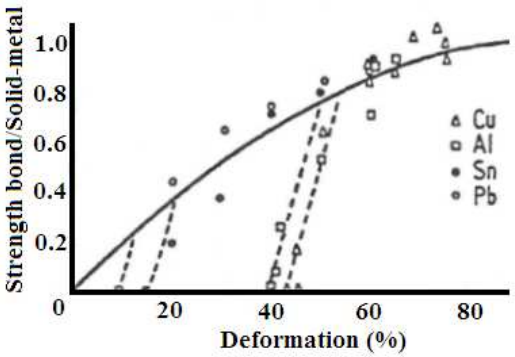

Figure 10.3: Threshold deformation (dotted line) for solid state welding. Experimental bond strength, plotted as a proportion of the strength of solid metal, compared with the theoretical maximum attainable strength (full line) [87].

Currently, four models exist to explain the physical phenomena during solid-state welding. These models take into account inter-phase interaction, dissolution, electrostatic interaction and brittleness [89]:

1. Recrystallisation model based on decreasing recrystallisation temperatures because of high deformations
2. Diffusion model based on hetero diffusion taking place in the contact zones and hence mutual diffusion into both work-pieces
3. Energy threshold model based on susceptibility of bonding and determined by the limit state of the polycrystalline materials. In this model the energy of the atoms in the bonding volume must be above a certain level to bond
4. Auto vacuum model based on the creation of vacuum micro volumes. Entrapped air interacts upon heating with the surfaces of the work-pieces, which finally dissociates into the material, leaving a micro vacuum. This is followed by sublimation and bond formation of the clean surfaces

A significant difference between diffusion bonding and high-speed resistance welding is time. Diffusion bonding can require 30 minutes or more of pressure at a temperature, which is one third of the materials melting point to ensure the required intimacy, the promotion of inter-atomic bonds and the elimination of surface oxides [90].

The reason for the HSRW process to belong to solid-state welding has two grounds. First, temperature, pressure and possible friction characteristics. These are achieved by either surface preparation or by applying a significant force to the material. Secondly, the current from the electrode wheels achieves application of heat, which is also a necessity for solid-state welding. The resistance welding processes are categorised by spot welding, seam welding, foil-butt seam welding, projection welding and upset welding.

Spot welding is very commonly used and dominant within the automotive industry. With spot welding the work-pieces are clamped between two copper electrodes, which pass a high direct current through an area of overlapped material whereby a local (i.e. spot) weld is formed to bond the material to a uniform structure. The spot weld is made with respect to the contact point of the copper electrodes (i.e. static), as shown in figure 10.4, and the high electrical conductivity and the resistance being the largest at the work-pieces overlap width. A larger contact area of electrode to work-piece requires a higher current, longer contact time and finally poorer weld qualities. Over time, the electrodes are subject to deformation and pick-up of the welded material. This contamination and deformation of the electrodes requires redressing or replacement.

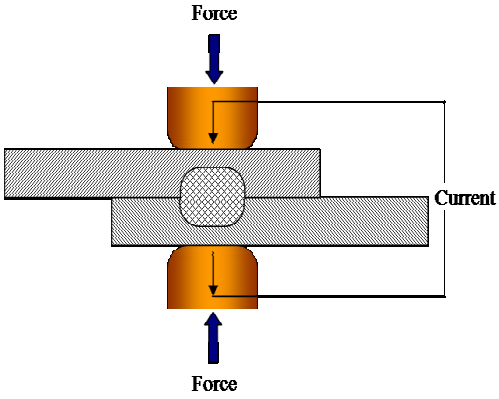

Figure 10.4: A spot weld process by which a weld (pool) is created at the interface of the work-pieces.

Seam welding is commonly described by the creation of overlapping spot welds and is similar to spot welding in that two copper electrode wheels pass a high current through a width of overlapped material. Due to the high electrical conductivity of copper, the resistance is highest at the overlap width. An alternating current frequency in combination with a weld speed determines the number of overlapping spot welds. Seam welding in the context of the particular description above results in a final sheet thickness, similar to the thickness of the non-deformed sheets.

Roll-spot welding corresponds to spot and seam welding. Roll-spot welding is essentially seam welding, yet with separated current pulses to form a series of separated weld nuggets on the weld interface line [90].

Mash seam welding (see figure 10.5) is a combination of resistance seam welding and metal forging. The weld is produced by material overlap whereby the overlap is approximately one to one and a half times the original material thickness. Heat is generated between the sheets by a high continuous current and an electrode force consequently mashes and joins the sheets. The final weld is only 10 to 25% bigger than the original sheet thickness [58]. Semi-mash seam welding is a mixture of seam and mash seam welding used in the assembly of for instance automotive parts (i.e. tailored

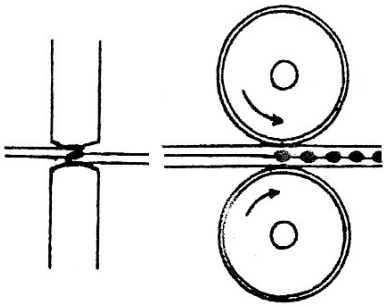

Figure 10.5: Schematic of a mash seam welding process whereby the electrodes drive the work-pieces and sequential weld nuggets are formed.

blanks) [].

With foil-butt seam welding the edges of the sheets are joined head to head. A thin strip of foil is introduced between the electrodes and work-pieces to increase the electrical contact resistance and to contain molten material in the weld nugget. This process is readily used for welding galvanised steels to prevent zinc contamination and deterioration of the electrodes.

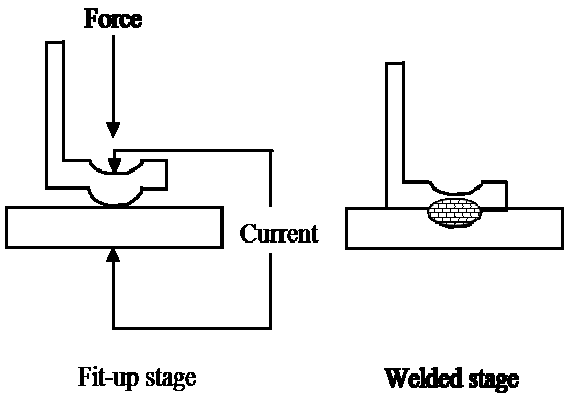

Figure 10.6: Schematic of projection welding before and after welding is shown. It illustrates the creation of the weld (pool) at the particular projection.

Projection welding is a variation of resistance welding where the current flow is concentrated at a geometric extension of the part that is welded, as shown on the right illustration in figure 10.6. The projection concentrates the current flow and localises the applied force, reducing the amount of current, required on allowing thicker sections to be welded. Nonetheless, the need for a projection may not be cost or process effective compared to spot welding.

Upset welding is similar to spot welding in the use of a current and an applied force. Effectively, joining the ends of two pieces of material with the same cross section instead of using a material overlap produces a butt weld. The term upset implies the extrusion of material, which exceeds the original geometry of the work-pieces and can be trimmed after joining. A continuous or semi-continuous version of this process can be used for the fabrication of pipes, tubing and wheel rims.

Despite the solid-state character, low-carbon steels are often bonded by fusion welding processes due to the time necessary for joining. Additionally, the HSRW process is sometimes considered fusion welding due to the nature of some defects (melting phenomena) experienced in hot welds. Fusion welding can be defined as a process that uses liquid formation of the base metal to make the joint. The main difference between the fusion and solid-state welding is the geometry whereby a solid-state weld will be similar after welding and a fusion weld will have remarkable differences from the original geometry fit-up. In comparison to other welding processes, solid-state welding does not use filler or additive materials [72, 80 to 86 and 89].

10.3 Weld nugget

Weld formation is commonly described as the development of weld nuggets or: "*The formation of a new material phase by the correspondence of each half cycle of an alternating current*

waveform and moving work-pieces" [28]. However, the actual weld nugget formation is very much dependent on the temperature that is generated within the material. The temperature over the weld interface line continuously differs because of the continuous alternating current of the sinusoidal waveform and hence the formation of the weld nuggets.

The total weld seam is considered as a series of adjacent spot welds (weld nuggets). Individual weld nuggets can clearly be seen when looking at the weld seam of a can body (see figure 10.7).

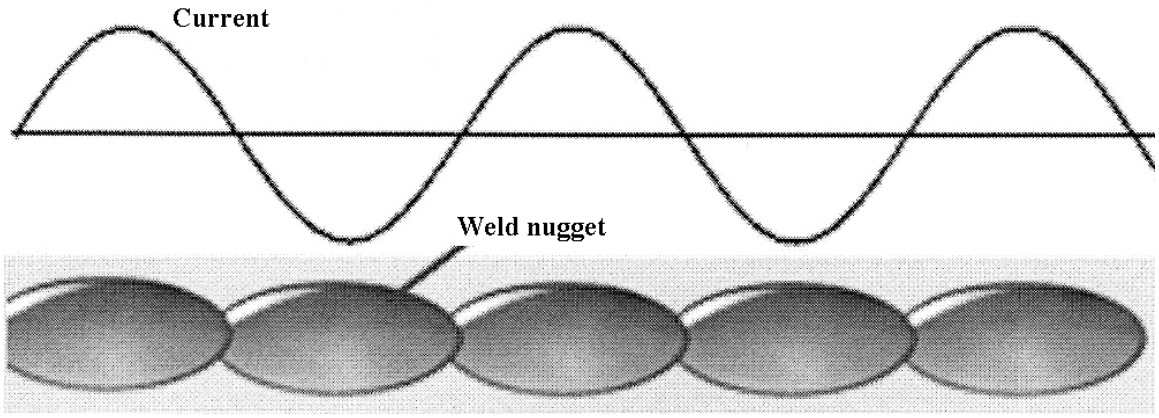

Figure 10.7: Schematic of the creation of the weld nugget at each half cycle of the applied welding current, whereby the number of weld nuggets is equal to the number of half cycles.

Often welding process design as found in the literature is in accordance with how the welding process is commonly described, spot weld - displacement - spot weld - displacement, etc. Nevertheless, the welding process is a continuous process in which the material is constantly moving with a certain speed and the welding current follows its own distinct path.

A good quality weld seam consists of overlapping weld nuggets caused by a minimum temperature, which should be controlled to ensure that each element has a certain minimum temperature to create a good solid phase joint. Yet, the temperature may not exceed the melting point, which would result in the creation of weld defects. Corresponding to the heating of the material is the temperature gradient over the height of the weld seam from interface to surface in relation to nugget development. The exact weld nugget shape is determined by the temperature profile (i.e. welding and process parameters); generally showing elongated cone-like microstructural formations.

The number of weld nuggets in a weld seam of a certain length is said to be governed by the frequency waveform. Since the main voltage is 50Hz, 100 weld nuggets per second can be generated, when a weld nugget is said to be formed for each half cycle. If for example the frequency is 100 Hz, then there are 12000 half cycles per minute and 12000 weld nuggets per

minute is the maximum that will be observed at this frequency. In the past, a step-up frequency converter was used to generate frequencies of 100 Hz, 150 Hz, etc. Instead of 100 weld nuggets per second, 1000 weld nuggets could be generated at a frequency of 500Hz. However, the frequencies on the newer welding machines are approximated by a solid-state transformer and have values of 252 Hz, 488 Hz or 710 Hz.

Since the weld should be formed at the weld interface line temperatures and temperature gradients are the main factors, which makes formation of weld nuggets clear. A low temperature gradient indicates a weld nugget growth towards the surface. With lower temperature gradients the weld nugget tends to curl to the smaller electrode wheel (i.e. the higher temperatures due to the higher current density). Larger temperature gradients induce a weld nugget to stay more at the interface line between the sheets. The maximum temperature is best approximated by the microstructure of the weld nuggets, whereby the amount of hardening or dendritic appearance indicates where most of the heat was generated. The basic welding parameters that control the formation of the weld nuggets are distinguished by two categories: process parameters (e.g. welding current, electrode wheel pressure, welding speed, etc) and material properties (e.g. geometry, coating, carbon content, etc). Both categories determine the actual length, penetration depth and shape of the weld nuggets. Variations within the parameters results in a range of weld nugget shapes or heat balance alterations and different, yet acceptable weld qualities.

Concerning the weld nugget development during resistance spot welding, a lot of literature can be found that uses analytical and experimental techniques to progressively estimate the effects of the welding parameters on the weld nugget formation and to construct a weld nugget growth model. For instance [92to 94] discuss a weld growth mechanism characterised by four stages: incubation, rapid growth, steadily decreasing growth and expulsion, which is consistent with the discussed dynamic resistance phenomena in chapter 6. The mechanisms for weld nugget formation in the HSRW process are in the literature limited to the correlation welding parameter-weld nugget size as shown in figure 10.4 and discussed in the previous chapters.

10.4 Mechanisms

In early investigations, resistance mash seam welding was regarded as a fusion welding process. Funk and Bergeman [95] suggested that melting and solidification of the weld were characteristics of a strong weld mechanism. They also indicated that resistance mash seam welding is a combination of resistance heating and mechanical forging, whereby the variables are roughly classified in [95]:

- Heat effective parameters: welding current, speed of rotation of the wheels

- Forge effective parameters: overlapping of the sheets and the electrode force

The forge effective parameters also affect the heating of the joint since the contact resistance and current density are also a variable of these two parameters. Later, Ferrasse and Piccavet [126] divided the resistance mash weld configurations into three distinctive categories:

1. Low energy level: not fusion, but diffusion welding takes place providing poor mechanical weld qualities
2. Intermediate energy level: larger molten zones with sufficient weld nugget development for creating a sound weld. Welds fail preferentially along the periphery of the weld centre
3. High energy level: molten weld nugget that is ejected form the weld interface

Uchihara et al [96] showed that resistance mash seam welds made of low strength steels (LSS) possess sufficient strength without melting, yet in welding high strength steels (HSS) melting was found necessary for obtaining a strong enough weld.

Within conventional resistance welding the quantitative effect of welding consist of resistance phenomena and evidently the path of the current flow. Welding at low speeds, below 10 m/min using a standard overlap width and equally sized electrode wheels results in a symmetrical weld nugget development; the weld nuggets initially formed on the geometrical centre between the electrodes (i.e. weld interface line). The temperature distribution is also symmetrical and the final weld size is a result of a fine balance between heat generation and development at the weld interface line and heat loss via the electrode wheels, steel sheets and environment [97].

In the HSRW process, the welding current flows via a more distinct path (i.e. current flow path), and becomes particularly significant; generating a Maximum Heat Development (MHD) site. The MHD should be generated on the weld interface line between the differently sized electrode wheels in order to correctly join the sheets. The MHD position can displace with respect to the electrode wheels as a consequence of variation in the contact

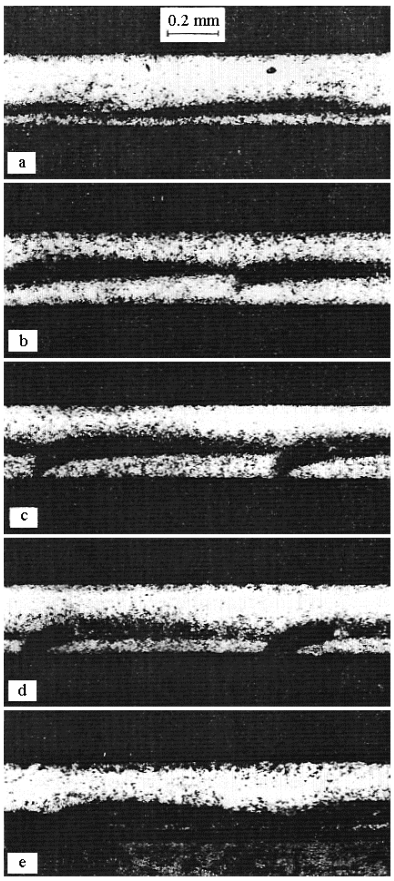

Figure 10.8: Overview of the heat pattern development with an increasing welding current from a to e [28].

resistance and hence current flow path. As a result a distinction is made between low and medium to high contact resistance for respectively a wide current path and welding range, and narrow current path and narrow to no welding range. A too high a contact resistance can cause severely deviating current flow paths between the electrodes, promoting the excess of comma and splash formation. When the point of initial formation of the weld nugget tends to move forward to the exit of the electrode wheels, with for example higher welding speeds; heating times become shorter and the contact resistance is not able to reduce before the electrode wheels are passed. In this way, current flow before the centre of the electrode geometry is less than at the exit side of the electrode wheels.

The heat distribution around the weld nugget changes from being symmetrical around the weld interface line towards the outside surface to a comma-shaped pattern towards the inside can surface of the weld seam, shown in figure 10.8. The comma-shaped heat pattern curves downwards to the smaller electrode wheel, where a higher current density or heat development is present. At the overlap edges the cooling effects are of the greatest magnitude because of the water-cooled electrode wheels. The position of maximum heat development relative to the contact area between the electrode wheels is the basis for weld formation and takes place in three distinct zones, as shown in figure 10.9:

- Zone 1: satisfactory weld nuggets are formed, because of sufficient heat abstraction and containment of the formed liquid at the geometrical centre of the weld interface line. The electrode force is properly applied to contain the liquid
- Zone 2: commas may occur, because heat is only extracted by the top electrode, which increases the heat concentration (i.e. liquid formation) towards the bottom. The absence of the electrode force in the lower area results in material ejection (i.e. comma formation)
- Zone 3: interfacial splash takes place, because no heat extraction by both electrode wheels can take place. The applied electrode force does not have an effective action on the interface resulting in ejection along the work-piece surfaces.

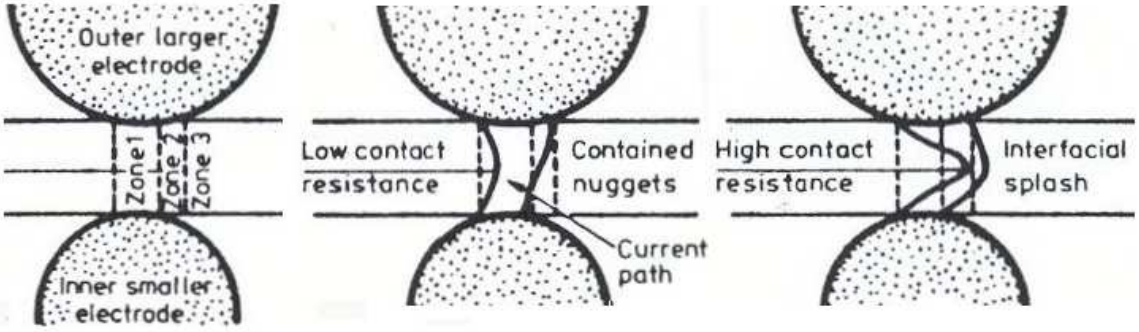

Figure 10.9: Schematic of the different maximum heating zones as defined by [28] with the different applied heat generations: high and low contact resistance. The effect of contact resistance on the region of maximum heat development: increased contact resistance increases the heating rate and influences current path and therefore the region of heat development.

Higher speeds result in more material ejected from the seam edges at the weld surface. It is considered that liquid material states originate from the weld nugget and so splash generally occurs when the weld nugget grows beyond the boundaries of a solid material, whereby the contact angle of the sheets edges becomes an essential factor.

Consequently, the third zone characteristics are minimised or avoided by effectively containing the liquid at its point of formation with for instance, a jockey system. The jockey system allows a longer effective electrode force essentially extenuating the MHD position beyond the exit. In this way, the weld nugget curl down effect is also reduced and a more symmetrical and smoother weld interface is created.

The movement of the MHD site to the exit of the electrode wheels also introduces the current flow lines to bend to the exit, creating a smaller area for joining of the work-pieces. In this way, a higher welding current to sufficiently heat the material could be needed, and narrower welding ranges are the result.

11 Microstructure

11.1 Low-carbon steel welds

In (ultra) low-carbon steel microstructural transformations, temperature-time and strain are the main indicative parameters; heating and cooling rates being controlled by the process and material parameters. These conditions (i.e. time-temperature-strain features) determine the final average grain sizes and types after transformation and are directly related to for instance, the strength of the material, where smaller average grain sizes result in stronger materials [66 and 98 to 100].

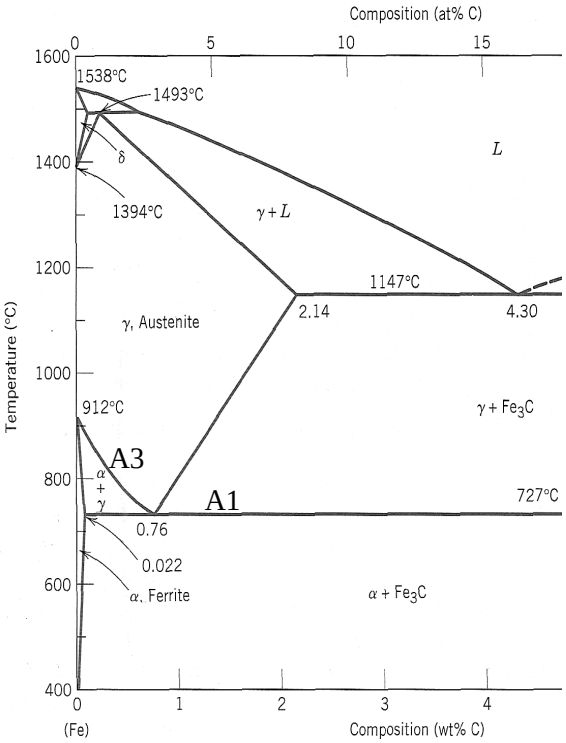

Figure 11.1: The iron-carbon phase diagram [66]. The A1-temperature line is at 727°C and the A3-temperature line is the line crossed upon cooling at the austenite to austenite-ferrite region.

Low-carbon steels can exist in three stable equilibrium heat-treated crystalline phases, namely austenite (above 850 °C), ferrite (below 850 °C) and cementite (below 680 °C) as indicated in figure 11.1 [66, 72 and 99 to 103].

When solidifying (ultra) low-carbon steels first δ-ferrite is formed. Formation of δ-ferrite is directly followed by an austenite cast microstructure (i.e. primary structure) formation. This microstructure consists of dendritic crystals and exists until phase transformation at the γ-α phase transition (i.e. between the A1- and A3-temperature) takes place. When transformation from austenite to α-ferrite takes place, dependant on cooling rate and steel compositions, the three most important secondary microstructures, which can be formed, are [73]:

1. Grain boundary ferrite (i.e. pro-eutectic ferrite): first formed structure upon austenite to α-ferrite phase transformation. Appears as a network of polygonal crystals on the former austenite grain boundaries. This microstructure is unwanted because of large grains inducing an unfavourable toughness and high crack initiation state
2. Side-plate ferrite (high-bainite or Widmannstätten-ferrite): formed by laminates from the grain boundary ferrite into the primary austenite grains. The laminates are separated

by small angle grain boundaries on which mostly martensite or austenite carbides are formed. This needle-shaped microstructure is undesirable because of the unfavourable toughness (i.e. effective large grains) and the presence of martensite (e.g. brittleness)

3. Needle-shaped ferrite: formed in the middle of the primary austenite grains. The laminates provide large-angle grain boundaries and induce high dislocation densities ($10^{14}/m^2$) and therefore considered favourable for the toughness of the material

In (ultra) low-carbon steels the HAZ can be characterised by four zones, classified by the Fe-C equilibrium phase diagram (figure 11.1) and the progress of the distance of the peak temperature to the melting zone. The HAZ transformations are dependent on chemical composition, cooling rates and peak temperatures, T_p.

- Coarse grain zone (~1100°C<T_p<T_m): austenite transformation and grain growth takes place. Tp and the cooling rate determine the grain size. Small cooling rates induce grain boundary ferrite and ferrite-pearlite structures. Higher cooling rates induce less grain boundary ferrite and more laminated microstructures (i.e. bainite and martensite)
- Fine grain zone (Ac3<T_p<~1100°C): the low T_p provides only little grain growth, yet transformation to austenite is still achieved. When cooling relative fine secondary grain structures are formed
- Partially transformed zone (Ac1<T_p<Ac3): relative low transformation temperatures mostly transform the carbon rich areas into austenite. Upon cooling the carbon rich areas form depending on the cooling rate pearlite, bainite or martensite
- Tempered zone (T_p<Ac1): no transformation takes place, but it is assumed that stresses are relieved and ageing phenomena take place. In the temperature range of 700°C to 750°C carbide formations are pronounced

Transformation to a new phase requires nucleation and growth of that new phase. Nucleation and growth of grains are important phenomena in low-carbon polycrystalline steels since they govern the kinetics of all non-martensitic phase transformations and recrystallisation processes that can take place under the process induced conditions. [66 and 98 to 100]. To date, the kinetics of phase transformations, despite various models, are still poorly understood and models for the description of these phase transformations are mostly based on the classical nucleation theory (CNT) [104] and the law of parabolic grain growth by Zener [105], which both describe the behaviour of individual grains in a bulk material.

Recrystallisation may occur during or after deformation and/or subsequent annealing, which is classified as, static and dynamic recrystallisation respectively. Recrystallisation in low-carbon

steels is significantly dependent on strain and strain rate. When applying an increasing strain (rate) the recrystallisation process will accelerate during and/or after deformation. Effectively, dependant on the amount of strain (rate) easier and faster dynamic and/or static recrystallisation is achieved [106 to 108]. Recrystallisation is usually accompanied by a reduction in the strength and hardness of a material and a simultaneous increase in the ductility [106 and 108].

A precise definition of recrystallisation is difficult as the process is strongly related to several other processes, such as recovery and grain growth. Additionally, the different mechanisms by which recrystallisation occurs are complex and in many cases controversial [106 to 112]. When comparing recrystallisation to phase transformations a similar principle is seen because of an (thermally) activated solid-state reaction; nucleation followed by growth of grains. Although the principle is similar, there are some differences. First, the driving force (i.e. removal of dislocations and their associated energies) is very small and secondly, nucleation occurs in an extremely heterogeneous manner and thus only a small number of grains per unit volume are created [109].

The weld microstructures can severely deviate from those provided by equilibrium conditions because with resistance mash seam welding rapid and continuous changing temperatures during heating and cooling are introduced. With this feature low-carbon steels deviate from the equilibrium microstructures and create polygonal ferrite, coarse ferrite islands, pearlite, martensite and rest-austenite. However, these microstructural components have a negative influence on the materials toughness. Continuous heating transformation (CHT) and continuous cooling transformation (CCT) diagrams can be used for predicting the microstructures.

In CHT diagrams the temperature, at which transformation to austenite takes place for a given heating rate can be derived as, for example, shown in figure 11.2 [113 and 114]. The CHT

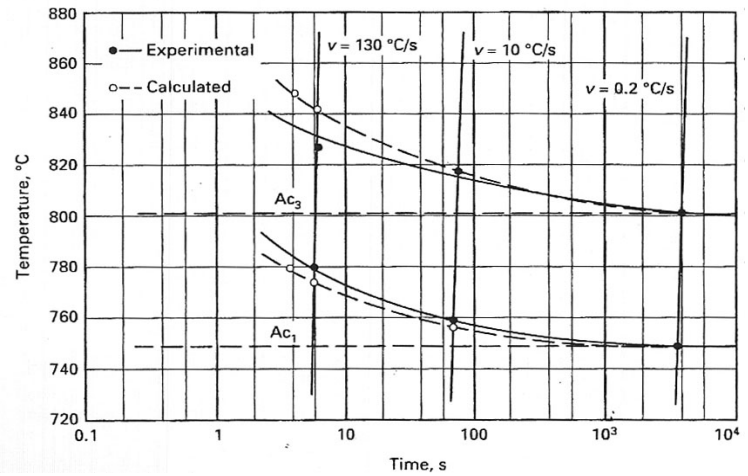

Figure 11.2: Continuous heating diagram for low-carbon steel. The steel phase that is formed is austenite. The heating rates increase from right to left. The dashed lines are calculated values and the solid lines are experimentally determined. The diagram shows a significant A1- and A3-temperature increase with an increase of the heating rate [1].

diagram shows that the A1-and A3-temperature or start and finish temperatures of the microstructural transformations are significantly delayed relative to the equilibrium phase diagram. Consequently, CHT diagrams are useful in predicting the effect of austenisation above the A1-, A3-temperature from which the hardening microstructures (e.g. martensite) are provided after quenching [113 and 114].

When quenching ultra high cooling rates are introduced causing an undercooling that surpasses the two-phase temperature range between the A1- and A3-temperature. Although the mechanism is not clear, it is known that carbon diffusion is not able to find equilibrium, causing martensite structures, which consist of over-saturated needle-shaped carbon islands enclosing areas with retained austenite [66 and 98].

As supported by the CHT diagram it is important to state what cooling curve and steel composition the CCT diagram is derived from. CCT diagrams, like the one shown in figure 11.3, predict the existing phases with a certain cooling rate and a particular steel composition at a final temperature [113].

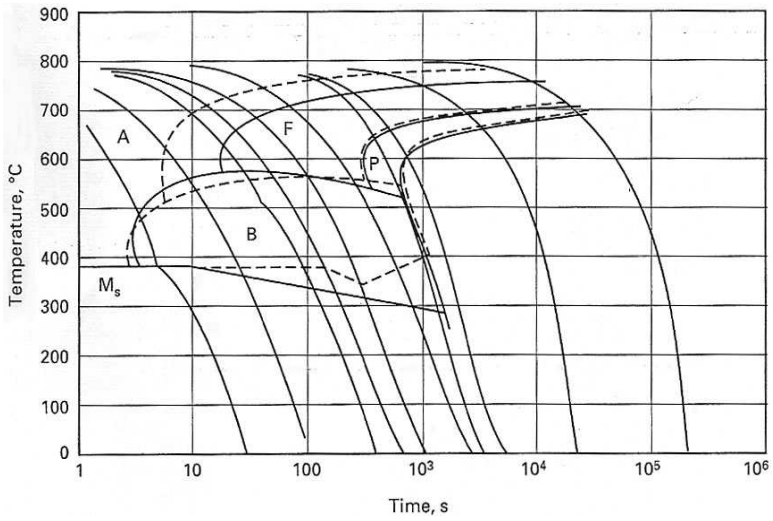

Figure 11.3: Continuous cooling transformation diagram for a steel containing 0.30% C, 0.64% Mn, 1.0% Cr, and 0.24% Mo. The temperature against the time and the curved cooling lines indicate which steel phases at a certain cooling rate in the material are formed. The cooling rates increase when going from right to left. The dashed lines are calculated values and the solid lines are experimentally determined [113].

In figure 11.3, the capitals indicate the regions ferrite, pearlite and bainite as the martensite forming start temperature. The construction of these diagrams is experimentally difficult and therefore calculations based on the John-Mehl-Avrami expression are used [113]. The most influential features when considering low-carbon steel are shifts of the ferrite and bainite phase noses to the left and the rising starting temperatures of the phase formations when decreasing the carbon content.

Most models are not constructed for such low-carbon percentages and therefore the outcomes are rather speculative having large scatter. The calculations only give an indication of when a phase is formed, provided by the cooling rates. Small alterations in the composition or austenisation temperature change the cooling rates significantly. Secondly, the CCT diagrams cannot be used to predict the response to thermal histories, which are different from the ones used to construct the CCT diagrams [113 and 115]. From these diagrams it is clear that changing the cooling rate has major influences on the distribution of the microstructural elements. Additionally, CCT diagrams are highly sensitive (i.e. the shifting of the transformation products) to chemical composition alterations, and the microstructural changes are directly related to mechanical property changes (e.g. hardness, brittleness).

11.2 High-speed resistance welds

In the literature virtually nothing is written on heating rates for high-speed resistance welding, and only cooling rates are discussed. The two characteristic parameters for the cooling rates are [73]:

1. The austenitising parameter: time for cooling between 1200^{o}C and 800^{o}C, which primarily determines the austenite grain size
2. The transformation parameter: time for cooling between 800^{o}C and 500^{o}C, which determines the nature and distribution of the transformation products.

Nevertheless, Williams et al [52] performed some microstructural examination after high-speed resistance welding and came up with the following (general) observations:

- The low-carbon steel consist of tempered martensite (upper and lower bainite) and some free ferrite (non-tempered martensite)
- The weld pulse centres show martensite type transformations together with low-carbon martensite in isolated areas
- Lamellar carbide precipitates further from the centre of the weld indicate slower cooling rates
- Adjacent to the weld area coalescence of carbides and acicular ferrite is formed, which indicates that the steel experienced a temperature just below the A_C3-temperature
- The naturally columnar metallic structures in the weld and heat-affected zone are difficult to resolve with light microscopy

The extent of hardening (martensite/bainite microstructures) within the microstructure depends largely on the heat input to the welded area. The higher the heat input, the higher the maximum hardness as a result of higher cooling rates. A different temperature balance by adjustment of the welding parameters leads to slower or faster cooling rates and consequently softer or harder microstructures.

The presence of acicular ferrite in the weld microstructure is the result of relatively fast cooling rates and provides a distinct increase in the toughness of the metal. Acicular ferrite is a fine pattern consisting of spikes that grows throughout the decomposing austenite grains. The fine microstructure is packed with dislocations pinned by secondary phases and grain boundaries that discourage fracture of crevices. The microstructure is obtained by the initiation of intra-granular nucleation of hypo-eutectoid ferrite in the austenite to promote competitive growth among the ferrite grains in order to generate the acicular microstructure [52].

Some further general observations made by Williams et al concerned the presence of, columnar weld microstructures, which consisted of tempered martensite (upper and lower bainite) and some free ferrites, possibly non-tempered martensite. They also found isolated occurrences of low-carbon martensite at the centre of the weld, indicating fast cooling rates with the surrounding slower cooled material in the form of lamellar carbide precipitates.

The weld microstructure depends on the temperature profiles at each material element within the weld seam. The microstructure might diverge from tempered base material to dendrite/solidification structures.

Research that has been done for several tinplate-packaging steel grades with varying welding currents focused on the grain formation and growth on the metal-metal interface and in the part of the base material where the microstructure and/or properties have changed due to the thermal cycles of welding, the HAZ. These results showed that ferrite grains appear to have grown over the interface line between the materials after welding, consequently a stimulation to identify the stage of the welding process at which this occurs, during heating or cooling, below or in the welding current range, etc. arose. In addition, the influence of non-equilibrium heating and cooling was also left out in these investigations [2].

Recrystallisation zones, which are soft regions, were found at the perimeter of the weld centre where DR tinplate material is recrystallised. Next to the recrystallisation zones a hardened microstructure was found, which highly depended on the carbon content. At 0.06 %C a very hard weld was found, as a consequence of bainite formation whilst at 0.04 %C the weld is as hard as the base material. Recent investigations were conducted to gain a better understanding of the

time-temperature profile (i.e. thermal history) and bond type(s) realised during welding, although this is still an approximation. [1, 2, 8 and 116]

Shimizu et al [44] shows some longitudinal pictures of heated steel at various temperatures in the right-hand side picture of figure 11.4. They related the grain size of the microstructures to each other and came up with an aspect ratio to determine a temperature at which the grains were formed

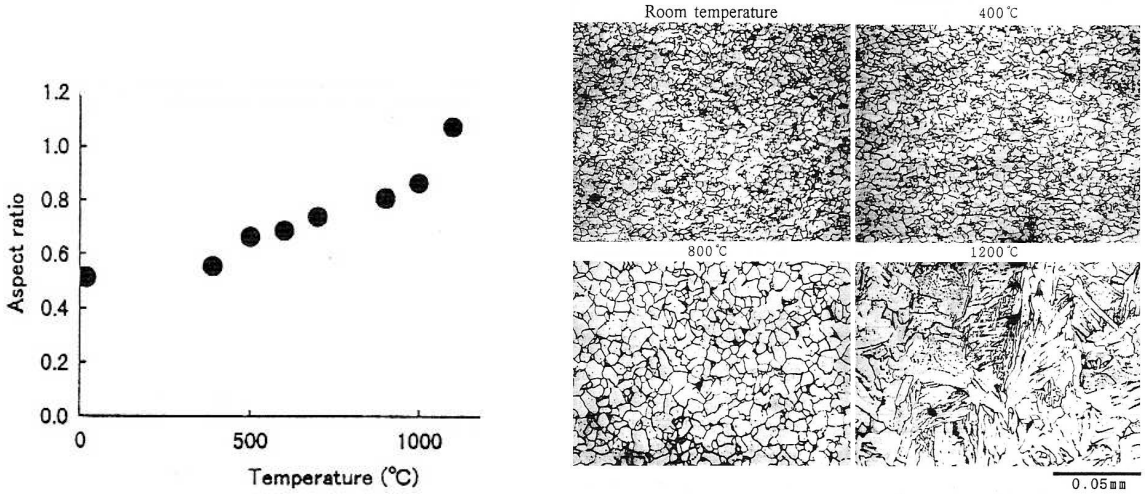

Figure 11.4: The left-hand side shows the relation between the temperature and aspect ratio of the grains. The right-hand side pictures show longitudinal cross-sections of heated steel at various temperatures [44].

12 Weld defects

In addition to the welding process and material parameters that produce good weld integrity, there are also a number of well-known defect phenomena as a consequence of the HSRW process. Nothing is found on the actual microstructural mechanisms or physical reasons for this phenomenon [1, 2 and 34].

12.1 Cavities

In metallographic examinations frequently noted features are variously shaped cavities, which cause problems during beading of the containers. The cavities appear to be contained completely within the weld. However, experiences have not shown the cavities to have any detrimental effect on weld integrity [3]. They are described as small, 40 to 100 µm, spherical cavities contained within the weld, formed by shrinkage of a liquid material state within the weld nugget see figure 12.1.

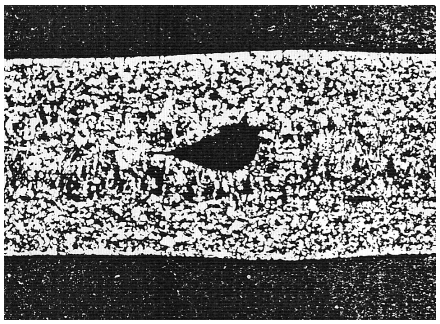

Figure 12.1: Example of a rather large shrinkage cavity at the weld centre.

Formation of shrinkage cavities is found to be related to energy input, speed of welding and thus parameter variation or the heating pattern [28] by means of:

- Low energy and relative high speeds, which create small oval / elongated cavities
- High energy and high speeds, which deliver larger spherical, not elongated cavities

At low energy levels, the weld nugget freezes the formation of cavities, whereas with high energies a larger time-period allows cavities to develop. The weld nugget also merges from the electrode force, which at a certain speed, becomes ineffective and produces a liquid material state on the surface whereby formation of cavities is inevitable.

Williams et al [51] showed that during the formation of the welding current range, very few welds are free of cavities or regularly porosity. For the majority of the cases, cavities occur as a single fine to medium sized spheres and frequently at the centre of the each weld nugget. However, there are instances where clusters of four or more cavities per weld nugget occur. Welds made at slower speeds, 15 to 20 m/min occasionally resulted in oval-shaped and elongated cavities at the trailing end of the weld nuggets.

Smaller oval-shaped cavities are formed at low energy levels and high speeds because in these areas material would solidify more rapidly. Larger spherical cavities appear at high energies and speeds because cooling of the material takes place over a considerable time, allowing cavities to

develop. The reason with high speeds is the contact time of the electrode and material, which is reduced (i.e. higher speeds reverse the success of the electrode force) to produce a good quality weld seam. If the energy becomes too high, the increasing electrode force to counter the formation of cavities results in formation of commas and splash.

12.2 Comma formation

Commas are defects that are mainly seen as an initial stage of splash formation. Consequences and the severity of the comma formation in the weld seam depend on factors such as beading and lacquering, and have a detrimental effect on the weld seam when exposed to the can content (i.e. pitting corrosion). The name, comma is deduced from the characteristic shape and appearance of these surface cracks and porosities. Waddell et al [28] found that an increasing welding current, increasing speed and reducing electrode force results in the formation of commas. Particularly at welding speeds above 36 m/min and at frequencies of 400 or 500 Hz, the presence of commas becomes notable.

If a wide operation window is needed, comma avoidance is of great importance. Particularly since it is noted that the formation of commas intensifies with increasing welding current and decreasing electrode force. Detailed examinations of commas make the phenomena geometrically classifiable into four groups (see figure 12.2):

1. Type ‘o’: open cavity with no associated material
2. Type ‘r’: raises large shiny commas with or without obvious cavitations
3. Type ‘a’: arrowhead shaped surface defects
4. Type ‘s’: small superficial surface spots

The predominant comma type is the ‘o’ type followed by ‘a’ and ‘s’ type commas, the rarest comma type is ‘r’. The ‘o’ type cavity has a heat pattern which is not symmetrical near the outside surface of the weld seam, but curves downwards to the inside surface, toward the smaller electrode wheel. The ‘r’ type commas are associated with lenticular nuggets that turn downwards to run into the surface of the sheet at the inside of the weld seam, eventually resulting in splash formation. Type ‘a’ is associated with a liquid material state at the surface of the weld seam, whilst the type ‘s’ commas are associated with weld nuggets extending to the tinplate surface and small areas which may have formed immediately below the weld seam surface.

Open comma cavities indicated that all four comma types are associated with the formation of a liquid phase and that commas according to [28] are a result of excessive expulsion of liquid material from the weld nuggets.

The typical comma shape at the outer surface changes to a spherical/elliptical shape parallel to the outer surface in the middle of the weld (see figure 12.3). This spherical/elliptical shape corresponds to the point were melting initially occurred [28]. A fine and columnar solidification pattern adjacent to the comma is found when examining the extruded material. It is also found that the internal surface of an open cavity is often covered with a thin layer of iron oxide. In the weld, adjacent to commas figure 12.3 shows that the open cavity extends to the edge of the weld. Weld pulses free from commas also showed material extrusion (i.e. deformation) at the weld seam edges at the interface, but covered the open cavities [28]. Jaques and Szczur [117] mention that a high welding current alone could not produce commas. An extra local heat input caused by friction energy or extra electrical resistance seemed to be necessary. They found commas extending ¼ to ½ way through the weld overlap and indicated that this defect can result in pitting corrosion, hardly visible under normal magnifications.

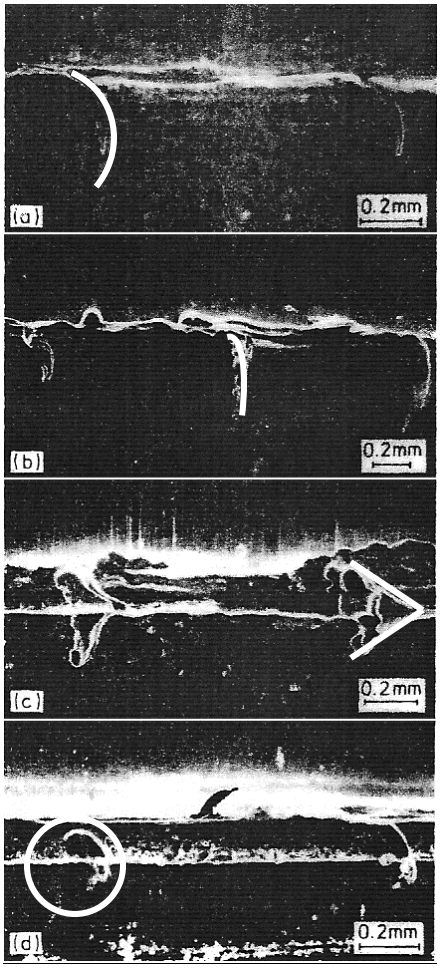

Figure 12.2: Classification of the commas: picture (a) is a type "o" comma, (b) is a type "r" comma, (c) is a type "a" comma and (d) is a type "s" comma. The pictures are a planar view of the weld seam. The commas are highlighted by the white illustrations. The distance scale on the bottom right of the pictures is 0.2 mm.

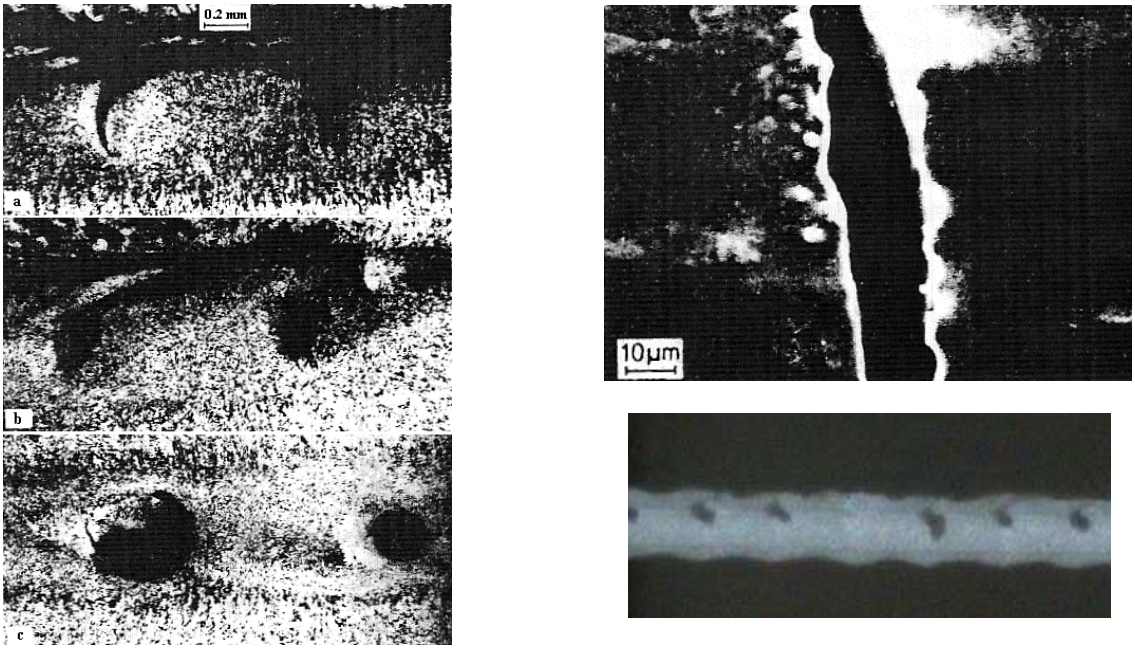

Figure 12.3: On the left-hand side successive planar sections through commas from the sheet surface (a) to the centre of the weld (c). On the right-hand side a planar view of an open cavity comma showing evidence of liquid formation is shown [28] and an overview of commas formed in each weld nugget.

Waddell et al [28] tried to qualitatively describe the effect of comma and splash formation in terms of maximum heat development, contact time of the electrode wheels and the tinplate surface (see figure 12.4).

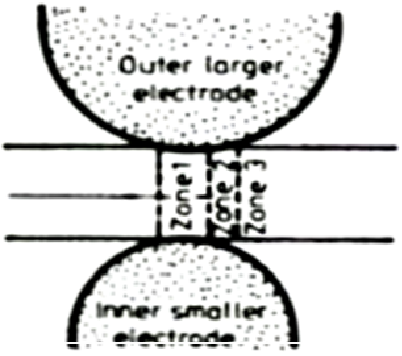

Figure 12.4: schematic of the idea on the qualitative effect of contact resistance on the formation of weld nuggets, commas and splashes.

The idea that maximum heat is generated in the first zone results in containment of the liquid material state before the onset of any defect formation, because the heat loss to and force of the electrode wheels. This would also confine the weld nugget formation on the weld interface line as opposed to the weld edges. If the maximum heat were generated in the second zone the material would only be in contact with the larger electrode wheel creating possibilities for comma formation. The heat loss to only the larger electrode wheel means that higher temperatures are confined to the inside of the can body, with the risk of a liquid material state. Without the electrode force (i.e. deformation) the material would then be ejected leaving a comma shaped defect. In the third zone no contact of the electrode wheels or an exerted electrode force can take place. Waddell et al suggested that this would cause ejection of liquid material along the weld interface line resulting in splash formation.

Elzinga [118 and 120] concluded that a higher electrode force and a thicker tin layer at the side of the smaller electrode wheel lead to less comma formation and that lower welding speeds increase the number of commas and a reduction in the material overlap width decreases the number of commas. These phenomena are related to the heat distribution which becomes coherent with slower welding speeds. With smaller material overlaps and higher electrode forces the welded steel better distributes over the weld to fill up commas. Elzinga indicates that commas are not cavities, which are created in the weld, but places that are not filled up with material during welding.

12.3 Splash formation

Splash, as shown in figure 12.5 is a defect that is defined as a liquid material state being forced from the weld seam. As mentioned before, splash formation defines that the upper limit for a weld of good quality. Splash formation is said to be a result of the weld nugget growing over the natural boundaries of the solid material overlap. However, splash encloses many factors that contribute to its formation and the extent of splash is controlled by the weld process parameters and the surface of the welded material as for instance Williams et al stated: "*A poor fit-up or mating of the surfaces being welded, too low or too high welding pressure, and an excessive welding current, can cause interfacial splash. Unsatisfactory tinplate surface quality can result in both surface and interfacial splash, the controlling factors being surface cleanliness, surface roughness and the degree of passivation of oxide on the tin surface.*" [51]

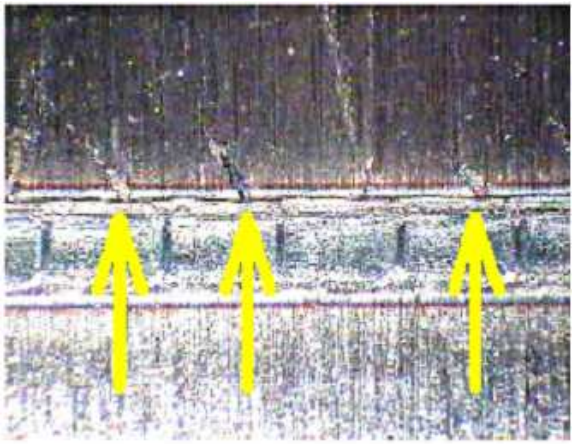

Figure 12.5: Photograph showing the splashes (arrows) at each weld nugget.

In this respect, surface films should be kept to a minimum, but compatible with the production requirements. The tendency of splash formation is mostly associated with a relatively high initial contact resistance and therefore, particularly with low tin level coated steels, higher forces are necessary for welding. A larger electrode force contributes to a reduction in splash and comma formation that finally, with low tin coating levels, could lead to a welding range with only 'conventional' splash. Applying a large enough welding current will result in fusion, but could also lead to (surface) splash formation [52]. In addition, welding speed also influences the weld nugget formation [52]. It has been reported that at slow welding speeds, long heating and large

contact length leave the generated liquid material state on the weld interface line at the point of formation by action of the electrode force. At higher speeds, the applied effective electrode force (contact length between electrodes and welded material) is relatively small and as a result, the ranges of good quality welding conditions significantly reduce [28].

The smaller electrode wheel gives rise to higher current densities; accordingly, splash formation is more readily seen on the inside of the can body. Some can body welding machines have a controlled vertical movement for the smaller electrode wheel to assist in aleviating the formation of splash.

Splash particles are left behind adjacent to the weld seam and are mainly seen when the contact time is reduced and the welding speed is increased. Splash formation is prone to occur in thin sheet steel with higher carbon contents due to the higher material resistivity. [118 to 120]

12.4 Cold welds, fishtailing and overheating

Incomplete bonding and tin bonds result from cold weld formation and are formed due to insufficient heat generated at the weld interface line, as shown in figure 12.6 [5].

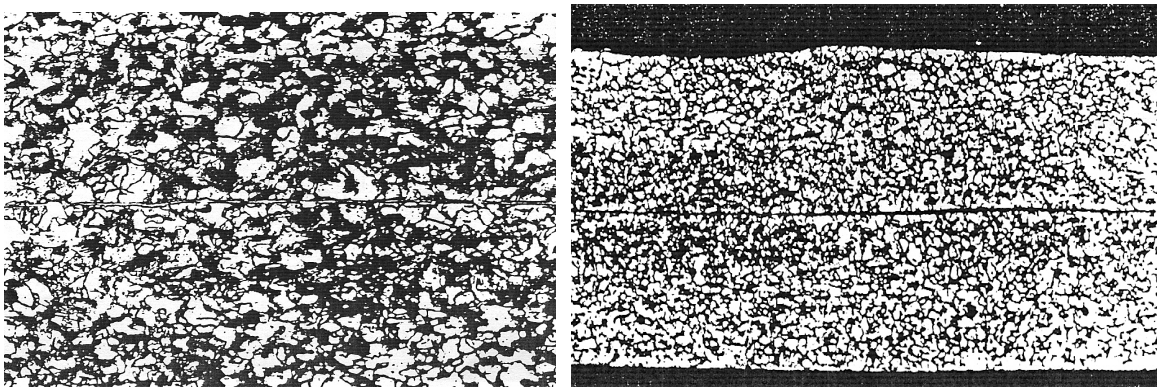

Figure 12.6: The left-hand side shows a picture of a weld interface line were tin is still situated in between the two work-pieces, a tin bond. The right-hand side picture shows an incomplete bond between the two work-pieces [5].

According to Norman [3], varying the welding parameters could result in a parameter area of tin-solder bonding, where essentially only tin coating is melted between the interfaces. Yet, such a joint can be acceptable for some end-application containers. The presence of tin-solder bonds creates an unsatisfactory cold-weld condition. Norman et al said that this is effectively a soldered joint. Tin bonds are apparently weak regions on the interface with a solder joint condition, which typically occur at lower welding currents [28]. The effect would be more pronounced with increasing welding speeds, because less contact time results in less heat generation between the electrode wheels and the sheet material.

Fishtailing is a defect that can cause problems after welding, i.e. during flanging and double seaming in the production of three-piece containers. Fishtailing is a phenomenon which takes place at the end of the weld seam as shown in figure 12.7 and is a result of material which is longitudinally extruded in relation to the welding direction beyond the end of the can body.

The reason for fishtailing is found in the process. As the wire gap becomes too wide, the electrode wheels further press the sheet material to a state of plasticity, which in combination with the electrode force extrudes the sheet material at the end of the can body. In order to overcome the problem of fish tailing the gap between the two wires (which circumscribe the electrode wheels) should lie between 0.5 and 1 mm. When the gap becomes smaller joining of stretched wire at the gap and fishtailing could occur.

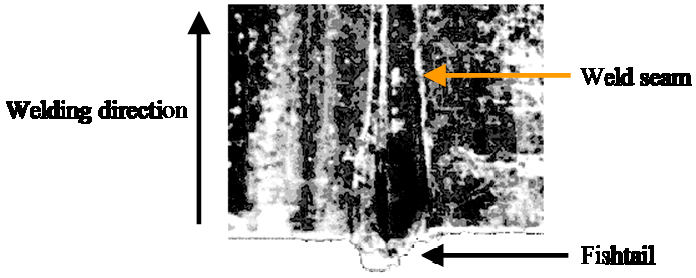

Figure 12.7: Microphotograph of a fishtail at the end of the can body after welding. The fishtail being the result of material longitudinally extruded in relation to the welding direction beyond the can body end.

Rare defects that are encountered with only embrittled work-pieces are split flanges, blowholes (see figure 12.87) and complete burn through of the weld [3]. These defects are encountered with embrittled work-pieces and are thus a consequence of over-heating the work-pieces.

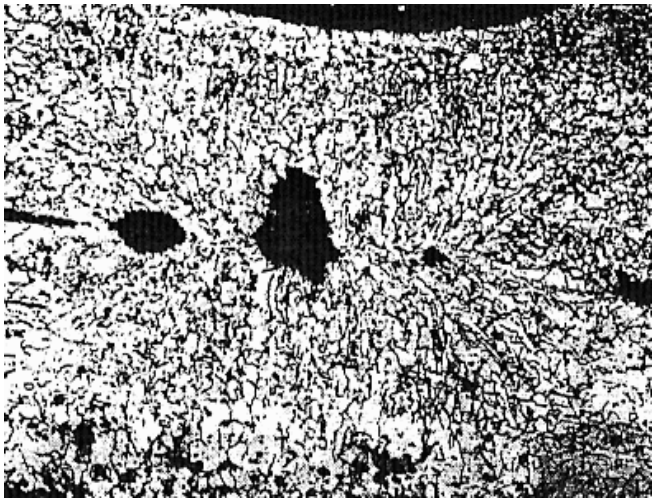

Figure 12.8: example of a blowhole found in an overheated weld made above the upper welding limit.

13 Modelling high-speed resistance welds

Numerical modelling techniques are employed to gain scientific insight into the welding process, both macroscopically and microscopically, but due to the inherent lack of user-control with pre-written commercial software, little understanding could be gained. In this way, only a weak basis for process control is attained. Furthermore, limitations exist in all models, which are sometimes difficult to understand.

Attaining high-speed welding data experimentally to develop welding current ranges using different parameters, is very time consuming, as is the detailed metallographic analyses that require high-precision cutting equipment. A computer model would therefore be justified in gaining more understanding of the process and comparing parameters without difficult or time/cost expensive tryout experiments, because as a best practice, canmakers will set weld combinations that work instead of trying different settings at greater risk.

Decisions on what parameters are chosen for a model need to be made. For simplicity and time related issues it can be counter-productive to take some process factors into consideration. For example, the age and type of welder can be a governing factor. All conditions and factors mentioned before leave a wide range of parameters to consider when establishing production conditions.

Previous attempts have been made at modelling welding processes using finite element (FE), methods [121 and 122] and theoretical analysis [7] using commercial and in-house codes. Particularly with high-speed welding differently reported approaches are outlined with additional consideration of modelling assumptions made for other applications involving heat transfer, such as defects in castings.

A mathematical model to simulate the cooling of the weld with high-speed resistance mash seam welding was developed by Boyd [123] to gain understanding of the mechanisms of heat loss in a weld seam of a container. Assumptions made in this model were:

- Temperature was considered to be constant through the thickness of the plate since heat was conducted away from the weld zone into the electrode wheels and can body
- No conduction along the can height was considered because that depended on the heat conduction rate of the material and the isolation of overlapping weld nuggets
- No increasing thickness of the weld to maintain the previous assumptions. However, the specific heat was increased at the overlap width, thereby establishing a 1-D conduction mechanism

The results for the heat loss correlated with the experimental findings, as convection and radiation losses were much smaller than conduction, especially loss of heat to the electrode wheels. The model was further developed by Boyd [124] with geometrical aspects considered by comparison to the collapse of a plasticity section and a graphics model. The assumption of constant plasticity within the model enabled consideration of a full homogeneous material. Within the model of Boyd longitudinal flow and shear forces were neglected to aid simplification. However, the graphics model did include a ridged topography as seen on the surface of a weld seam. A reducing contact area of the upper electrode wheels would improve the quality of the weld.

The modelling of DC resistance welding to produce continuous container weld seams was performed by Brifcani [125]. He considered electro-thermal aspects in the absence of deformation on a simplified 2-D cross-section mesh using a commercial FE code, ANSYS. Although Brifcani distinguished the limitations of the model, considerable data was generated to determine current flow in the steel sheet and the transient temperature distribution in the sheet and electrodes. Brifcani noted that the increasing resistance of the steel caused weld instability as the temperature increased (i.e. temperature dependent resistivity) and that excessive heating was caused by current flow ahead of the welding front. The effects of thermal conduction are also negligible because the speed of the material exceeds the speed of thermal diffusion in steel. It was determined that problems associated with DC welding were not prevalent in AC welding due to the cyclic character of the current, which yields similar temperature conditions at the formation of each weld nugget.

Using the commercial code SYSWELD Ferrasse and Piccavet [126] modelled the mash seam welding process for 0.7 mm thick low-carbon steel sheet. A fixed transverse 2-D model with observed geometries of the electrode wheels and the steel sheet was constructed. The conductive heat flow through the transverse and longitudinal directions was considered to remain significantly lower than the studied welding speeds. The model allowed examinations of the distribution of thermal patterns within the weld zone and was validated using infrared surface temperature scanning techniques. Photomicrographs of actual samples were used to determine specific isotherms. The nature of the 2-D model was justified with lower currents; the plastic deformation (mash) took place before any signs of melting were detected with most of the heat generation concentrated at the weld interface line. Instead of a continuous growing weld zone, the (Joule) heating effect was limited to a static region.

Modelling of the mash seam welding process is for a greater part conducted within industry [127 to 129]. Here electro-thermal models in the commercial code ABAQUS was written. This

takes into account the copper wire and current, which is assumed to flow through the outer surfaces of the copper wires. The short run time of the model assumes that no heat flow establishes either from the electrode wheels or the tinplate sheets. Another assumption within the model is the use of a deformed mesh (lattice) to which the current is applied. Limitations of the model are the 2-D character of the mesh, whereby lack of accurate understanding of contact resistance inhibits development to a 3-D model. The welding process was further modelled using ABAQUS by Wen [130]. Two 2-D meshes were constructed, one transverse and one longitudinal cross-section, within which coupled thermal-mechanical computations were performed. The (Joule) heating effect from different current frequencies was investigated on the longitudinal section. Within this work it is important that deformation and heat generated at the electrode wheel-tinplate interface and overlap width are taken into account. However, the model is limited by no use of contact resistance. Besides this the model only has a 2-D mesh. Results from the model showed that higher temperatures were uniformly generated at the electrode wheel-tinplate contact and overlap (i.e. where the heating effect is applied). However, it did not take into account the loss of heat to the atmosphere and copper electrode wheels and the effect of larger current densities at the sharp edges of the mesh. Within modelling of projection welding, using ABAQUS, this aspect was also shown by Sun [131]. This model assumed a defined line of symmetry and limitations regarded no work-hardening effect; also no prevalent stress or strain in the projection, prior to welding were taken into account.

Cross-sectional and longitudinal 2-D FE models were developed by Murakawa et al [132]. They used a thermal-elastic-plastic theory to examine the effects of the waveform, value of the welding current and welding speed on the formation of the weld nugget. Their model is split into three stages. First, the deformation from the electrode wheels is calculated to compute the electric fields whereby the current densities are given. Thereafter, the heating effect is estimated and the thermal field is calculated. This three stage cycle is repeated using small time steps until a satisfactorily weld is made. However, the model is for joining three sheets with a total thickness of 1.9 mm at speeds between 1.4 to 1.6 m/s using electrode wheels with similar diameters. The results are small deformations compared to the original sheet thickness and the model appears to be giving difficulties in correctly defining contact elements during heating and deformation between the electrode wheels-tinplate and tinplate overlap width. Nevertheless, a continuous applied current resulted in non-uniform nugget growth due to periodic instability, closely linked to the contact area between the electrode and the sheet material. As a result Murakawa et al stated that discontinuous settings lead to better weld nuggets due to a sufficient available time for electrode cooling.

The measurement of dynamic electrical resistance of the electrode to sheet interface was modelled by Thieblemont et al [133]. In this model the interaction of thermal and electrical phenomena are simulated in an axi-symmetric FE model. The goal was to provide temperature information for the automotive industry, where the problem of spot welded zinc coated sheets lies within over-heating at the electrode to sheet interface resulting in insufficiently large weld nuggets and faster electrode deterioration. The model takes into account heat loss to the atmosphere and water-cooling of the electrodes and uses surface contact elements to determine where the heating takes place. The model predicts temperature distributions for uncoated and zinc coated steel sheets and shows that the resistances of the faying weld interface and electrode-sheet interface play the most significant role during the early stages of welding. In contrast with a 3-D model for high speed resistance welding, spot welding is a process, which can be modelled with a defined line of symmetry. However, the concept of contact resistance still holds when modelling the high-speed welding process.

Gould [7] proposed a model to analyse the effect of forging and heating in forming a mash seam weld since both play a different role in accomplishing a solid-state bond. He stated that forging proceeds along the weld interface line, whereby the actual strains can be derived from the joint configuration. The results from the forging indicate that the effective bonding must occur by the addition of thermal energy in the mash seam welding, and the role of thermal energy appears to predominate. Gould indicates that the thermal energy has two other functions, namely: dissolution of retained surface oxides and contaminants, and recovery of the residual deformed weld interface line structure. Heat generation in mash seam welding is through resistance heating over the weld area.

The modelling of a moving heat source is investigated by Hansen et al [134] for submerged arc welding and Brown et al [35] for high-speed resistance welding of containers. Hansen et al did their work in ABAQUS, using elements in the finite element mesh accounting for the moving heat source and thereby placing a higher weighting on determining stress fields, focussed on the effects of thermal expansion from filler metal contraction. A detailed description of heat generation and thermal distribution was considered less important than a generalised description when coupled with stress fields and deformations. The moving heat source for the high-speed welding model is different in the sense that material flows through a static mesh and is subjected to boundary conditions at a theoretical electrode wheel-sheet material contact area [35]. Brown and Suthar also state that the possibility of a full 3-D stress analysis for high-speed resistance welding is very difficult because the mechanical properties of the material from room temperature to melting point, as a function of prevalent strain rates are required. The assumptions, which have

to be made to account for conditions, attributed to melting and deformation could impede the effectiveness of the model as they validated their model to the RTZ only. A typical example of the inclusion of a liquid phase due to melting within a weld is modelled by Pavlyk and Dilthey [135]. They implemented thermo-fluid models to investigate the influence of convection on temperature distribution and weld pool geometry in electric arc weld pools with the commercial code FIDAP, which is specifically designed for computational fluid dynamics. The model considers thermo-capillary forces, volume expansion and heat exchange mechanisms including loss of heat due to evaporation, radiation and convection. They included FIDAP due to fluid flow affecting the overall heat and mass transfer in the weld pool, which affect weld shape and temperature distribution. The model [135] is made for Gas Tungsten Arc (GTA) welding; thereby the validation of the model could be achieved experimentally with a static weld pool. The dynamic character of high-speed welding gives quantification difficulties, with infrared measurements serving as validation, only giving surface temperatures at the contact of the upper electrode wheel and the outside of the welded can body. The suitability of infrared measurements as a method can also be questioned because splash formation on the inside of the can and commas inside the weld could disturb this.

14 Discussion

To date, worldwide welded steel containers represent the most predominant form of packaging for food, aerosol and general line products, whereby around 90% of the world's food containers are three-piece cans. In obtaining this situation, the production of three-piece cans has developed very quickly from the sceptical unease in its early conception (hand work) of soldered seam containers to the very fast (80 to 115m/min) and highly automated welding process nowadays. Three-piece can manufacture still holds a little over half of the can market sectors for aerosol, food, and general line containers. However, the deep drawn processes are also used for aerosol; food and speciality can applications and rapidly took almost half of the marked and are still taking over from the welded can market. Laser welding is also impending in the manufacture of three-piece cans, but because it is not yet able to compete with the present three- and two-piece container production speeds and manufacturing technologies, it has not yet found commercial acceptance. The literature on laser welding also shows some inconsistency as a consequence of this. However, the development and relation to other processes is clear from the wide variety of literature sources.

An adequate starting point to describe in detail, the (fundamental) aspects, understanding and control of the complex and dynamic nature of high speed resistance seam welding shows that the seam welding process is firstly required for a range of hot-rolled and coiled low-carbon steel grades and tinplate classifications to meet customers demands of for instance tomato soup or deodorant producers. The welding of containers is only one process feature in the production line of the three-piece can manufacture. Although the production process consists mainly of forming operations welding is a major influential process step. Before and after welding, limitations and restrictions on the tinplate, and welding machine determine what happens to the material of the can body and its properties in the final product. All other process steps are pointed out in various literature sources and are soundly based and understood, except for the welding process, which seems to be less studied from the scientific perspective.

Most high-speed resistance welding literature before the 1990s is based on phase angle/shift control, variation and on their development and optimisation. Today, the current is no longer interrupted via phase angle control, but by amplitude control whereby the preceding literature could turn out to be obsolete. However, the essence of the process with respect to the material appearances and microstructures because of differently used tinplate grades and heating phenomena remains, and the earlier literature contributes to a better understanding of the welding process. To date, the classic theory of coalescence in the absence of melting is considered valid

and is invariably discussed in terms of its variable parameters, i.e. within the welding range. The process and material related factors mentioned below are given in the majority of the literature to be most important in order to utilise the appropriate weld quality with the HSRW process.

Process	Material
Power supply	Coating type
Electrodes and wire contact	Thickness of the work-piece
Weld current	Coating layer thickness
Electrode force	Grain orientation
Weld speed and frequency	Steel chemistry; carbon content
Material overlap width	Heat treatments

The parameters above are repeatedly investigated and reported in the various literature sources to operate the welding process to its maximum welding speed and optimum welding range. Since the complexity and wide variety in the HSRW process is opposed by these process and material parameters, the dynamic character of the process makes it sometimes difficult to classify the process to a specific weld mechanism. However, as the HSRW process name indicates, resistance, predominantly contact resistance is the main and indicative feature that the parameters have in common and which in the literature is studied over and over to show the effect of heat generation and temperature balances on the final joint and its associated (mechanical) properties, i.e. to classify the weld in the welding range. Additionally, several studies discussed the difference in static and dynamic contact resistance and found that this distinction should be made to get an idea of what is actually happening during welding. The main reason for this is that there is a large difference between static and dynamic contact resistances.

Some sources show that the welding range can be defined in terms of microstructures by the examination of longitudinal sections of a HSRW weld. The point where it is not possible anymore to produce sound welds is associated with the occurrence of detectable defects. Melting, under certain conditions (e.g. high welding current) can occur, accounting for defects where molten metal is ejected from the inside of the weld seam, which affects the appearance and corrosion resistance of the weld. However, the examination method for the determination of the upper limit becomes too sophisticated and time consuming when the appearance commas are considered as the limiting stage. Defects from the cold weld situation are also difficult and time consuming to quantify on the microscopic level, but easy mechanical test methods makes them readily detectable.

Very little is known or published on the actual mechanism of weld formation (i.e. nugget formation and bonding phenomena) within high-speed resistance welding. The idea on weld formation at a particular maximum heat development zone seams to hold for phenomena seen in the HSRW process. The dynamic nature of the process permits only a few milliseconds for heating and deformation to produce a proper weld seam. However, the process is governed by dynamic and original (static) contact resistance. Therefore a full explanation of weld formation should also include volume and melting point of coating, bulk resistivity and how these influence the dynamic resistance. The existing explanations are based on large parameter studies or data-mining in combination with statistical analyses and are rather ambiguous and indistinguishable. Even though a lot of time and resources are invested in understanding the process and associated materials, especially related to protective layers with several thicknesses; however, the process has been studied without thoroughly examining the behaviour of the materials during processing.

On the atomic level, weld nugget development (sub-macroscopic level) and classification of solid-state and fusion bonding phenomena a variety of literature can be found to describe parts or specific conditional settings of the bonding mechanism(s). Actually, within the resistive heating phenomena many can be found on the theoretical basis of heating and cooling, but predominantly with static resistance welding phenomena. However the few sources discussing dynamic contact resistance all exclude joining by solid-state welding.

Although the science seems to remain quite complex not a lot is found on microstructural phenomena in high-speed resistance welds, probably as a consequence of the fact that metallographic examination can be complex and particularly time consuming. In the published literature, one criterion of the microstructure was initiated on the determination of the lower limit, which is dependant on the structure on the weld interface line. This criterion is defined as a percentage of incomplete bonding, tin bonds and grains situated across the weld interface line, some literature sources also mention grain growth at the weld interface.

Furthermore, as mentioned before, there are a lot of limitations and unrecognisable phenomena occurring in this process. The relationships of many of these phenomena to each other or to the welding process are not clearly understood. Nevertheless, some ideas on the actual bonding formation exits based on welding parameter and process parameter variations, which can probably be attributed to the fact that literature that is published concerning improved weldability. The phenomenological approach in this is missing.

Modelling can help to provide a more profound understanding of the HSRW process and thereby improve the process capability. Modelling the HSRW process is very difficult, given all of the different parameters that should be included. In previous attempts only 2-D models written

in commercial packages appear to exist. They provide a great deal of useful information, otherwise unattainable form experimental studies. A lot of useful information would be gained from a 3-D model; however, this should be written from the ground up with an in-house code. The benefit of an in-house developed codes compared to a commercial code is the inherent knowledge of the assumptions and limitations that the user has. Additionally, during the development, the user has access to the source code allowing suitable changes to be made to materials and process properties or constants throughout the analysis. Significantly, all types of codes are numerical approximations therefore an exact answer is probably not possible and validation of the experimental findings is therefore important for both commercial and in-house codes. In contrast with in-house codes, commercial codes are advantageous in the user-friendly matter making the model development less time-consuming.

15 Conclusions

In this literature review an appraisal of all facets of high-speed resistance mash seam welding tinplate packaging steels for three-piece can manufacture lead to the following key conclusions:

The high-speed resistance mash seam welding process developed rapidly into a very fast, and highly automated welding process, which despite other much suitable processes is still able to maintain more than half of the steel container packaging market.

Three-piece container production consists mainly of forming operations whereby many limitations and restrictions on the tinplate influence the welding procedure. Nevertheless, welding is a major influential process step, with a lifetime effect to what happens to the can body material and its properties in the final product.

The welding process is characterised by the (contact) resistance, which shows the effect of heat generation and temperature balances on the final joint and associated metallurgical features. The contact resistance is subject to the welding parameters and tinplate properties to operate the process to its maximum speed and optimum welding range, whereby the dynamic character of the welding process makes it difficult to classify the process to a specific class.

The welding process is defined in terms of the can manufacture specifications, yet very little is known or published on the actual mechanism of weld formation (i.e. nugget formation and bonding phenomena). The existing explanations are based on some rather ambiguous and indistinguishable assumptions. A lot of time and resources have been invested in large parameter studies or data-mining in combination with statistical analyses to find material-process connections. However no study looked at the behaviour of the materials during processing.

Given all the different parameters that should be included, only 2-D models of the HSRW process written in commercial codes appear to exist. Even though modelling the process is very difficult, it provides a great deal of useful information, otherwise unattainable form experimental studies. Both commercial and in-house codes are numerical approximations and require validation by experimental studies.

On assessment of all the conclusions above the following main conclusion is deduced:

Despite the simple principles of the welding process the actual process is rather complex, involving aspects of many different scientific phenomena, which give rise to many limitations, and inexplicable phenomena. The relationships of many of these phenomena to each other or to the welding process are not yet clearly understood.

16 Recommendations for future work

This literature gives a contribution to the incomplete research on the materials tin layer and microstructural development during the welding process. To further deepen the understanding of the mash seam welding process and to provide a basis for optimisation in resistance mash seam welding of container applications, future research should focus on the particular influences of the metallurgical and physical alterations on the weld interface upon process performance in the complete welding range and the specific mechanisms for the formation of the joint.

If possible, the microstructural development should be analysed by assessing the thermal balances based on dynamical resistance (history). It is likely that the tin layer also has significant influence on the thermal history due to its resistivity and the associated changes during heating and deformation. Influence of the metallic coating layer on the weld formation requires studies on physical and metallurgical consequences to provide different dynamic contact resistance (i.e. changes in the thermal history) and weld ranges. Hereby precise cross sectioning of the welds is a first requirement. Time-temperature-force assessment, and thermal and microstructural prediction could be done best by modelling and validating this to experiments.

References

1 Elzinga E. and De Haas M., "*Personal Communication*", Corus Research Development & Technology, IJmuiden Technology Centre, The Netherlands, 2006.

2 Twisk F. and De Haas M., "*Some Observations of the Microstructure of High-Speed Welds*", Internal Document, Corus Research Development & Technology, IJmuiden Technology Centre, The Netherlands, October 2004, 15p.

3 Norman G. F., "*Welding of Tinplate Containers - An Alternative to Soldering*", Metal Box Limited, London, United Kingdom, Paper No.20 1st International Tinplate Conference, International Tin Research Institute, London, United Kingdom, October 1976, pp. 239 to 248.

4 Sodeik M. Täffner K. and Weber F., "*Fundamentals of Modern Canmaking and Materials Development for Three-Piece Can Manufacturing*", Rasselstein Hoesch AG, Neuwied, Germany, Transactions of the Iron and Steel Institute of Japan, Vol.28 No.8, Japan, March 1988, pp. 663 to 671.

5 Gregory L., Szczur J. and Squires I., "*The Australian Steelmakers Experience with the Welding of Tinplate Cans*", New Zealand Institute of Welding, Paper No.10 Art and Science of Welding conference, Auckland, New Zealand, October 1985, pp. 75 to 82.

6 Klärner T., "*Ausgewählte Probleme des Rollennahtschweißens in der Emballagenindustrie*", Umformtechnik Vol.25 No.2, Zwickau, Germany, February 1991, pp. 57 to 65.

7 Gould J.E., "*Theoretical Analysis of Welding Characteristics during Resistance Mash Seam Welding of Sheet Steel*", Research Supplement, Welding Journal Vol.82 No.10, 2003, pp. 263-s to 267-s.

8 Elzinga E., "*Lasbaarheid en Kontaktweerstand van Materialen voor de Driedelige Bus*", Internal Document, Hoogovens Research & Development, IJmuiden Technology Centre, The Netherlands, July 1991, 83p.

9 Sodeik M., "*Influence of Material Properties on Side Seam Welding of Cans made of Tinplate*", Rasselstein Hoesch GmbH, Neuwied, Germany, Paper No.16 2nd International Tinplate Conference, London, International Tin Research Institute, London, United Kingdom, October 1980, pp. 161 to 175.

10 Coles A-M. and Evans C.J., "*The Welded Tinplate Can*", Tin and its Uses No.139, International Tin Research Institute, Greenford, United Kingdom, 1984, pp. 1 to 5.

11 Silbereis J., "*Electric welding of canbodies - Hindsight and insight*", Tin International Vol.59 No.7, July 1986, pp. 241 to 243.

12 Kuguminato H., Ryu N. and Kikuchi T., "*New Tin Free Steel for Cans Weldable without Edge Grinding*", Kawasaki Steel Technical Report Vol.34, Kawasaki, Japan, March 1996, pp. 37 to 39.

13 Church F.L., "*Laser Welding Proves its Worth in Can Manufacturing*", Modern Metals Vol.42 No.9, October 1986, pp. 104 to 113.

14 Saito T., Miyazaki Y., Sakiyama T., Takahashi Y. and Mizuhashi N., "*Welding Technology for Uncoated and Coated Steel for Automobiles, Household Electric Appliances, and Containers*", Nippon Steel Technology Report Vol.65, Japan, April 1995, pp. 25 to 31.

15 Uchihara M. and Fukui K., "*Tailored Blanks of High Strength Steel - Comparison of Welding Processes*", Welding Research Abroad Vol.49 No.4, April 2003, pp. 19 to 26.

16 Irving B., "*Cans, Tailored Blanks and Fuel Tanks*", Welding Journal Vol.73 No.7, July 1994, pp. 34 to 38 (even).

17 Sharp C.M. and Nilsen C.J., "*The Development and Implementation of High Speed Laser Beam Welding in the Can Making Industry*", Welding Journal Vol.67 No.1, January 1988, pp. 25 to 31.

18 Evans C.J., "*Can-Making Today*", Tin and its Uses No.153, International Tin Research Institute, Greenford, United Kingdom, 1987, pp. 1 to 4.

19 Schmitz B. and Defourny J., "*Laser Welding, Resistance Spot Welding, Adhesive Bonding, Competing or Concurring Process for Sheet Metal*", American Society for Metals International, USA, 1993, pp. 427 to 432.

20 Siewert J. and Sodeik M., "*Seamless Food Cans Made of Tinplate*", Paper No.13 1st International Tinplate Conference, International Tin Research Institute, London, United Kingdom, October 1976, pp. 154 to 164.

21 Fidler F., "*Two-Piece Container Developments - Some Influences of Tin*", Metal Box Limited, London, United Kingdom, Paper No.15 2nd International Tinplate Conference, International Tin Research Institute, London, United Kingdom, October 1976, pp. 169 to 177.

22 Panknin W., Schneider C. and Sodeik M., "*Plastic Deformation of Tinplate in Can Manufacturing*", Sheet Metal Industries Vol.53 No.8, Germany, August 1976, pp. 137 to 138 and 140 to 142.

23 Sodeik M., Täffner K. and Weber F., "*Fundamentals of Modern Canmaking and Materials Development for Two-piece Can Manufacturing*", Rasselstein Hoesch AG, Neuwied, Germany, Transactions of the Iron and Steel Institute of Japan, Vol.28 No.8, Japan, March 1988, pp. 672 to 677.

24 Habberly P.J., "*Market Requirements of Metal Packaging*", Ironmaking and Steelmaking Vol.18 No.1, January 1991, pp. 16 to 20.

25 Büchler A., "*Comeback der Dreiteildose*", Neue Verpackung No.9, Germany, September 1991, pp. 160 to 162.

26 Gardner J.F., "*The Springback of Metals*", Journal of Transactions of the American Society for Materials Engineering Vol.79, November 1955, pp. 1 to 9.

27 Elzinga E., "*Welding and Rolling Direction*", Internal Document, Corus Research Development & Technology, IJmuiden Technology Centre, The Netherlands, June 2005, 29p.

28 Waddell W., Thomas D.E. and Williams N.T., "*High Speed Seam Welding of Low Tin Substrates*", Metal Construction Vol.18, March 1986, pp. 156 to 161.

29 Dantas S.T., De Massaguer P.R., Mori E.E.M. and Shirose I., "*Performance of Metallic Packaging for Carbonated Beverages: Evaluation of Welded and Soldered Cans*", Instituto de Tecnologica de Alimentos, Campinas, Brasil, Paper No.42 3rd International Tinplate Conference, International Tin Research Institute, London, United Kingdom, October 1984, pp. 467 to 481.

30 Elzinga E., "*Axiale en Radiale Weerstand van Driedelige Bussen uit 0,12 mm Materiaal*", Internal Document, Hoogovens Research & Development, IJmuiden Technology Centre, The Netherlands, October 1992, 5p.

31 Elzinga E., "*Determination of Axial and Radial Strength on 3-Piece Cans, ø 52 x 115 mm*", Internal Document, Hoogovens Research & Development, IJmuiden Technology Centre, The Netherlands, March 1992, 3p.

32 Sauer R. and Sodeik M., "*Mechanical Behaviour of Food Cans Under Radial and Axial Load*", Paper No. 3rd International Tinplate Conference, International Tin Research Institute, London, United Kingdom, October 1984, pp. 152 to 167.

33 Sauer R. and Sodeik M., "*Mechanisch Verhalten der Verpflegungdosen unter Radial und Axial laden*",Technical Scientific Supplement, Verpackungs-Rundschau Vol.36 No.6, June 1985, pp. 35 to 42.

34 Elzinga E, "*Everything you always wanted to know about The Seam Welding Process*", Internal Document, Corus Research Development & Technology, IJmuiden Technology Centre, The Netherlands, February 2003, 30p.

35 Brown S.G.R. and Suthar B.S., "*Modelling the Effects of Process Variables on Thermal Behaviour during High Speed Resistance Welding of Tinplate*", Materials Science and Technology Vol. 20 No.12, December 2004, pp. 1585 to 1589.

36 Schaerer G. and Weil W., "*Soudronic Welding Technique - A Promoter of Tinplate Containers*", Soudronic AG, Switzerland, Paper No. 21 3rd International Tinplate Conference, International Tin Research Institute, London, United Kingdom, October 1984, pp. 268 to 280.

37 Hamann C., "*Geschweißte Weißblechdosen - Teil I*", Blech Rohre Profile Vol.32 No.9, Germany, September 1985, pp. 520 to 523 und "*Geschweißte Weißblechdosen- Teil II*", Blech Rohre Profile Vol.32 No.10, Germany, October 1985, pp. 549 to 552.

38 Klärner T., "*Ausgewählte Probleme des Rollennahtschweißens in der Emballagenindustrie*", Umformtechnik Vol.25 No.2, Germany, February 1991, pp. 57 to 65.

39 Elzinga E., Stevels J.T. and Van Haastrecht G.C., "*Improvement of Welding Three-piece Cans*", Hoogovens Research & Development, IJmuiden Technology Centre, The Netherlands, Paper No.5 6th International Tinplate Conference, International Tin Research Institute, London, United Kingdom, October 1996, pp. 61 to 65.

40 Brown M., "T*rapezium Wire fills Quality Gap*", The Canmaker, February 1997, pp. 30.

41 Rosenthal D., "*Mathematical Theory of Heat Distribution during Welding and Cutting*", Research Supplement, Welding Journal Vol.20 No.5, May 1941, pp. 220-s to 234-s.

42 Haigh S.J., "*Preliminary Results of Electrical Characterisation of Body Plate for Welding*", Technical Record, Metal Box Limited Research & Development, London, United Kingdom, 1982, pp. 1 to 5.

43 Ichikawa M and Saito T, "*The Effect of Contact Resistance on the Weldability of Can Materials*", Nippon Steel Corporation, Sagamihara, Japan, Paper No. 4th International Tinplate Conference, International Tin Research Institute, London, United Kingdom, October 1988, pp. 446 to 452.

44 Shimizu N, Hayashida T, Nishimoto N, Fukai J and Miyatake O, "*Relation between Equivalent Contact Resistance and Resistance Seam Weldability for Beverage Cans*", Tetsu-To-Hagane (Journal of Iron and Steel Institute of Japan) Vol.84, No.4, Japan, April 1998, pp. 249 to 254.

45 Shimizu N., Nishimoto N., Morita S., Fukai J., Baba S. and Miyatake O., "*Effect of Differential Tin Coatings on Resistance Seam Weldability of Low Tin-coated Steel for Beverage Cans*", Tetsu-To-Hagane (Journal of Iron and Steel Institute of Japan) Vol.86, No.8, Japan, August 2000, pp. 519 to 525.

46 Tan W., Zhou Y., Kerr H.W. and Lawson S., "*A Study of Dynamic Resistance during Small Scale Resistance Spot Welding of Thin Ni Sheets*", Journal of Applied Physics D: Applied Physics Vol. 37 No.14, June 2004, pp. 1998 to 2008.

47 Dickinson D.W., Franklin J.E. and Stanya A., "*Characterization of Spot Welding Behaviour by Dynamic Electrical Parameter Monitoring*", Research Supplement, Welding Journal Vol.59 No.6, June 1980, pp. 170-s to 176-s.

48 Elzinga E., "*Enige Opmerkingen over de Grootte van de Lasrange en de Riptest*", Internal Document, Hoogovens Research & Development, IJmuiden Technology Centre, The Netherlands, July 1988, 5p.

49 Elzinga E., "*The Sensibility of Canbodies to Deformation (The "Smile"-Test)*", Internal Document, Hoogovens Research & Development, IJmuiden Technology Centre, The Netherlands, November 1986, 14p.

50 Simon F.E., Toner D.F. and Kuessel N.E., "*The Influence of Tinplate Surface Characteristics on Wire Welding*", Campbell Soup Corporation and Ross Laboratories, USA, Paper No.16 5th International Tinplate Conference, International Tin Research Institute, London, United Kingdom, October 1992, pp. 170 to 177.

51 Williams N.T., Thomas D.E., and Wood K., "*High Speed Seam Welding of Tinplate Cans, Part 1 - Equipment Development, Weldability Lobes and Metallurgical Characteristics*", Metal Construction Vol.9 No.4, April 1977, pp. 157 to 160.

52 Williams N.T., Thomas D.E., and Wood K., "*High Speed Seam Welding of Tinplate Cans, Part 2 - Influence of Welding Parameters and Material, and Production Implications*", Metal Construction Vol.9 No.5, May 1977, pp. 202 to 204 and 206 to 208.

53 Renard J.F. and Gellez J, "*Tinplate Specification for New Applications*", Sollac, France, Paper No. 5th International Tinplate Conference, International Tin Research Institute, London, United Kingdom, October 1992, pp. 1 to 13.

54 Various authors, "*A Simple Guide to Finishing Processes in the Iron and Steel Industry*", British Iron & Steel Federation, The Fanfare Press Limited, London, United Kingdom, 1953.

55 Various authors, "*Tinplate - Electrolytic Tinning*", British Iron & Steel Federation, The Fanfare Press Limited, London, United Kingdom, 1953.

56 Giefers H. and Nicol M., "*Equation of State Study of Several Iron-Tin Inter-metallic Compounds*", University of Nevada, Las Vegas, USA.

57 Hansen M. and Anderko K., "*Constitution of Binary Alloys*", 2nd edition, McCraw and Hill, General Electric company, Business Growth Services, Schenectady, New York, USA, 1958, ISBN: 0-9316-9018-8.

58 American Society for Metals International and the Materials Information Society, "*Alloy Phase Diagrams*", 10th edition, American Society for Metals Handbook Vol.3, USA, 1993, ISBN: 0-87170-381-5.

59 Winter M., http://www.webelements.com, University of Wales and WebElements Limited, Wales, United Kingdom, August 2006.

60 Asano H., Higashi M., Higuchi S. and Ichikawa M., "*Coated Sheet Steel for Welded Cans*", Nippon Steel Corporation - Research & Development, Technical Report No.25, Japan, April 1985, pp. 47 to 54.

61 Elzinga E. and Bisel, "*Lasbaarheid van Verpakkingsstaal met Verschillende Metallische Deklagen*", Internal Document, Hoogovens Research & Development, IJmuiden Technology Centre, The Netherlands, August 1990, 10p.

62 Elzinga E., "*De Invloed van de Legeringslaagdikte op de Lasbaarheid van Vetind Staal*", Internal Document, Hoogovens Research & Development, IJmuiden Technology Centre, The Netherlands, December 1986, 10p.

63 Stevels J.T., "*Is Lager Gelegeerd Staal beter Lasbaar*", Internal Document, Hoogovens Research & Development, IJmuiden Technology Centre, The Netherlands, March 1997, 8p.

64 Tylecote R.F., "*Investigations on Pressure Welding*", British Welding Journal Vol.1 No.3, March 1954, pp. 117 to 135.

65 Holtzclaw Jr. H.F., Robinson W.R. and Odom J.D., "*General Chemistry*", 9th edition, D.C. Heath and Company, Toronto, Canada, 1991, ISBN: 0-6692-4429-5.

66 Callister Jr. W.D., "*Materials Science and Engineering - An Introduction*", 6th edition, John Wiley & Sons, University of Utah, USA, 2003, ISBN: 0-4711-3576-3.

67 Jones L. and Atkins P., "*Chemistry: Molecules, Matter, and Change*", 4th edition, W.H. Freeman & Company, New York, USA, 1999, ISBN: 0-7167-3595-4.

68 Anonymous author, "*Materials Science - Bonding in Solids, Structures of Solids*", http://chemed.chem.purdue.edu/genchem/topicreview/bp/materials/material1.html, Purdue University, West Lafayette, USA, 2006.

69 Bullard J.W., "*Bonding in Solids*", http://www.mse.uiuc.edu/info/mse182/t57.html, University of Illinois, Illinois, USA, 1999

70 Dutch S., "*Minerals, Atomic Bonding and Metallic Bonding*", http://www.uwgb.edu/dutchs/EarthSC202Notes/minerals.htm, University of Wisconsin, Green Bay, USA, January 2001.

71 Various authors, http://www.dunneplaat-online.nl/smartsite9719.htm?goto=13747, FDP, Hechtingsinstituut, NIL, NIMR, TNO and FME-CWM, The Netherlands, February 2006.

72 Various authors, http://www.keytosteel.com, INI International, Key to Metals Group and Step-Commerce AG, Switzerland, 2006

73 Den Ouden G., "*Lastechnologie*", 3rd edition, Delft University Press, Delft, The Netherlands, 2000, ISBN: 9-0407-1285-9.

74 Beddoes J. and Biddy M.J., "*Principles of Metal Manufacturing Processes*", Elsevier Butterworth-Heinemann, Oxford, United Kingdom, 2003, ISBN: 0-3407-3162-1.

75 American Society for Metals International and the Materials Information Society, "*Welding, Brazing and Soldering*", 10th edition, American Society for Metals Handbook Vol.6, 1993, USA, ISBN:0-8717-0382-3.

76 Gales A. and Bodt H.J.M., "*Verbinden van Dunne Plaat en Buis*", FDP, Hechtingsinstituut, NIL, NIMR, TNO and FME-CWM, Paper No.TI.03.13, The Netherlands, May 2003, 11p.

77 Van der Sluis H.H. "*Soldeerprocessen voor Dunne Plaat en Buis*", FDP, Hechtingsinstituut, NIL, NIMR, TNO and FME-CWM, Paper No.TI.03.17, The Netherlands, May 2003, 12p.

78 Gales A., "*Lasprocessen voor Dunne Plaat en Buis*", FDP, Hechtingsinstituut, NIL, NIMR, TNO and FME-CWM, Paper No.TI.03.14, The Netherlands, May 2003, 10p.

79 Gould J.E., "*Mechanisms of Bonding for Solid-Sate Welding Processes*", 11th American Society for Metals Conference: Joining of Advanced and Specialty Materials, November 1995, pp. 259 to 267.

80 Bull S., "*Surface Requirements for Joining*", http://www.staff.ncl.ac.uk/s.j.bull/mmm373/solid/, Newcastle University, New Castle, United Kingdom, January 2001.

81 Tylecote R.F., "*The Solid Phase Welding of Metals*", Saint Martin's Press, United Kingdom, 1968, ISBN: 0-7131-3173-X.

82 Milner D.R. and Rowe G.W., "*Fundamentals of Solid-State Welding*", Metallurgical Reviews Vol.28 No.7, July 1962, pp. 433 to 478.

83 Bay N., "*Mechanisms Producing Metallic Bonds in Cold Welding*", Research Supplement, Welding Journal Vol.62 No.5, May 1983, pp. 137-s to 142-s.

84 Tylecote R.F., Howd D. and Furmidge J.E., "*The Influence of Surface Films on the Pressure Welding of Metals*", Research Supplement, British Welding Journal Vol.5 No.1, January 1958, pp. 21-s to 38-s.

85 Wright P.K., Snow D.A. and Tay C.K., "*Interfacial Conditions and Bond Strength in Cold Pressure Welding by Rolling*", Metals Technology Vol.5 No.1, January 1978, pp. 24 to 31.

86 Mohammed H.A. and Washburn J., "*Mechanism of Solid State Pressure Welding*", Research Supplement, British Welding Journal Vol.54 No.9, September 1975, pp. 302-s to 310-s.

87 Brick R.M., "*Hot Roll Bonding of Steel*", Research Supplement, Welding Journal Vol.49 No.9 , September 1970, pp. 440-s to 444-s.

88 McEwan K.J.B. and Milner D.R., "*Pressure Welding of Dissimilar Metals*", British Welding Journal Vol.9 No.7, July 1962, pp. 406 to 420.

89 Nikitin A.S., "*Examination of the Mechanism of Formation of Solid - Phase Welded Joints*", Welding International Vol.12 No.11, November 1998, pp. 904 to 906.

90 Linnert G.E., "*Welding Metallurgy - Carbon and Alloy Steels, Volume 1: Fundamentals*", 4th edition, American Welding Society, USA, 1994, pp. 520 to 534 and pp. 587 to 589.

91 Mitchell J.W. and Soltis M., "*Semi-Mash Seam Welding*", Welding Journal Vol.52 No.8, August 1973, pp. 509 to 516..

92 Gould J.E., "*An Examination of Nugget Development during Spot Welding, using both Experimental and Analytical Techniques*", Research Supplement, Welding Journal Vol.66 No.1, January 1987, pp. 1-s to 10-s.

93 Cho Y. and Rhee S., "*Experimental Study of Nugget Formation in Resistance Spot Welding*", Research Supplement, Welding Journal Vol.82 No.8, August 2003, pp. 195-s to 201-s.

94 Harlin N., Jones T.B. and Parket J.D., "*Weld Growth Mechanisms during Resistance Spot Welding of Two and Three Thickness Lap Joints*", Science and Technology of Welding and Joining Vol.7 No.1, January 2002, pp. 35 to 41.

95 Funk E.J. and Bergeman M.L., "*Electrical and Metallurgical Characteristics of Mash Seam Welds"*, Research Supplement, Welding Journal Vol.35 No.6, June 1956, pp. 265-s to 274-s.

96 Uchihara M., Hirose Y., and Fukui K., "*Tailored Blanks of High Strength Steel Sheets - Weldability and Formability"*, Paper No. 31st International Symposium on Automotive Technology and Automation Conference, June 1998, Germany, pp. 253 to.

97 Westgate S.A., "*The High Speed Resistance Seam Welding of Nominally 1.2mm Steel Sheet*", The Welding Institute, Cambridge, United Kingdom, June 1984, 31p.

98 Porter D.A. and Easterling K.E., "*Phase Transformations in Metals and Alloys*", 2nd edition, Chapman & Hall, United Kingdom, 1992, ISBN: 0-7487-5741-4.

99 Offerman S.E., Van Dijk N.H., Sietsma J., Grigull S., Lauridsen E.M., Margulies L., Poulsen H.F., Rekweldt M.Th. and Van der Zwaag S., "*Phase Transformations in Steel Studied by 3DXRD Microscopy*", Nuclear Instruments and Methods in Physics Research Section B: Beam Interactions with Materials and Atoms Vol.246 No.1, May 2006, pp. 194 to 200.

100 Offerman S.E., Van Dijk N.H., Sietsma J., Grigull S., Lauridsen E.M., Margulies L., Poulsen H.F., Rekweldt M.Th. and Van der Zwaag S., "*Grain Nucleation and Growth During Phase Transformations*", Science Vol.298 No.5595, November 2002, pp. 1003 to 1005.

101 Anonymous authors, "*Steel Alloys - Carbon Steels*", http://www.materialsengineer.com, Materials Engineer-Metallurgical Consultants, Orlando, USA, June 2006.

102 Krielaart G.P., Onink M., Brakman K.M., Tichelaar F.D., Mittemeijer E.J. and Van der Zwaag S., "*Thermodynamic Analysis of Isothermal Transformations of Hypo-Eutectoid Fe-C Austenites*", Zeitschrift für Metallkunde Vol.85 No.11, November 1994, pp. 756 to 765.

103 American Society for Metals International and the Materials Information Society, "*Properties and Selection: Irons, Steels, and High Performance Alloys*", 10th edition, American Society for Metals Handbook Vol.1, USA, 1993, ISBN: 0-8717-0380-7.

104 Christian J.W., "*The Theory of Transformations in Metals and Alloys*", 2nd edition, Pergamon Press, Oxford, United Kingdom, 1981, ISBN: 0-0804-4019-3.

105 Zener C., "*Theory of Growth of Spherical Precipitates from Solid Solution*", Journal of Applied Physics Vol. 20 No.10, October 1949, pp. 950 to 953.

106 Various authors, "*Wikipedia - The Free Encyclopaedia*", http://en.wikipedia.org, 2006.

107 Sun W.P. and Hawbolt E.B., " *Comparison between Static and Metadynamic Recrystallisation - An Application to the Hot Rolling of Steels*", Institute of Iron and Steel of Japan Vol.37 No.10, October 1997, pp. 219 to274.

108 Roucoules C., Hodgson P.D., Yue S. and Jonas J.J., "*Softening and Microstructural Change Following the Dynamic Recrystallisation of Austenite*", Metallurgical Transactions part A Vol.25A No.2, February 1994, pp. 389 to 400.

109 Rios P.R., Siciliano Jr. F., Sandim H.R.Z., Plaut R.L. and Padilha A.F., "*Nucleation and Growth during Recrystallisation*", Materials Research Vol.8 No.3, 2005, pp. 225 to 238, Brazil.

110 Humphreys F.J. and Hatherly M., "*Recrystallisation and Related Annealing Phenomena*", Oxford: Pergamon press, 1996, pp. 85 to 126, United Kingdom.

111 Cooperation for material knowledge, http://www.matter.org.uk/glossary/detail.asp?dbid=339, The University of Liverpool, UK, 2000 to 2006.

112 Doherty R.D., Hughes D.A., Humphreys F.J. Jonas J., Jensen D.J. and Kassner M.E., "*Current Issues in Recrystallisation: A Review*", Materials Science and Engineering A Vol.237, 1997, pp. 219 to 274.

113 American Society for Metals International and the Materials Information Society, "*Heat Treating*", 10th edition, American Society for Metals Handbook Vol.4, USA, 1993, ISBN: 0-87170-379-3.

114 Melander M. and Nicolov J., "*Heating and Cooling Diagrams for the Rapid Heat Treatment of Two Alloy Steels*", Journal of Heat Treating Vol.4 No.1, June 1985, pp. 32 to 38.

115 Van der Wolk P.J., Wang J., Sietsma J. and Van der Zwaag S., "*Modelling the Continuous Cooling Transformation Diagram of Engineering Steels using Neural Networks Part I: Phase Regions*", Zeitschrift fuer Metallkunde/Materials Research and Advanced Techniques Vol.93 No.12, pp. 1199 to 1207.

116 Moerman J., "*Mikrostruktuuronderzoek aan de Rolnaadlas van de Driedelige Bus*", Internal Document, Hoogovens Research & Development, IJmuiden Technology Centre, The Netherlands, April 1996, 24p.

117 Jaques S. and Szczur J., "*Tinplate and the Welded Can*", Paper of the Australian Iron and Steel Proprietary Limited, Port Kembla, New South Wales, Australia, pp. 17 to 26.

118 Elzinga E., "*Kommavorming in Vetind Blik ten gevolge van Soudroniclassen*", Internal Document, Hoogovens Research & Development, IJmuiden Technology Centre, The Netherlands, February 1988, 10p.

119 Elzinga E., "*De Invloed van de Lasbaarheid en de Breedte van de Overlap op de Kommavorming*", Internal Document, Hoogovens Research & Development, IJmuiden Technology Centre, The Netherlands, March 1988, 5p.

120 Elzinga E., "*The Formation of Commas*", Internal Document, Hoogovens Research & Development, IJmuiden Technology Centre, The Netherlands, December 1989, 8p.

121 Gutierrez-Miravete E., Giamei A.F., Cowles Jr. J.H., and Bruskotter M., "*Recent Developments in Welding Modelling*", The Minerals, Metals & Materials Society, Modelling of Casting, Welding and Advanced Solidification Processes VII, USA, 1995, pp. 825 to 831.

122 Taylor G.A., Hughes M. and Pericleous K., "*The Application of Three Dimensional Finite Volume Methods to the Modelling of Welding Phenomena*", University of Greenwich & Centre for Numerical Modelling and Process Analysis, London, United Kingdom, 2000, 8p.

123 Boyd A.J., "*Mathematical Model of Weld Cooling*", Technical Record, Metal Box Limited - Research & Development, London, United Kingdom, January 1981.

124 Boyd A.J., "*Geometric Aspects of Soudronic Weld Formation*", Technical Record, Metal Box Limited - Research & Development, London, United Kingdom, April 1981.

125 Brifcani M., "*Modelling of DC Resistance Welding*", Technical Document, Crown Technology - Research & Development, United Kingdom, January 1994.

126 Ferrasse S. and Piccavet E., "*Thermal Modelling of the Mash Seam Welding Process Using FEM Analysis*", Institute of Metals, Minerals & Mining Communications Limited, Mathematical Modelling of Weld Phenomena IV, London, United Kingdom, April 1998, pp. 494 to 519.

127 Davies T., Jones I.B., Beaverstock R.C. and Wadsworth J.E.J., "*FE Modelling of the Mash Seam Welding Process - Three-Piece Food Can Manufacture*", Internal Document, Corus Research Development & Technology, IJmuiden Technology Centre, The Netherlands, 2001.

128 Beaverstock R.C., "*General FE Support - Mash Seam Welding*", Internal Document, British Steel, United Kingdom, January 2000.

129 Den Uijl N., "*Corus Resistance Weld Modelling Projects*", Internal Document, Corus Research Development & Technology, IJmuiden Technology Centre, The Netherlands, March 2006, 15p.

130 Wen S., "*Preliminary Investigation on Modelling of Can Body Seam Welding*", Transport Applications, Corus Research Development & Technology, Swinden Technology Centre, United Kingdom, 2001.

131 Sun X., "*Effect of Projection Height on Projection Collapse and Nugget Formation - A Finite Element Study*", Research Supplement, Welding Journal Vol.80 No.9, September 2001, pp. 211-s to 216-s.

132 Murakawa H., Minami H. and Kato T., "*Finite Element Simulation of Seam Welding Process*", Transactions of the Joining Welding and Research Institute Vol.30 No.1, January 2001, pp. 111 to 117.

133 Thieblemont E., Gobez P., Bollinger E. and Chevrier J.C., "*Resistance Spot Welding: Measurement of Dynamic Electrical Resistance of the Electrode Sheet Interface*", The Minerals, Metals & Materials Society, Modelling of Casting, Welding and Advanced Solidification Processes V, USA, 1991, pp. 165 to 171.

134 Hansen J.L., Hattel J. and Lorentzen T., "*Modelling Moving Heat Source and Residual Stresses in Submerged Arc Welding*", The Minerals, Metals & Materials Society, Modelling of Casting, Welding and Advanced Solidification Processes IX, USA, 2000, pp. 814 to 821.

135 Pavlyk V. and Dilthey U., "*A Numerical and Experimental Investigation of Heat and Fluid Flow in Electric Arc Weld Pools*", The Minerals, Metals & Materials Society, Modelling of Casting, Welding and Advanced Solidification Processes IX, USA, 2000, pp 830 to 837.

Additional reading

1. Opprecht P., "*Überlappt- und Quetschnahtschweißen*", Bänder Bleche Rohre Vol.26 No.2, Berlin, Germany, February 1978, pp. 68 to 71.
2. Schaerer G., "*Food and Beverage Can Manufacture by Soudronic Welding Technology*", Soudronic AG, Berdietkon, Switzerland, Paper No.17 2nd International Tinplate Conference, International Tinplate Research Institute, London, United Kingdom, October 1980, pp. 176 to 186.
3. Panknin W., "*New Developments in Welding Can Bodies*", L. Schuler GmbH, Groeppingen, Germany, Paper No.20 3rd International Tinplate Conference, International Tinplate Research Institute, London, United Kingdom, October 1984, pp. 265 to 267.
4. Habenicht G., "*Neues Schweißverfahren für die Weißblechdosen-Herstellung*", Neue Verpackung No.5, München, Germany, May 1984, pp. 38 to 48.
5. Sauer R., Täffner K. and Sodeik M., "*Neuere Entwicklungen im Bereich Weißblecherzeugung und Dosenherstellung*", Metall Vol.41 No.9, Germany, September 1987, pp. 880 to 885.
6. Church F.L., "*S.M.E. Clinic Explores Canmaking Technology*", Modern Metals Vol.44 No.9, October 1988, pp. 52 to 74 (even).
7. Hollaender J., "*Influence of Welding Conditions on the Quality of Welded Seams of Tinplate Cans"*, Verpackungs-Rundschau Vol.40 No.9, Germany, September 1989, pp. 71 to 78.
8. Sauer R., Sodeik M., Täffner K. and Weber F., "*Anwendungstechnische Entwicklungen für Verpackungsblech bei der Rasselstein AG*", Stahl und Eisen Vol.108 No.22, Germany, October 1988, pp. 1107 to 1114.
9. Draugelates U., Bouafi B., Sommer D. and Siebert D., "*Simulation of the Forming of Mash Seam Welded Sheets*", Steel Research Vol.65 No.6, July 1994, pp. 238 to 241.
10. Adonyi Y., "*Steel Property and Welding Parameter Effects on Can Flange Cracking*", US Steel, 77th annual American Welding Society Convention Abstracts, USA, April 1996, pp. 48 to 49.
11. Kersten W., "*Werkstoffeinflusse auf das Hochleistungslängsnahtschweißen von Dosen*", Technische Forschung Stahl, Rasselstein AG, Germany, 1989.

12. Kikuchi T., Mochizuki K. and Kuguminato H., "*Relationship between Dynamic Contact Resistance and Weldability of Can Materials"*, Journal of the Surface Finishing Society of Japan Vol.47 No.1, Japan, January 1996, pp. 62 to 66.
13. Draugaletes U., Bouaifi B. and Daniel S., "*Effect of the Post-Weld Treatment on the Weld Properties of Mash Seam Welded and Laser Beam Welded Sheets"*, Welding Research Abroad, Vol.46 No.12, December 1998, pp. 27 to 32.
14. Kim K.C. and Lee M.Y., "*Effect of Welding Conditions on Resistance Weldability of Tin Coated Sheet Steels"*, RIST Journal of Research & Development Vol.14 No.2, South Korea, June 2000, pp. 143 to 149.
15. Suthar B.S., "*Numerical Modelling of the High Speed Resistance Seam Welding Process*", Engineering Doctorate, University of Wales, Swansea, United Kingdom, 2006.

16. Elzinga E., "*Onderzoek naar Overbordelcapaciteit, Scheurvorming en Lasstruktuur bij de Driedelige Bus*", Internal Document, Hoogovens Research & Development, IJmuiden Technology Centre, The Netherlands, March 1995, 36p.
17. Stevels J.T., "*Dikte Reductie Lasnaad*", Internal Document, Hoogovens Research & Development, IJmuiden Technology Centre, The Netherlands, November 1996, 14p.
18. Moerman J., "*Karakterisering van de mechanische eigenschappen van een lasstructuur*", Internal Document, Hoogovens Research & Development, IJmuiden Technology Centre, The Netherlands, February 1999, 3p.
19. Dunnebier J.C., Van der Heide J. and Stevels J., "*Tinplate for Quality, High-Speed Welding*", Canmaker Conference: The Leading Edge, Houston, USA, November 1998
20. Landkroon J.P.S., "*Tin Gloss and Roughness*", Internal Document, Hoogovens Research & Development, IJmuiden Technology Centre, The Netherlands, April 2003, 16p.

21. Zhang, Qingan, Gao, Jiasheng, Chen, Huifen, He and Yizhu, "*Mechanism of Fracture of a Mash Seam Welded Joint in Interstitial-Free (IF) Steel*", Journal of Materials Engineering No.2, 1998, pp. 44 to 46.
22. Tokaji K. and Minagi A., "*Fatigue Crack Propagation of Mash Seam Welded Joints*", Journal of the Japan Welding Vol.18 No.4, Japan, April 2000, pp. 634 to 641.

23. Tokaji K., Shiota H., Minagi A. and Miyata M., "*Fatigue Strength of Mash Seam Welded Joints*", Fatigue and Fracture of Engineering Materials and Structures Vol.23 No.5, Japan, May 2000, pp. 453 to 459.

24. Vaidyanath L.R., Nicholas M.G. and Milner D.R., "*Pressure Welding by Rolling*", British Welding Journal Vol.5 No.1, January 1959, pp. 13 to 28.

25. Panknin W. and Sodeik M., "*Untersuchen uber das Warmpressschweissen von Stahl*", Bänder Belche Rohre Vol.11 No.3, Germany, March 1970, pp. 161 to 164.

26. Sodeik M., "*Cold Weld Seizing during Deep Drawing and Ironing of Steel Sheet*", Deutsche Gesellschaft für Metallkunde, Germany, 1975, pp. 158 to 179.

27. Partridge P.G. and Ward-Close C.M., "*Diffusion Bonding of Advanced Materials*", Metals and Materials Vol.5 No.6, June 1989, pp. 334 to 339.

28. Fenn, R. "*Solid phase welding - An Older Answer to New Problems*", Metallic and Materials Technology Vol.16 No.7, July 1984, pp. 341 to 342.

29. Baron J., "*An Update on Mash Seam Resistance Welding*", Welding Journal Vol.73 No.7, July 1994, pp. 35 to 39 (odd).

30. Jones T.B., "*Weldbonding - The Mechanism and Properties of Weldbonded joints"*, Sheet Metal Industries Vol.72 No.9, September 1995, pp. 27, 30 and 31.

31. Geiemann T.J. and Davenport III F.H., "*Tailored Blank Welding by The Resistance Mash Seam Process*", Material and Body Testing, IBEC, 1995, p108.

32. Fukui K., Yasayama M., Taka T. and Ogawa K., "*Development of Joining Technology on Aluminium and Low-Coated Steel Sheets*", Technical Reports, Sumitomo Research No.59, September 1997, pp. 35 to 38.

33. Uchihara M., Takahashi M., Kurita M., Hirose Y. and Kukui K., "*Properties of Mash Seam Weld for Tailored Blanks*", Sumitomo Metals Vol.50 No.3, Japan, March 1998, pp. 41 to 48.

34. Haiping S., "*Blank Welding High-Strength Steels*", Dissertation, Ohio State University, Ohio USA, 2000, pp. 8 to 20.

35. Han C.W., Uhm S.H. and Lee C.H., "*Weldability Criteria for Mash Seam Tailored Blank Welds in Ultra Low Carbon Steels Applied to Automotive Bodies*", Science and Technology of Welding and Joining Vol.7 No.6, June 2002, pp. 403 to 407.

36. Krallics G. and Lenard J.G. "*An Examination of the Accumulative Roll-Bonding Process*", Journal of Materials Processing Technology Vol.152 No.3, March 2004, pp. 154 to 161.

37. Flax S., "*Modern Application of resistance welding - 1*", Welding and Metal Fabrication Vol.39 No.8, August 1971, pp. 289 to 293.

38. Flax S., "*Modern Application of resistance welding - 2*", Welding and Metal Fabrication Vol.39 No.9, September 1971, pp. 322 to 326.

39. Flax S., "*Modern Application of resistance welding - 3*", Welding and Metal Fabrication Vol.39 No.11, November 1971, pp. 406 to 408.

40. Slee K.V. and Moore G.R., "*New Approach to Quality Assurance in Resistance Welding*", Welding and Metal fabrication Vol.41 No.6, June 1973, pp. 204 to 205 and 207.

41. Sitte G., "*Mash Seam Resistance Welding of Transformer Core Plates*", Zeitschrift für Metallkunde Vol.18 No.4, April 1976, pp. 385 to 388.

42. Johnson K.I., "*Resistance Seam Welding - A New British Standard*", Metal Construction Vol.13 No.5, May 1981, pp. 294 to 295.

43. Picket K.M., Shi M.F. Bhatt K.K. and Selvaraj J., "*Structure Property Relationships of Resistance Mash Seam Welding Tailored Blanks with Post Treatment*", Microstructural Science Vol.20, 1993, pp. 87 to 102.

44. Adams Jr. C.M., "*Cooling Rates and Peak Temperatures in Fusion Welding*", Research Supplement, Welding Journal Vol.37 No.5, May 1958, pp. 210-s to 215-s.

45. Yuan Z.X., Jia J., Guo A.M., Shen D.D. and Song S.H., "*Cooling-Induced Tin Segregation to Grain Boundaries in a Low Carbon Steel*", Scripta Materialia Vol.48 No.2, January 2003, pp. 203 to 206.

46. Desai C.S. and Abel J.F., "*Introduction to the Finite Element Method - A Numerical Method for Engineering Analysis*", Van Nostrand Reinhold Company, New York, USA, 1972, ISBN: 0-4422-2083-9.

47. Lancaster J.F., "*Metallurgy of Welding*", 6th edition, Abingdon Publishing, United Kingdom, 1999, ISBN: 0-0466-9010-7.

48. Rogers G.F.C. and Mayhew Y., "*Engineering Thermodynamics - Work and Heat Transfer*", 4th edition, Prentice Hall, United Kingdom, 1992, ISBN: 0-5823-0500-4.